Published in final edited form as:
Clin Orthop Relat Res. 2005 March ; (432): 242–251.

Selective Retention of Bone Marrow-Derived Cells to Enhance Spinal Fusion

George F. Muschler, MD[*,†,a], **Yoichi Matsukura, MD, PhD**[†], **Hironori Nitto, MD, PhD**[†], **Cynthia A. Boehm, BS**[†], **Antonio D. Valdevit, MS**[†], **Helen E. Kambic, PhD**[†], **William J. Davros, PhD**[‡], **Kirk A. Easley, MS**[§], and **Kimerly A. Powell, PhD**[†]

*From the Department of Orthopaedic Surgery, The Cleveland Clinic Foundation, Cleveland, OH.

†From the Department of Biomedical Engineering, Lerner Research Institute, The Cleveland Clinic Foundation, Cleveland, OH.

‡From the Department of Radiology, The Cleveland Clinic Foundation, Cleveland, OH.

§From the Departments of Biostatistics and Epidemiology, The Cleveland Clinic Foundation, Cleveland, OH.

Abstract

Connective tissue progenitors can be concentrated rapidly from fresh bone marrow aspirates using some porous matrices as a surface for cell attachment and selective retention, and for creating a cellular graft that is enriched with respect to the number of progenitor cells. We evaluated the potential value of this method using demineralized cortical bone powder as the matrix. Matrix alone, matrix plus marrow, and matrix enriched with marrow cells were compared in an established canine spinal fusion model. Fusions were compared based on union score, fusion mass, fusion volume, and by mechanical testing. Enriched matrix grafts delivered a mean of 2.3 times more cells and approximately 5.6 times more progenitors than matrix mixed with bone marrow. The union score with enriched matrix was superior to matrix alone and matrix plus marrow. Fusion volume and fusion area also were greater with the enriched matrix. These data suggest that the strategy of selective retention provides a rapid, simple, and effective method for concentration and delivery of marrow-derived cells and connective tissue progenitors that may improve the outcome of bone grafting procedures in various clinical settings.

Bone grafting is widely used in orthopaedic surgery to treat acute fractures, fracture nonunions, and bone defects, and to achieve therapeutic arthrodesis. Each year, approximately 500,000 bone grafting procedures are done on patients in the United States.[4] The efficacy of the grafts used in these procedures generally is considered to be derived from their osteoconductive and osteoinductive properties.[2,10,14,22]

Osteoconduction can be defined as a scaffold function provided by a graft material that facilitates the attachment and migration of cells that contribute to new tissue formation.[25]

Correspondence to: George F. Muschler.

Correspondence to: George F. Muschler, MD, Department of Orthopaedic Surgery (A41), The Cleveland Clinic Foundation, 9500 Euclid Ave, Cleveland, OH 44195. Phone: 216-444-5338; Fax: 216-445-1638; E-mail: muschlg@ccf.org..

[a]One of the authors (GFM) has or may receive payments or benefits from a commercial entity (DePuy Acromed, Raynham, MA), under a license agreement with The Cleveland Clinic Foundation, related to this work.

Each author certifies that his or her institution has approved the animal protocol for this investigation and that all experimentation was done in conformity with ethical principles of research.

One or more of the authors have received funding from the Musculoskeletal Transplant Foundation (MTF, Edison, NJ); Grant R01 AR-42997 from the National Institutes of Health (Bethesda, MD); and from The Cleveland Clinic Foundation (Cleveland, OH).

Osteoinduction broadly refers to biologic stimuli from diffusible or matrix-bound peptide growth factors and cytokines that promote osteoblastic progenitors to migrate, proliferate, and differentiate. The prototypical stimuli are the family of bone morphogenetic proteins (BMPs), but many factors contribute. Osteogenic and non-osteogenic cells, including endothelial cells,[39] may elaborate inductive factors.[5,10,14,15]

Although osteoconduction and osteoinduction must be present in a successful graft site, the efficacy of any osteoconductive material or osteoinductive stimulus depends entirely on the presence of a sufficient number of osteogenic progenitors in the graft or graft site (the osteogenic potential). Were it not for the presence of osteogenic cells in most graft sites, the implantation of an osteoconductive material or the delivery of an osteoinductive stimulus alone would be ineffective. Fortunately, osteogenic cells are present in viable local bone and periosteum and also are found in adjacent soft tissues, muscle, or fat.[6,31,33] Osteogenic cells also may be transplanted into the graft site with autogenous bone graft or bone marrow.

Despite the presence of osteoblastic progenitors in virtually all graft sites, many clinical settings are likely to be deficient in osteoblastic progenitors. These settings include atrophic nonunited fractures; large or segmental bone defects; regions of scarring after infection, trauma, or previous surgery; regions of previous radiation therapy; regions of osteonecrosis; and patients who are immuno-compromised because of systemic illness or chemo-therapy. The concept that the number of osteoblastic progenitor cells in many graft sites is suboptimal is supported by the large volume of animal and clinical data[10,15,22–24,27] indicating that the addition of bone marrow-derived cells to almost any osteoconductive or osteoinductive material results in a considerable improvement in outcome.

Recognizing the potential biologic value and low risk of surgical complications,[41] many surgeons have used bone marrow aspirated from the iliac crest as an adjuvant to bone grafting procedures, even in the absence of practical means of concentrating cells in the operating room.[8,11–13,32,35,36,38] Efforts have provided information to assist surgeons in optimizing methods for the use of bone marrow-derived cells. For example, it has been shown that the concentration of bone marrow-derived cells in a bone marrow aspirate is diluted rapidly by peripheral blood as the volume of the aspirate is increased. However, this effect can be reduced by limiting the volume of aspiration from a given needle site to 2 cc or less.[19] Using established means for assay of connective tissue progenitors from human bone marrow, some investigators have begun to characterize the effects of clinical variables (age, gender, and disease) on the population of connective tissue progenitors.[16,27]

To provide surgeons with practical means of concentrating and delivering bone marrow-derived cells for optimization of bone grafting procedures, we observed that connective tissue progenitor cells and other bone marrow-derived cells can be concentrated rapidly from bone marrow aspirates using selected materials with surface properties that facilitate the rapid attachment of osteoblastic progenitors.[18] One such material is allograft bone chips. We also reported that a cellular graft using allograft chips that is enriched fourfold in the number of connective tissue progenitors performs significantly better than allograft chips combined with bone marrow alone.[28] However, this improvement was shown to require the presence of a fibrin clot environment provided by nonanticoagulated bone marrow or blood.[28]

The current experiment was designed to expand on these observations by testing the hypothesis that demineralized cortical bone powder provides an effective alternative substrate for selective retention and to confirm that concentration of connective tissue progenitors using the selective retention strategy significantly improves the radiographic and mechanical performance of demineralized cortical bone powder used with or without conventional bone marrow aspirate in spinal fusions.

MATERIALS AND METHODS

Demineralized canine allograft cortical bone powder was used as the matrix for attachment and delivery of cells. All allograft matrices used in these experiments were prepared under sterile conditions from allograft bone from Beagles (femurs and humeri) at Osteotech, Inc. (Eatontown, NJ), using methods identical to those used to process demineralized human cortical bone allograft matrix for clinical use. Graft preparation was in accordance with the standards of the American Association of Tissue Banks.[1] Cortical bone was frozen with liquid nitrogen, milled to a powder, and then washed in alcohol-based solvents and detergents to remove fats and cellular debris. The matrix then was demineralized to less than 5% wt/wt residual calcium in 0.6 mol/L HCl, adjusted to neutral pH, and lyophilized. A range of particle size from 425 μm to 850 μm in diameter was selected. To limit the potential for histocompatibility differences between donors that might compromise paired comparisons between matrices, the graft matrices used in each dog were derived from one donor.

Allograft-bone marrow composites were evaluated in an established canine posterior segmental spinal fusion model.[20,21,26] Twelve male Beagles (Marshall Farms, North Rose, NY) were used (age, 12–15 months; weight, 11.8–13.4 kg). Study animals were cared for in accordance with the Principles of Laboratory Care and The Guide for the Care and Use of Animals.[29]

Detailed methods for the surgical procedure, animal care, and specimen harvest have been reported.[21] Briefly, localized fusions were done at three spinal fusion sites in each animal (L1–L2, L3–L4, and L5–L6). Each fusion site was separated by one normal mobile segment. Graft site preparation was done under constant irrigation using a high-speed burr (TURQ-3, 3-mm fluted ball; Anspach, Palm Beach Gardens, FL). The fusion site included the facet joints at each level and the space between the lamina at each site. Each animal received grafts of all three materials under evaluation, one at each site. To limit the potential for surgical bias and to ensure equal distribution of materials at each of the three graft sites, the site assigned to each material was determined randomly after site preparation. Twelve cards (two sets of six possible combinations of three materials in three sites) were prepared at the beginning of the experiment. Site assignments then were made intraoperatively by randomly drawing a card from this set of possible combinations after site preparation was complete. Internal fixation was applied to each segment using stainless-steel plates (0.125 inches × 0.4 inches × 1.4 inches) placed on either side of the spinous processes. These plates were fixed using threaded bolts (2-56 thread, 0.5 inches long) passing through each spinous process with locking nuts. Each animal received preoperative prophylactic antibiotics of penicillin G (500,000 units) given intramuscularly, then 250 mg ampicillin given orally each day for 5 days. Acepromazine and acetaminophen were used for perioperative pain. No external immobilization was used.

All animals were euthanized 12 weeks postoperatively using an overdose of pentobarbital. The lumbar spine was harvested intact. Plate fixation was removed. Quantitative assessment of the bone formation in each fusion segment was done using helical radiography, CT scanning, and three-dimensional (3-D) image analysis. The spines were frozen at −20°C until preparation for mechanical testing. Each fusion segment then was tested mechanically to failure for assessment of mechanical properties. The cross-sectional area of the fusion mass bridged with firm mineralized bone tissue then was assessed as a union score for each site.

The following cell-matrix composites were evaluated: demineralized cortical bone powder (DCBP) alone − DCBP (1.5 cc) + saline (1.5 cc); DCBP + aspirated bone marrow (ABM) − DCBP (1.5 cc) + ABM (1.5 cc); and enriched DCBP + ABM − enriched DCBP composite (1.5 cc) + ABM (1.5 cc). This enrichment was designed to result in an approximately fivefold increase in the number of osteoblastic progenitors.

After induction of general anesthesia, and before beginning the approach to the spine, a 3-mm skin incision was made using a Number 11 blade over the anterior aspect of the proximal humerus. Previous experience has shown that the proximal humerus in a canine is a reliable source of hematopoietic bone marrow containing osteoblastic progenitors and that the yield of cells and progenitors from the humerus is more reliable than aspirates taken from the iliac crest in a canine. A Lee-Lok bone marrow aspiration needle (Lee Medical, Ltd., Minneapolis, MN) was inserted through one cortical site. Ten separate 2-cc bone marrow aspirates were harvested from the proximal humeri with each dog under general anesthesia (five aspirates were harvested from each side). Aspiration sites were separated by approximately 1 cm by changing the direction and depth of the needle placement. Samples were aspirated into 10-mL syringes (Becton Dickinson and Co, Franklin Lakes, NJ). One aspirate on each side was harvested without heparin to provide a marrow clot. Four additional aspirates on each side were harvested into syringes containing 1 cc sodium heparin solution (1000 units/cc). Each syringe was inverted several times to ensure complete mixing with the heparin solution. The eight heparinized aspirates were pooled (approximately 30 cc total volume) to provide a noncoagulated, single-cell suspension of bone marrow-derived cells diluted in blood. A 1-cc aliquot of the pooled sample was used to assay the concentration of nucleated cells using a hemacytometer.

肝素化浓度

For preparation of the enriched composite, a 1.5-cc volume of demineralized cortical bone powder was loaded into a 10-cc syringe using a nylon mesh at the tip of the syringe to prevent passage of the powder out of the syringes. The cellularity of marrow aspirates and the prevalence of connective tissue progenitors varies significantly between humans[19] and dogs.[28] Therefore, to control for variation between dogs with respect to the number of cells and connective tissue progenitors transplanted, a sample of heparinized bone marrow containing 600 million nucleated cells was prepared for each dog. This then was passed through the matrix at a flow rate of 0.5 cc per minute (a linear flow rate of approximately 25 cc/minute) to prepare the enriched cell-matrix composite. The number of cells and osteoblastic progenitors present in the effluent solution from each preparation was assayed to determine the number of cells and osteoblastic progenitors selectively retained in the matrix. Sample preparation took approximately 20 minutes.

Once the enriched composite was returned to the operating suite, the final composite preparation was completed. Demineralized cortical bone powder (1.5 cc) was moistened with 1.5 cc of saline to form the DCBP-alone graft material. Demineralized cortical bone powder (1.5 cc) was mixed physically with 1.5 cc of the clotted nonheparinized bone marrow aspirate to form a paste of the DCBP + ABM material. Similarly, the enriched composite (1.5 cc) was mixed physically with 1.5 cc of the nonheparinized bone marrow aspirate to form a paste of the enriched DCBP + ABM material.

The number of osteoblastic progenitors in each sample was assayed using an established colony-forming assay.[16,19,27,28] This assay was used to determine the number of colonies formed after culture of a defined number of nucleated cells. Colonies assayed in this way include cells that can differentiate into bone and phenotypes other than bone (cartilage, fat, muscle, and fibrous tissue). This population of tissue-derived cells has been defined broadly as connective tissue progenitors.[23] When cultured under conditions that promote proliferation and osteoblastic differentiation, approximately 90% of all connective tissue progenitor colonies express alkaline phosphatase (ALP), an early marker of bone differentiation. The number of ALP-positive connective tissue progenitors can be used as an assay of osteoblastic progenitors.

Briefly, heparinized marrow suspensions were centrifuged at 1500 rpm for 10 minutes. The buffy coat was pipetted and re-suspended in 5 cc of alpha minimal essential medium (Gibco BRL, Grand Island, NY). Nucleated cells were counted using a hemacytometer. Cells were

plated at a density of 125,000 cells/cm^2 on 4-cm^2 slides (Lab-tek chamber slides, Fisher Scientific, Pittsburgh, PA). The culture medium consisted of 90% alpha minimum essential medium, 10% fetal bovine serum (Lot no. 6MO109, BioWhittaker, Walkersville, MD), dexamethasone (10^{-8} mol/L), and ascorbic acid (50 μg/cc). Slides were incubated at 37°C in 5% CO_2. The medium was changed once at Day 7. On Day 9, the slides were stained in situ for determination of ALP activity. Cell clusters containing eight or more cells also expressing ALP were counted as connective tissue progenitors.

To assay the number of cells and connective tissue progenitors delivered in each graft site, the matrix loading process was done and controlled in four steps. A heparinized suspension of bone marrow-derived cells and blood obtained by aspiration was prepared. Then the heparinized suspension was passed through the matrix under controlled conditions to allow selective retention of cells by adhesion of cells to the matrix surface. Next, the effluent containing cells that did not adhere to the matrix was collected. Finally, the initial sample and the effluent sample were assayed for nucleated cells and connective tissue progenitors.

Using the cell count and connective tissue progenitor data, calculations were done that showed the retention and selection of cells and connective tissue progenitors in the graft. These parameters included the number of cells and connective tissue progenitors retained in the graft, binding efficiency for nucleated cells and connective tissue progenitors (fraction of cells and connective tissue progenitors retained), selection ratio for connective tissue progenitors versus nucleated cells (relative efficiency of retention for connective tissue progenitors versus other nucleated cells), and fold increase in concentration for cells and connective tissue progenitors (relative change in concentration from the initial marrow aspirate to the final graft).

The raw data for each implanted cell-matrix composite included the number of nucleated cells and connective tissue progenitors in the original sample (N_O, CTP_O) and in the load effluent (N_{LE}, CTP_{LE}). The following calculations then were done for each implanted cell–matrix composite graft.

The number of cells and connective tissue progenitors retained in the matrix (N_R and CTP_R) was determined by the following equations: $N_R = N_O - N_{LE}$ and $CTP_R = CTP_O - CTP_{LE}$. The binding efficiency (BE) for connective tissue progenitors and nucleated cells (CTP_{BE} and N_{BE}) was calculated as follows: $N_{BE} = N_R/N_O$ and $CTP_{BE} = CFU_R/CTP_O$. The selection ratio (SR) for connective tissue progenitors versus nucleated cells was calculated in terms of the binding efficiency ratio ($SR = CTP_{BE}/N_{BE}$). A selection ratio greater 1.0 implies positive selection or enrichment of connective tissue progenitors with respect to other marrow cells. The fold increase in concentration (ΔC) for cells and connective tissue progenitors was calculated as a ratio of the concentration in the final graft versus the concentration in the initial sample: $N_{\Delta C} = (N_R/\text{graft volume}) \div (N_O/\text{aspirate volume})$; $CTP_{\Delta C} = (CTP_R/\text{graft volume}) \div (CTP_O/\text{aspirate volume})$ = [CTPs] in the graft/[CTPs] in the marrow aspirate.

There were minor differences in the volume of graft implanted in these three groups. In preparing each sample, 1.5 cc of demineralized cortical bone powder first was hydrated with 1.5 cc saline. After hydration, the volume of the matrix was increased to approximately 1.7 cc as a result of swelling of the matrix particles and collection of a layer of fluid in the spaces between particles. The resulting consistency was like that of wet sand. There was no observable change in the volume of the matrix after the enrichment process. This was not surprising, because the volume contributed by the 148 ± 50 million cells retained in the enriched matrix after passing the heparinized bone marrow sample through the matrix was small (≤ 0.05 cc, if compressed as a pellet) and readily accommodated the space between bone matrix particles. When the matrices in the DCBP + ABM group and the enriched DCBP + ABM group were combined with clotted bone marrow, the formed clot fragments seemed to be retained in the

matrix, displacing some of the fluid that was retained between particles after the loading process. After mixing, the graft was allowed to set for 10 to 15 minutes. Any excess fluid was allowed to drain from the matrix before implantation. Therefore, the final volume of the graft was the same (approximately 2.0 cc) in the DCBP + ABM group and the enriched DCBP + ABM group, but slightly lower in the DCBP-alone group (approximately 1.7 cc). This preparation method achieved the goals of the study and ensured that any differences between the DCBP + ABM group and the enriched DCBP + ABM group in the final number of cells and progenitors that were delivered to the graft site was the direct result of increases in the concentration of cells and progenitors achieved during the process or selective attachment. These differences were not attributable to any differences in the volume of the graft material that was transplanted into the graft site.

Quantitative assessment of the fusion mass was done using helical radiography, CT scanning, and automated three-dimensional image-processing techniques to determine the volume of each fusion mass (bone volume), the cross-sectional area at the center of each fusion mass (fusion area at center slice), and the mean bone mineral density (BMD) of the fusion mass (bone density).

A three-dimensional data set was acquired of all segments from L1–L6 in each spine using a Somatome Plus 40 CT scanner (Siemens Medical System Inc., Iselin, NJ). Scanning was done for 30 seconds at 120 kV(p), 210 mA, 1 second helical mode, 2-mm collimation, and at a table speed of 2 mm/second with a Siemens BMD phantom. Images were reconstructed using a bone algorithm and an image-to-image overlap of 1 mm.

Original software (D–image Dog 2 for Unix system), developed in the Department of Biomedical Engineering of our institution, was used to manipulate and observe the three-dimensional CT data. The area of the fusion mass (center slice area) was calculated by adding the number of segmented pixels in the transaxial plane at the middle section with a value of more than 1400 (366 Hounsfield units), then multiplying this sum by the appropriate pixel area (1 mm^2). The volume of the fusion mass (bone volume) was calculated by adding the segmented voxels with a value of more than 1400 units in the specified region of interest in 11 image slices (the center slice plus five slices above and five slices below the middle disc cross section) and multiplying this sum by the appropriate voxel volume (1 mm^3). The mean mineralization density (bone density) was calculated for the entire fusion mass and referenced to the density of a phantom. As previously described,[21] before testing, each specimen was thawed for 24 hours at room temperature. Testing was done on an MTS Bionix 858 Materials Testing System (MTS, Minneapolis, MN) using a custom four-point bending device. After three sinusoidal conditioning cycles, load displacement data were collected nondestructively with the specimens in flexion and extension and left and right bending. Failure testing then was done in right bending using the ramp function at 8 mm/second. Lateral bending was selected as the mode of failure because lateral bending stiffness was correlated most closely with union status in previous studies.[20,26] Load displacement curves were used to determine stiffness, maximum load, displacement to failure, and total energy to failure. Failure in all segments occurred in the transaxial plane through the midportion of the fusion mass, at the level of the disc space.

Immediately after mechanical testing, the surface of the fractured specimen was examined using a metal probe. By comparing both sides of the fracture surface, the degree of union was scored from 0 to 4 based on a regional grid system described previously.[20,21,26,28] A score of 4 represents complete fusion of both facet joints and the entire lamina. Scores of 0, 1, 2, 3, and 4 represent union across approximately 0%, 25%, 50%, 75%, and 100% of the cross-sectional area of the grafted volume, respectively. Scoring was done by two observers (YM and GFM), who were blinded with respect to the material grafted at each site.

An ordered logistic regression using the proportional odds model,[17] which adjusted for the correlation of observations in the same animal and potential differences between graft sites, was used to compare union scores for the three cell-matrix composites. Pairwise comparisons were made between cell-matrix composites. Repeated measures analyses of CT data (fusion volume, fusion area, and bone density) and mechanical stiffness data were done by SAS Proc Mixed (SAS, Inc., Cary, NC), which provided estimates of the means for each cell-matrix composite. The reported p values were two-sided, and a p value of 0.05 or less was considered statistically significant.

RESULTS

One animal had a deep wound infection involving the region of plate fixation overlying the enriched DCBP + ABM site; this dog was euthanized 3 weeks after surgery and was replaced, maintaining data from 12 animals and 36 graft sites for analysis.

Concentration and selection of connective tissue progenitors did improve graft performance, confirming the initial hypothesis that a stepwise improvement in union score would be seen when marrow cells were added to the matrix (DCBP versus DCBP + ABM) and when marrow cells and connective tissue progenitors were concentrated additionally using the selective retention strategy (DCBP + ABM versus enriched DCBP + ABM). The total union score was greatest for the enriched DCBP + ABM group (mean, 2.3) and was greater than the DCBP-alone group (mean, 0.5) (p = 0.009) and the DCBP + ABM group (mean, 1.3) (p = 0.04) (Table 1). The union scores in the DCBP + ABM group also were superior (p = 0.05) to those in the DCBP-alone group.

The union score data also showed an effect of graft site. In this experiment, grafts at the most proximal site (L1–L2) scored lower (p = 0.03) than grafts at the more distal sites. This finding has been observed in some previous experiments using this model, but does not impair the statistical comparison between materials, because the materials were distributed equally by site.[20,21,26,28]

Improved performance with the enriched DCBP +ABM graft also was reflected in the overall data for union rate (achievement of a union score greater than 0). The union rate was highest (p =0.018, Fisher's exact test) in the enriched DCBP + ABM group, in which eight of 12 grafts healed (67%). The union rate for the DCBP + ABM group was six of 12 grafts (50%), compared with two of 12 grafts (17%) in the DCBP-alone group. Unions with higher scores also were most common in the enriched DCBP + ABM group, in which six of 12 sites (50%) achieved a score of 3.0 or higher. In contrast, only two of 12 (17%) sites in the DCBP + ABM group and only one of 12 (8.3%) sites in the DCBP-alone group achieved a score in this range (p = 0.097 and 0.034, respectively; Fisher's exact test).

Concentration and selection of connective tissue progenitors also was associated with improved mechanical performance. The enriched DCBP + ABM group showed greatest mechanical stiffness (mean, 13.8 ± 7.7 N/mm). This was greater (p = 0.006) than the mechanical stiffness in the DCBP-alone group (9.4 ± 3.3 N/mm). In contrast, the stiffness in the DCBP + ABM group (11.0 ± 4.5 N/mm) also was not greater (p = 0.25) than that in the DCBP-alone group (Table 2).

The data on maximum load, displacement to failure, and total energy to failure only could be calculated from specimens with bony fusion in which failure was associated with a defined yield point. Data for these parameters, therefore, were limited to only those graft sites that successfully fused. The mechanical performance of these fused segments did not differ among the three composites (with adjustment for union score) and was consistent with previous reports using this model (data not shown).[20,26,28]

Fusion volume and fusion area data also support the initial hypothesis of stepwise improvement when marrow cells and connective tissue progenitors were concentrated additionally using the selective retention strategy (DCBP + ABM versus enriched DCBP + ABM). Fusion volume and fusion area in the enriched + ABM group were greater than those in the DCBP + ABM group ($p = 0.02$ and $p = 0.05$, respectively) (Table 3). Similarly, the fusion volume and fusion area in the enriched + ABM group were superior to the DCBP-alone group ($p = 0.001$ and $p = 0.005$, respectively). The DCBP + ABM group also was superior to the DCBP group for fusion volume and fusion area ($p = 0.001$ and $p = 0.04$, respectively). There were no differences between groups in the mean density of the bone formed.

Data measuring cell and connective tissue progenitor retention in the enriched graft also support the initial hypothesis that demineralized cortical bone powder provides an effective substrate for selective retention and concentration of connective tissue progenitors. The enriched DCBP + ABM group delivered more cells ($p < 0.001$) (Table 4). The mean concentration of marrow-derived cells implanted in the enriched DCBP + ABM group was increased by a factor of 2.3 ± 0.5 by the loading process. The total number of cells implanted with the graft was 269 ± 41 million cells, in contrast to an estimated 122 ± 20 million cells in the DCBP + ABM group.

The enriched DCBP + ABM group also delivered more connective tissue progenitors (Table 5). The mean number of connective tissue progenitors implanted in the enriched DCBP + ABM group was increased by a factor of 5.6 ± 3.9 by the loading process. The mean number of connective tissue progenitors implanted with the graft was 39,400 ± 24,500, in contrast to an estimated 7400 ± 4080 connective tissue progenitors in the DCBP + ABM group ($p < 0.001$).

Connective tissue progenitors adhered selectively to the cortical bone powder. Overall, 61% (± 14%) of connective tissue progenitors that were exposed to the matrix were retained. In contrast, only 23% (± 8%) of all nucleated cells in bone marrow were retained. This represents a positive selection of connective tissue progenitors over other marrow-derived cells of 3.0 (± 1.5)-fold.

DISCUSSION

This experiment was designed to test the hypothesis that demineralized cortical bone powder provides an effective alternative substrate for selective retention and to recon-firm our previous observation[28] that the concentration of connective tissue progenitors using the selective retention strategy significantly improves the performance in spinal fusions of an already effective osteoconductive matrix material, either with or without the addition of a conventional bone marrow aspirate.

These data show that demineralized cortical bone powder can be used as a substrate for rapid intraoperative concentration of bone marrow-derived cells. The addition of a simple aspirate of bone marrow to demineralized cortical bone powder resulted in an improvement in union score, fusion area, and fusion volume. This finding is consistent with results of numerous reports[3,9,11–13,30,34,36–38] suggesting the benefit of adding cells harvested by aspirated bone marrow to a graft site. Moreover, these data also support the hypothesis, and our previous observation, that the efficacy of a graft can be increased through preparation of an enriched composite of marrow cells, using the surface of the matrix as a means of selectively attaching and retaining marrow-derived cells and connective tissue progenitors for transplantation into a graft site. Enrichment of the matrix in this way resulted in increases in union score, fusion area, and fusion volume beyond those achieved by using a bone marrow aspirate alone. This enriched matrix was far superior to the allograft matrix alone.

We did not directly compare the enriched matrix preparation with the contemporary gold standard of autogenous cancellous bone. However, the mean union score of 2.3 achieved in

this study by an enriched DCBP + ABM graft is within the range of union scores (2.0–3.0) reported using autogenous cancellous bone in this model.[20,21,26] In contrast, the union score of 1.3 achieved by addition of a simple bone marrow aspirate to the allograft matrix was not in this range.

Connolly et al[7] were the first to suggest that concentration of bone marrow-derived cells could be used to enhance the performance of a cellular bone graft. They showed that increasing the concentration of cells (approximately fourfold) from rabbit bone marrow using density gradient separation resulted in increased bone formation in diffusion chambers. Although this method seemed to be effective, it required the use of a centrifuge in the operating room. In contrast, the selective retention method described in the current study does not require a centrifuge, nor are cells exposed to other potentially toxic agents (Percoll or Ficol) that must be removed later in processing. The selective retention method proposed by us also has the opportunity to exclude cells that do not attach, reducing the population of cells that compete with the retained cells and connective tissue progenitors after implantation.

Using selective retention, cell-matrix composites enriched in the concentration and prevalence of osteogenic connective tissue progenitors can be prepared rapidly in the operating room. However, this and a previous study[28] should be viewed only as initial feasibility studies that show the value of selective retention. Many variables in the processing require improvement before this method is practical for clinical use, as discussed later. Despite promising performance in this established canine spinal fusion model, direct clinical evaluation in selected treatments is necessary to show clinical value. Several clinical assessments are being done.

Optimal use of this method in the operating room requires selection of matrices with an appropriate porous structure, surface area, surface chemistry, and handling properties for processing and for implantation. Although only one structure was assessed in the current study, it is interesting to compare the selective retention characteristics of the demineralized cortical bone powder used in this study with that of the allograft cancellous chips used in a previous study.[28] Using similar loading techniques, demineralized cortical bone powder, with greater available surface area than cancellous chips, showed a greater increase in connective tissue progenitor concentration, greater relative selection of connective tissue progenitors versus other cells in marrow, and higher overall union scores than those achieved using cancellous chips alone as the matrix substrate.

Optimization of a selective retention strategy for clinical use also requires practical methods for control of the rate and pattern of fluid flow through the matrix in the operating room. In this study, preparation of the cell matrix composites was done in a separate laboratory under a laminar flow hood, using a customized nylon mesh to retain the matrix and a variable vacuum manifold to control flow rates. However, controlled fluid flow conditions must be made practical and convenient for use in an operating room with a limited set of specialized materials and equipment.

Optimization also may involve improved methods to harvest bone marrow before processing. Clinical aspiration of bone marrow has been shown to be a simple, safe, and effective means of harvesting connective tissue progenitors in considerable numbers.[16,19,27] Appropriate techniques for harvesting bone marrow by aspiration have been defined and can be taught and learned readily.[19] No patient has reported pain, swelling, infection, or hematoma at the aspiration site that required a change in pain medication, limited progress in rehabilitation, or prolonged hospitalization. However, future techniques should limit the time that is required for marrow harvest and the dilution of bone marrow cells with peripheral blood that has been shown to occur when aspiration volume from any given site is not limited to 2 cc or less using a static single-hole needle.[19]

Optimization of these methods also may include improvements in our understanding of the individual biologic features of patients and patient selection. However, current data suggest that few patients would be excluded. In three previous reports of clinical bone marrow harvest and subsequent experience, it was shown that connective tissue progenitors can be harvested from the iliac crest of almost all patients,[16,19,27] regardless of age or gender. The only exceptions, in our experience, arise in sclerotic regions of bone in patients with osteopetrosis and in patients with marrow-packing disorders such as myelofibrosis. We also showed that there is considerable variation in the concentration and prevalence of connective tissue progenitors in the bone marrow of patients. This variation is partly a function of age and gender.[27] There is a slow decline in marrow cellularity with age in men and women. In women, this decline in marrow cellularity is compounded by a decline in the prevalence of connective tissue progenitors, a finding that may be related to the pathophysiology of bone loss and estrogen deficiency after meno-pause.[27] However, only a small part of the variation in connective tissue progenitor concentration and prevalence in the tissues of patients is attributable to identified clinical factors. Other uncharacterized factors of genetics, systemic health (or disease), medications, tobacco and alcohol use, and local tissue conditions must account for this variation.[27]

Given the wide variation in connective tissue progenitor concentration among patients, it seems likely that, in some individuals, a deficiency in the number of cells and connective tissue progenitors may result in a clinically important reduction in the osteogenic potential, systemically or in specific tissue regions. In the context of a bone grafting procedure, a deficiency of connective tissue progenitors could limit the value of implanted osteoconductive materials and osteoinductive materials (BMPs), by reducing the number of available target cells. If so, the strategy of selective retention, or other means of enriching the local population of connective tissue progenitors, might offer a means of reversing or limiting this effect, and improve clinical outcomes.

Regardless of the variation that may exist among patients in concentration of connective tissue progenitors in local tissues, the available data suggest that increasing connective tissue progenitor concentration in a graft site will improve local osteogenesis, even in healthy individuals. One of the most striking findings of our study is that relatively modest enrichment of the connective tissue progenitor population results in significantly enhanced bone graft performance, even in young, healthy Beagles. This is a biologic setting in which the graft site is comprised entirely of normal bone and healthy minimally traumatized soft tissues. One would not expect this setting to be deficient in osteoblastic progenitors. Therefore, the finding of improved results with only a modest increase in the number of cells and connective tissue progenitors suggests that the number of osteogenic progenitors may be suboptimal in the majority of graft sites, even in small graft sites in otherwise healthy patients. It also may imply that augmentation of the cell and progenitor pool may be desirable and even necessary in a wide range of clinical settings to achieve an optimal bone healing response, including settings in which effective osteoconductive materials or osteoinductive growth factors or both may be used. This possibility is supported by the findings of Yasko et al,[40] who showed in a small femoral defect model in young, healthy rats that the combination of whole bone marrow and a highly osteoinductive preparation of BMP-2 was significantly more effective than the BMP-2 preparation alone.

读不懂啊？？

The optimal number of cells or progenitors required in a graft site is not known. Our study evaluated only one level of enrichment, which delivered a mean of 5.6-fold more connective tissue progenitors and a mean of 2.3-fold more marrow-derived cells than would be delivered by a simple bone marrow aspirate alone. Whether delivery of a larger number of cells or connective tissue progenitors will result in greater improvements in efficacy is speculation.

There is reason to predict, however, that there will be an upper limit of cell density that is desirable in a wound site. In a graft site, the capacity for diffusion of oxygen, carbon dioxide, and other nutrients is limited. As greater numbers of cells are delivered, these demands continue to increase and may exceed the capacity of diffusion into the graft site to support cell survival. As a result, beyond some threshold concentration, additional increases in the number of cells in a graft site might reduce the efficacy of the graft by inducing more profound hypoxia in the graft site and greater cell death.[24] The optimal number of connective tissue progenitors for transplantation and the optimal composition of the population of other marrow-derived cells needs to be determined experimentally. This is a topic of ongoing investigation.

漂亮　需要引用

We think the methods presented here for preparation of cellular grafts containing an enriched population of bone marrow-derived cells in an implantable matrix are valuable for optimizing the performance of bone-grafting materials using an integrated tissue engineering strategy. The elements of this conceptual framework are: efficient collection of tissue-derived cells containing stem cells and progenitor cells; rapid concentration and selection of a population of bone marrow-derived cells that includes cells that are capable of osteoblastic differentiation using the surface of an implantable matrix as the means of cell selection; delivery of these cells at a concentration sufficient to repopulate the graft site with bone-forming cells; delivery of cells in an environment in which their survival will not be precluded or threatened by the metabolic environment present in the graft site after implantation; choice of a matrix with surface and three-dimensional properties (pore size and architecture) that facilitate proliferation and migration of the desired cell population throughout the region in which the tissue is required; and creation of a biologic environment that contains an appropriate repertoire of cells and inductive stimuli to initiate all critical processes of local bone healing, including revascularization of the graft site and proliferation and differentiation of transplanted osteogenic cells. We think that this strategy, beginning with rapid, simple, safe, and inexpensive methods for concentration and delivery of bone marrow-derived cells and connective tissue progenitors, may improve the outcome of bone grafting in a wide range of clinical settings. Similar methods using bone marrow-derived cells also might be applied to various tissue engineering applications.

Acknowledgment

We thank Chizu Nakamoto, MD, PhD, for assistance in preparing this manuscript.

References

1. American Association of Tissue Banks. American Association of Tissue Banks; McLean, VA: 1998. Standards for Tissue Banking.
2. Bauer TW, Muschler GF. Bone graft materials: An overview of the basic science. Clin Orthop 2000;371:10–27. [PubMed: 10693546]
3. Boden SD, Martin GJ Jr, Morone M. The use of coralline hydroxyapatite with bone marrow, autogenous bone graft, or osteo-inductive bone protein extract for posterolateral lumbar spine fusion. Spine 1999;24:320–327. [PubMed: 10065514]
4. Bone Grafts and Bone Substitutes. Orthopaedic Network News 2000;11:8–9.
5. Burwell RG. The function of bone marrow in the incorporation of a bone graft. Clin Orthop 1985;200:125–141. [PubMed: 3905105]
6. Caplan AI. Mesenchymal stem cells. J Orthop Res 1991;9:641–650. [PubMed: 1870029]
7. Connolly J, Guse R, Lippiello L, Dehne R. Development of an osteogenic bone-marrow preparation. J Bone Joint Surg 1989;71A:684–691. [PubMed: 2732257]
8. Connolly JF, Guse R, Tiedeman J, Dehne R. Autologous marrow injection as a substitute for operative grafting of tibial nonunions. Clin Orthop 1991;266:259–270. [PubMed: 2019059]
9. Cornell CN, Lane JM, Chapman M. Multicenter trial of Collagraft as bone graft substitute. J Orthop Trauma 1991;5:1–8. [PubMed: 2023034]

10. Fleming JE Jr, Cornell CN, Muschler GF. Bone cells and matrices in orthopedic tissue engineering. Orthop Clin North Am 2000;31:357–374. [PubMed: 10882463]
11. Garg NK, Gaur S. Percutaneous autogenous bone-marrow grafting in congenital tibial pseudarthrosis. J Bone Joint Surg 1995;77B:830–831.
12. Garg NK, Gaur S, Sharma S. Percutaneous autogenous bone marrow grafting in 20 cases of ununited fracture. Acta Orthop Scand 1993;64:671–672. [PubMed: 8291415]
13. Healey JH, Zimmerman PA, McDonnell JM, Lane JM. Percutaneous bone marrow grafting of delayed union and nonunion in cancer patients. Clin Orthop 1990;256:280–285. [PubMed: 2364614]
14. Khan SN, Bostrom MP, Lane JM. Bone growth factors. Orthop Clin North Am 2000;31:375–388. [PubMed: 10882464]
15. Ludwig SC, Boden SD. Osteoinductive bone graft substitutes for spinal fusion: A basic science summary. Orthop Clin North Am 1999;30:635–645. [PubMed: 10471768]
16. Majors AK, Boehm CA, Nitto H, Midura RJ, Muschler GF. Characterization of human bone marrow stromal cells with respect to osteoblastic differentiation. J Orthop Res 1997;15:546–557. [PubMed: 9379264]
17. McCullagh P. Regression models for ordinal data (with discussion). J R Stat Soc 1980;42B:109–142.
18. Muschler, GF. Method of preparing a composite bone graft. US patent 5,824,084. 1998 Oct 20.
19. Muschler GF, Boehm C, Easley K. Aspiration to obtain osteoblast progenitor cells from human bone marrow: The influence of aspiration volume. J Bone Joint Surg 1997;79A:1699–1709. [PubMed: 9384430][Published erratum in J Bone Joint Surg 80A:302, 1998.]
20. Muschler GF, Huber B, Ullman T. Evaluation of bone-grafting materials in a new canine segmental spinal fusion model. J Orthop Res 1993;11:514–524. [PubMed: 8340824]
21. Muschler GF, Hyodo A, Manning T, Kambic H, Easley K. Evaluation of human bone morphogenetic protein 2 in a canine spinal fusion model. Clin Orthop 1994;308:229–240. [PubMed: 7955688]
22. Muschler, GF.; Lane, JM. Spine fusion: Principles of bone fusion. In: Herkowitz, HN.; Garfin, SR.; Balderston, RA., et al., editors. The Spine. WB Saunders; Philadelphia: 1999. p. 1573-1589.
23. Muschler GF, Midura RJ. Connective tissue progenitors: Practical concepts for clinical applications. Clin Orthop 2002;395:66–80. [PubMed: 11937867]
24. Muschler GF, Midura RJ, Nakamoto C. Practical modeling concepts for connective tissue stem cell and progenitor compartment kinetics. J Biomed Biotechnol 2003;2003:170–193. [PubMed: 12975533]
25. Muschler GF, Nakamoto C, Griffith L. Principles of clinical cell-based tissue engineering. J Bone Joint Surg 2004;86A:1541–1558. [PubMed: 15252108]
26. Muschler GF, Negami S, Hyodo A. Evaluation of collagen ceramic composite graft materials in a spinal fusion model. Clin Orthop 1996;328:250–260. [PubMed: 8653966]
27. Muschler GF, Nitto H, Boehm CA, Easley KA. Age- and gender-related changes in the cellularity of human bone marrow and the prevalence of osteoblastic progenitors. J Orthop Res 2001;19:117–125. [PubMed: 11332607]
28. Muschler GF, Nitto H, Matsukura Y. Spine fusion using cell matrix composites enriched in bone marrow-derived cells. Clin Orthop 2003;407:102–118. [PubMed: 12567137]
29. National Research Council. National Academy Press; Washington, DC: 1996. Guide for the Care and Use of Animals.
30. Ohgushi H, Goldberg VM, Caplan AI. Repair of bone defects with marrow cells and porous ceramic: Experiments in rats. Acta Orthop Scand 1989;60:334–339. [PubMed: 2665415]
31. Owen M, Friedenstein AJ. Stromal stem cells: marrow-derived osteogenic precursors. Ciba Found Symp 1988;136:42–60. [PubMed: 3068016]
32. Paley D, Young MC, Wiley AM, Fornasier VL, Jackson RW. Percutaneous bone marrow grafting of fractures and bony defects: An experimental study in rabbits. Clin Orthop 1986;208:300–312. [PubMed: 3522026]
33. Pittenger MF, Mackay AM, Beck SC. Multilineage potential of adult human mesenchymal stem cells. Science 1999;284:143–147. [PubMed: 10102814]

34. Ragni P, Lindholm TS, Lindholm TC. Vertebral fusion dynamics in the thoracic and lumbar spine induced by allogenic demineralized bone matrix combined with autogenous bone marrow: An experimental study in rabbits. Ital J Orthop Traumatol 1987;13:241–251. [PubMed: 3330547]

35. Takagi K, Urist MR. The role of bone marrow in bone morphogenetic protein-induced repair of femoral massive diaphyseal defects. Clin Orthop 1982;171:224–231. [PubMed: 6754199]

36. Tiedeman JJ, Connolly JF, Strates BS, Lippiello L. Treatment of nonunion by percutaneous injection of bone marrow and demineralized bone matrix: An experimental study in dogs. Clin Orthop 1991;268:294–302. [PubMed: 2060222]

37. Tiedeman JJ, Garvin KL, Kile TA, Connolly JF. The role of a composite, demineralized bone matrix and bone marrow in the treatment of osseous defects. Orthopedics 1995;18:1153–1158. [PubMed: 8749293]

38. Tiedeman JJ, Huurman WW, Connolly JF, Strates BS. Healing of a large nonossifying fibroma after grafting with bone matrix and marrow: A case report. Clin Orthop 1991;265:302–305. [PubMed: 2009671]

39. Villanueva JE, Nimni ME. Promotion of calvarial cell osteogenesis by endothelial cells. J Bone Miner Res 1990;5:733–739. [PubMed: 2396500]

0. Yasko AW, Lane JM, Fellinger EJ. The healing of segmental bone defects, induced by recombinant human bone morphogenetic protein (rhBMP-2): A radiographic, histological, and biomechanical study in rats. J Bone Joint Surg 1992;74A:659–670. [PubMed: 1378056][Published erratum in J Bone Joint Surg 74A:1111, 1992.]

41. Younger EM, Chapman MW. Morbidity at bone graft donor sites. J Orthop Trauma 1989;3:192–195. [PubMed: 2809818]

TABLE 1

Union Scores by Animal, Material, and Site

Animal	DCBP-Alone			DCBP + ABM			Enriched + ABM		
	L1–L2	*L3–L4*	*L5–L6*	*L1–L2*	*L3–L4*	*L5–L6*	*L1–L2*	*L3–L4*	*L5–L6*
1		0				2.0	0		
2			2.5	0				3.0	
3		3.5		2.5					4.0
4	0				4.0				4.0
5	0					0		0	
6	0				2.5				1.5
7	0					4.0		3.0	
8		0				0	0		
9		0		0					3.0
10			0		0		2.5		
11			0	0				4.0	
12			0		0.5		0		
Site subtotal	0	3.5	2.5	2.5	7.0	6.0	2.5	10.0	12.5
Total score		6.0			15.5			25.0	
Mean		0.5			1.3*			2.3†	
Median		0			0.3			2.1	

* = Significantly greater than DCBP-alone (p = 0.05)

† = Significantly greater than DCBP + ABM (p = 0.04) and DCBP-alone (p = 0.009).

TABLE 2

Mechanical Stiffness Data

Graft Material	Stiffness (N/mm)	
	Mean ± SD	95% CI
DCBP-alone (n = 12)	9.4 ± 3.3	6.1, 12.7
DCBP + ABM (n = 12)	11.0 ± 4.5	7.7, 14.3
Enriched + ABM (n = 12)	13.8 ± 7.7*	10.5, 17.1

* = Greater than the DCBP-alone group (p = 0.006) but not greater than the DCBP + ABM group (p = 0.06)

TABLE 3

Computed Tomography Data

Outcome	DCBP-Alone (n = 12)	DCBP + ABM	Enriched + ABM (n = 12)
Fusion volume (mm^3)	2260 ± 459	2624 ± 533*	2953 ± 616†
Fusion area (mm^2)	102 ± 28	121 ± 31‡	140 ± 38§
Bone density	1876 ± 54	1849 ± 42	1854 ± 47

* = Greater than the DCBP-alone group ($p < 0.01$)

† = Greater than the DCBP + ABM ($p = 0.02$) and DCBP-alone group ($p < 0.0001$)

‡ = Greater than the DCBP-alone group ($p < 0.04$)

§ = Greater than the DCBP + ABM ($p = 0.05$) and the DCBP-alone groups ($p = 0.005$)

TABLE 4

Concentration of Cells in Cortical Bone Powder

Dog Number	Cells (Pooled Heparinized Sample) (× 10^6/cc)	Cells (Nonheparinized Sample) (× 10^6)	Cells Loaded in Matrix (× 10^6)	Cell Retained in Matrix (× 10^6)	Efficiency of Cell Attachment (%)	Cells Retained in Matrix (× 10^6/cc)	Total Cells Implanted (× 10^6)	Fold Increase in Cells
1	72	108	725	125	17	83	233	2.2
2	117	176	648	58	9	39	234	1.3
3	88	132	600	131	22	87	263	2.0
4	80	120	661	185	28	123	305	2.5
5	74	111	630	156	25	104	267	2.4
6	76	115	642	92	14	61	207	1.8
7	78	117	632	218	34	145	335	2.9
8	84	126	627	98	16	65	224	1.8
9	88	132	600	139	23	93	271	2.1
10	68	102	704	164	23	109	266	2.6
11	64	96	677	212	31	141	308	3.2
12	82	123	600	195	33	130	318	2.6
Mean	81	122	646	148	23	99	269	2.3
SD	14	20	40	50	8	33	41	0.5

TABLE 5

Concentration of CTPs in Cortical Bone Powder

Dog Number	CTP (Pooled Heparinized Sample) CTPs/cc	CTP (Nonheparinized Sample) CTPs/cc	CTPs Loaded in Matrix CTPs/cc	CTPs Retained in Matrix CTPs/cc	Efficiency of CTP Attachment (%)	CTPs Retained in the Matrix CTPs/cc	Total CTPs Implanted CTPs/cc	Fold Increase in CTP	Selection Ratio CTPs vs Cells
1	2749	4123	87000	63990	74	42660	68113	16.5	4.3
2	5154	7731	28512	17302	61	11535	25033	3.2	6.8
3	3866	5799	72000	50426	70	33618	56225	9.7	3.2
4	9389	14084	77337	54489	70	36326	68573	4.9	2.5
5	3034	4551	25830	15402	60	10268	19953	4.4	2.4
6	2064	3096	17334	5234	30	3489	8330	2.7	2.1
7	9828	14742	79632	63072	79	42048	77814	5.3	2.3
8	8356	12534	62700	47882	76	31921	60416	4.8	4.9
9	4403	6605	30000	18014	60	12009	24619	3.7	2.6
10	3696	5544	38016	16416	43	10944	21960	4.0	1.9
11	2644	3966	27757	15667	56	10445	19633	5.0	1.8
12	4027	6041	29400	16035	55	10690	22076	3.7	1.7
Mean	4934	7401	47960	31994	61	21329	39395	5.6	3.0
SD	2717	4075	25523	21856	14	14570	24568	3.9	1.5

Techniques in Foot & Ankle Surgery 7(2):84–89, 2008

SPECIAL FOCUS

The Role of Intraoperative Bone Marrow Aspirate Stem Cell Concentration as a Bone Grafting Technique

Kimberly Jacobsen, MA, Karolynn Szczepanowski, MA, Loay A. Al-Zube, MSc, J. Kim, MSc, and Sheldon S. Lin, MD
Department of Orthopaedics
New Jersey Medical School
University of Medicine
and Dentistry of New Jersey
Newark, NJ

■ ABSTRACT

Despite the recapitulative nature of bone, a large percentage of nonunions still occur. Many exogenous substances have been administered to aid in the arthrodesis process, yet few have proven efficacious relative to time and cost. With recent advancements in bone biology involving cellular and molecular signaling, it is now possible to selectively retain bone progenitor cells from a patient's bone marrow. The commercially available product, Cellect™ Cellect selective cell retention device has gained attention for its fast and cost-effective intraoperative concentration of these bone progenitor cells from bone marrow aspirate. Application of this concentrate within a bone graft matrix of either tricalcium phosphate granules or demineralized bone matrix is a novel grafting technique that facilitates bony bridging of osseous defects.

Keywords: Cellect, selective cell retention (SCR), nonunions, graft matrix, mesenchymal stem cell

■ HISTORICAL PERSPECTIVE

Bone is a unique tissue due to its ability to both maintain regulatory metabolic turnover and regenerate due to injury. However, despite the recapitulative nature of bone, an increase of 46% of nonunions still may occur after long-bone fracture.[1] Although a variety of treatments are available to aid in osseous bridging due to these defects, few implants or techniques have been completely successful.

Several approaches have been used to elicit bone formation and promote bone healing. The standard technique used to facilitate the arthrodesis process is the application of autogenous bone graft. Iliac crest graft harvesting remains today's gold standard because autogenous graft is currently the only material that contains the 3 essential bone formation elements. However, autogenous bone graft (ABG) comes with significant costs.

Harvest is associated with significant clinical morbidity in terms of pain, scarring, increased surgical time, prolonged hospitalization, delayed rehabilitation, increased blood loss, increased risk of infection, and surgical complications (fracture, hematoma, neuroma, etc). A review of the literature reveals that complications arise in as many as 31% of the procedures, and 27% of patients undergoing ABG continue to feel pain at 24 months after surgery.[2] Often the quantity of available graft may be less than optimal. For these reasons, an impetus exists to develop and validate alternative graft processes that are capable of replicating the performance of the iliac crest graft while eliminating the associated complications.

Due to the rapidly advancing knowledge of bone biology, it is now possible to exploit the potential advantages that cellular and molecular expression information has to offer. The cellular events that allow bone healing to occur include chemoattraction, migration, proliferation, and differentiation. The mesenchymal stem cell (MSC) population is the fundamental ancestor of this assemblage.[3] Bone marrow is a milieu containing these unique progenitor cells that possess the ability to differentiate into bone, cartilage, tendon, and other connective tissues.[4] Using aspirative techniques with the aid of cell retention technology and an osteoconductive scaffold, surgeons are able to selectively choose bone progenitor cells and use their differentiation capacity in the presence of a nonunion for better bone healing.

Several experimental approaches have been used to elicit the formation of bone within defects and to promote

Address correspondence and reprint requests to Sheldon S. Lin, MD, Department of Orthopaedics, New Jersey Medical School, University of Medicine and Dentistry of New Jersey, 90 Bergen St, DOC 7300, Newark, NJ 07103. E-mail: linss@umdnj.edu.

their healing.[4–6] Methodology used in such studies has been based on a strategy of ex vivo expansion of pluripotent MSCs that are loaded into a carrier system. This approach is based on the hypothesis that such a technique decreases the need for osteoblast progenitor cell chemotaxis into the defect as well as need for massive proliferation. The potential benefits of direct osteogenic progenitor cell implantation lie within its potential to produce more rapid, uniform, and reliable bone defect healing.

A review of the literature of ex vivo expansion of autologous and allogenic stem cell augmentation has demonstrated favorable results. Bruder et al analyzed autologous MSCs isolated from bone marrow, grown in culture and loaded into porous ceramic cylinders consisting of hydroxyapatite (65%) and β-tricalcium phosphate (TCP) ceramic (35%) in canine segmental bone defect model. The results demonstrated significant effect of the stem cell augmentation. At 16 weeks, the atrophic nonunion occurred in all of the femora that had untreated defect, with small amount of trabecular bone at the cut ends. In contrast, radiographic union was established rapidly at the interface between the host bone and the implants loaded with MSCs. In the percentage of histological and morphometric analysis, which demonstrated that both woven and lamellar bone had filled the pores of the implants that had been loaded with MSCs, the amount of bone was significantly greater ($P < 0.05$) than that found in the pores of the implants that had not been loaded with cells.[7]

Arinzeh et al analyzed the application of allogenic MSCs in a critical-sized canine segmental defect. For defects treated with allogenic MSC implants, no adverse host response could be detected at any time point.[5]

Histologically, by 8 weeks, a callus spanned the length of the defect and lamellar bone filled the pores of the implant at the host bone-implant interface. At 16 weeks, new bone had formed throughout the implant. The results were consistent with those seen in implants loaded with autologous cells. Implants loaded with allogenic or autologous stem cells had significantly greater amounts of bone within the available pore space than did cell-free implants at 16 weeks ($P \leq 0.05$).[5]

Although the concept of ex vivo expansion of MSCs has demonstrated its potential clinical role in surgical arthrodesis, concerns regarding sterility issues and logistics of ex vivo expansion have led to lack of clinical acceptance.

The Cellect selective cell retention (SCR) system is a recently developed alternative to ex vivo expansion of MSCs for use in arthrodesis procedures. This intraoperative Cellect™ process uses a pioneering selective retention technology that consists of osteogenic progenitor cell concentration/augmentation, achieving a 3- to 4-fold increase in osteoprogenitor cell concentration using a minimally invasive approach at the time of surgery. Mesenchymal stem cells possess the unique ability to differentiate into a number of phenotypes. The stem cell activity and differentiation is regulated by a series of naturally occurring growth factors that guide them to form bone-producing cells.[8] The bone marrow is an ideal source of stem cells containing 2 primary stem cell lineages: hematopoietic and mesenchymal, the latter of which contains the potential to differentiate into the osteoprogenitor cell. Analysis of the bone marrow aspiration reveals that 50 million cells may be obtained in 2 mL of aspiration, of which only 1 per 20,000 cells being part of the osteoprogenitor lineage.[9] Therefore, the strategy behind this selective retention technology provides a rapid, safe, simple, and inexpensive method for intraoperative concentration and delivery of bone marrow–derived cells that may improve the outcome of bone grafting.

Few studies exist regarding the effect of MSC augmentation on bone repair. Kadiyala et al presented data regarding the application of bone graft prepared with SCR technology in canine defect model. Using the process described above, 4 different bone graft materials were evaluated: autologous bone, enriched SCR allograft matrix, allograft matrix saturated with whole bone marrow, and allogenic matrix alone. At 4 weeks, all samples of the enriched SCR matrix (100%) and autograft (100%) groups demonstrated early evidence of cortical bridging. At 16 weeks, only the enriched SCR matrix group and autograft group showed complete cortical bridging by radiograph and micro–computed tomography. In contrast, sites grafted with the allograft matrix alone (50%) or with bone marrow saturation (67%) consistently lagged in healing progression. This study exhibits the potential role of this intraoperative SCR process.[6]

An intraoperative iliac crest aspirate may be taken from a patient using an anterior or posterior approach. Alternatively, marrow may be aspirated from other locations such as the distal tibia or calcaneus. Allograft size requirements of varying volumes are easily accommodated because the bone marrow–seeded graft material is easily separated after being run through the selective retention device. Once the aspirate is isolated, prehydrated Conduit TCP granules or LifeNet CEL25 demineralized bone matrix.

(DBM) is loaded into the Cellect selective retention device. The marrow aspirate, in conjunction with heparin, is then added to this prehydrated matrix using a uniquely developed cartridge that aids in the selection of osteoblastic progenitor cells. The Conduit TCP granules are a synthetic porous ceramic graft material that closely mimics the mineral phase that comprises 70% bone. Conduit TCP is a scaffold that allows for neovascularization and is resorbed as normal bone healing progresses. The LifeNet CEL25 model uses a DBM cortical fiber/cancellous chip matrix.[10] Also used in

conjunction with heparin, this model incorporates DBM's osteoinductive and osteoconductive effects on growth factor expression. Both the Conduit and the Life-Net CEL25 work in conjunction with the Cellect selective retention device to create an osteogenic graft material that is rich in cells and void of many of the morbidities associated with standard ABG harvesting procedures.

Similar devices such as the Wright Medical IGNITE Power Mix and techniques such as the graft reaming technique have recently been introduced; however, neither of these methods serves to concentrate bone marrow osteoprogenitor cells. The IGNITE system uses a simil bone marrow aspirate coupled with DBM but does not use a mechanism to concentrate any type of bone marrow cell. Moreover, the graft reaming technique takes a combination of bone marrow and bone graft reaming, necessitating a larger incision and thus higher degree of morbidity. Once again, this reaming technique does not incorporate a means by which cells are concentrated. A fundamental advantage of the Cellect system is its ability to use a larger volume of bone marrow from which osteogenic progenitor cells are isolated before implantation with TCP or DBM matrix.

■ INDICATIONS AND CONTRAINDICATIONS

The cell retention model can be used for osseous defects that occur to the extremities, pelvis, and spine due to trauma or surgical intervention. The Cellect system is indicated for the delivery of autograft, allograft, or artificial bone graft at an osseous surgical site.

This system is not to be used in patients that have fractures of the growth plate, segmental defects, fractures with insufficient vascular supply proximal to graft site, infection at the site of injury, or insufficiency in soft tissue coverage. Metabolic bone disorders or systemic diseases that effect bone healing are also relatively contraindicated with this system. This system may be used concurrently with a rigid fixation device or contained osseous defect.

Cell retention technology is designed to be used in conjunction with heparin and may be associated with bleeding or thrombocytopenia. Therefore, this system should not be used in patients that have heparin hypersensitivity.

■ PREOPERATIVE PLANNING

Potential limitations are noted in patients who would have a low volume of concentrated stem cells, which may be due to the age and sex of the patient as well as to systemic diseases that may be present. The issue of the relationship between ''high risk'' patients and number of osteogenic progenitor cells contained within an aspirate sample is a ''double-edged sword'' because these are the patients who would ideally benefit from this procedure.

The aging bone shows decreases in both mass and strength.[11] Previous studies have documented a significant age-related decline in the number of nucleated cells harvested per aspirate for both men and women ($P = 0.002$).[12] These progenitor cells may therefore be lacking in both quality and quantity. These findings suggest that patients with age-related bone loss and postmenopausal osteoporosis may not provide adequate numbers of cells.

Furthermore, studies also suggest that patients with systemic complications due to corticosteroid use or alcohol abuse have decreased activity of bone marrow cells.[13] Likewise, patients who are managing chronic diseases such as diabetes mellitus are known to have a 40% decrease in DNA of collagen content of the callus, which correlates to callus cellularity.[14] This decrease in DNA callus cellularity may be indicative of decreased concentration of bone marrow aspirate and an individual assessment should be considered with such patients.

■ TECHNIQUE

The following protocol for bone marrow harvesting and utilization is from DePuy's manual for Cellect-Cell Capture Technology.[10] Either an anterior or posterior approach may be used to harvest the aspirate. For an anterior approach, manually palpate to locate the anterior superior iliac spine and make a 2-mm incision with a #11 blade. The initial trajectory should be medially in line with the pelvic wing as gauged by the inner and outer tables. The needle should be aimed posterior to the iliac tubercle for entry into the medullary canal just beneath it. Gently tap the needle into the cortex of the bone and use a mallet to further the needle in the bone. Either 1 or 3 aspiration holes with needles can be used.

The posterior approach uses the same incision size and blade, yet the surgeon needs to palpate the patient to locate the superior aspect of the posterior superior iliac spine. The initial trajectory approach is approximately 40 degrees lateral from the parasagittal plane and 35 to 40 degrees inferior from transverse plane. Gently tap the needle into the cortex of the bone and use the mallet to further drive the needle in further.

A single-needle approach should be advanced 1 cm through the trajectory where 2 mL of marrow can be aspirated. Then advance another centimeter to take another 2 mL of aspirate. Continue this procedure until the syringe is full.

A triple-needle approach may also be used using either the anterior or posterior approach. Once the cortex

has been penetrated, continue to advance the needle until all 3 aspiration holes are engaged. Continue to pull back on the plunger of the syringe until 6 mL of aspirate is retrieved. Advance the needles 3 cm to pull another 6 mL of aspirate out. Remove the full syringe and replace it with new one. With this method, the needle can be advanced approximately 5 to 7 mL parallel to the iliac crest.

The Cellect protocol has a specified heparin to marrow ratio. The syringe should be prefilled with heparin at a concentration of 1000 U/mL. A 12-mL marrow aspirate should be added to the heparin. The heparin to marrow aspirate is the same for both the Conduit TCP granule method and the LifeNet CEL25 DBM method.

The matrix of choice (either TCP or DBM) needs to be prehydrated with saline for 1 minute before dispensing the bone marrow into the cartridge. After prehydration of the matrix, the marrow is dispensed within the cartridge. The selective retention-device syringe pump is activated when the pump handles are depressed. Two cycles of depressing the device are needed. After activation, the clotting ports are opened, and the bone marrow (or platelet-rich plasma, available commercially) and heparin are added to the system. Visible saturation is critical before using the material. Wait 2 to 3 minutes before removing the graft from the cartridge for implantation into the defect. The selective stem cell matrix is now ready for clinical application.

■ POSTOPERATIVE MANAGEMENT

The postoperative management after this procedure and fixation is the same standard of care as for any

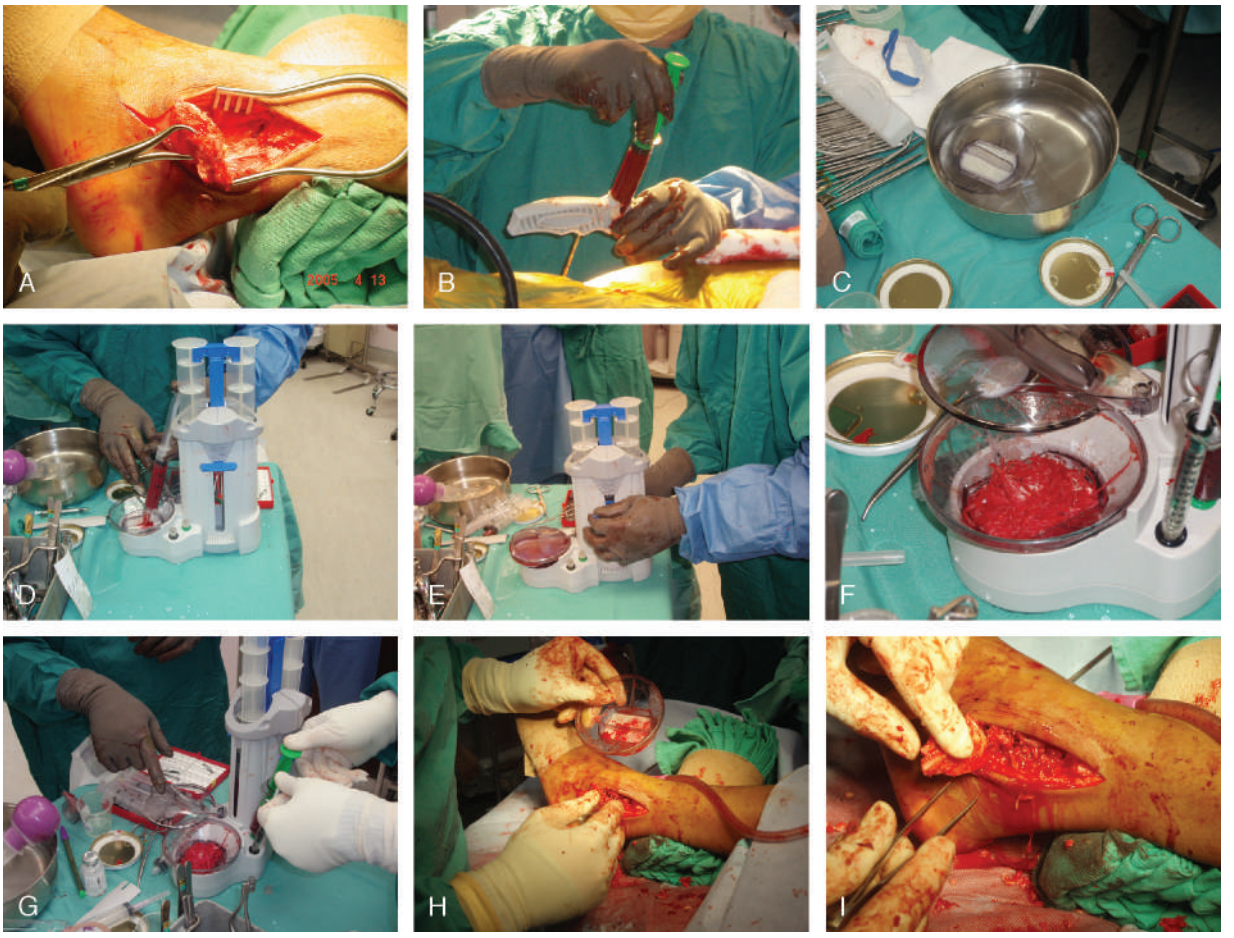

FIGURE 1. Intraoperative pictures: initial incision and fibular osteotomy (A), iliac crest bone marrow extraction (B), graft cartridge prehydration in saline (C), addition of bone marrow to prehydrated graft cartridge (now inserted into the Cellect selective retention device; D), handle depression (bone marrow filtration; E), close-up view of graft material (F), depression of "clotting syringes" (green: bone marrow + heparin, white: thrombin; G), implantation of graft material (H), and close-up view of implanted graft material (I).

other fracture or arthrodesis. Monitoring for infection, immobilization, and fixation of the bone is essential. This system should only be considered if a rigid fixation is used and soft tissue covering is sufficient.

CASE REPORT

A 44-year-old woman with sickle cell disease presents with avascular necrosis of the talus, leading to severe ankle arthritis. The patient undergoes ankle fusion using a lateral approach and fibula sparing technique. Due to the higher risk of nonunion secondary to avascular necrosis, the ankle fusion is performed using rigid internal fixation in conjunction with SCR via Cellect using LifeNet DBM graft (Fig. 1). See also preoperative and follow-up images (see Fig. 2).

POSSIBLE CONCERNS, FUTURE OF THE TECHNIQUE

The study of bone biology has allowed the exploitation of cellular and molecular markers for better bone healing. Through the use of intraoperative concentration of autologous bone marrow aspirate, we have decreased the morbidity of iliac graft harvesting, eliminated the disease transmission from allograft, and eliminated adverse immunologic reaction due to donor rejection.

Future directives for this procedure may involve the use of growth factor augmentation including osteoinductive agents such as bone morphogenetic proteins, angiogenic signaling, or platelet-derived growth factor to activate the stem cell–concentrated graft and complex. This may be accomplished through staged reconstruction that comprised 3 steps: (1) concentration of the bone marrow

FIGURE 2. Preoperative and postoperative x-rays. A–C, Anteroposterior, lateral, and oblique views of left ankle (preoperative) showing avascular necrosis and anterior osteophytes. D–F, Anteroposterior, lateral, and oblique views of left ankle (status postankle arthrodesis + Cellect SCR).

aspirate using the Cellect protocol, (2) expansion of the progenitor cells in vitro with growth factor augmentation, and (3) finally implanting the modified and expanded cell line into the osseous defect.

Cellect is one of several commercially available bone marrow aspirate stem cell systems. It has not been determined clearly if one system has clinically significant advantages over another. However, minor subtleties exist between the different brands in terms of aspiration kits, and the Cellect selective retention device offers the added component of a concentration mechanism of an osteogenic progenitor cell. The iliac crest carries the greatest number of mesenchymal pleuri potential cells, when compared to other areas that contain marrow.

■ ACKNOWLEDGMENTS

This work was supported by funding from DePuy Orthopaedics, Inc, a Johnson & Johnson Company.

■ REFERENCES

1. Sen MK, Miclau T. Autologous iliac crest bone graft: should it still be the gold standard for treating nonunions? *Injury*. 2007;38(Suppl 1):S75–S80.
2. Gupta AR. Perioperative and long-term complications of iliac crest bone graft harvesting for spinal surgery: a quantitative review of the literature. *Int Med J*. 2001;8: 163–166.
3. Kraus KH, Kirker-Head C. Mesenchymal stem cells and bone regeneration. *Vet Surg*. 2006;35:232–242.
4. Bruder SP, Jaiswal N, Ricalton NS, et al. Mesenchymal stem cells in osteobiology and applied bone regeneration. *Clin Orthop Relat Res*. 1998;355 Suppl:S247–S256.
5. Arinzeh TL, Peter SJ, Archambault MP, et al. Allogenic mesenchymal stem cell regenerate bone in a critical-sized canine segmental defect. *J Bone Joint Surg Am*. 2003;85A: 1927–1935.
6. Brodke D, Pedrozo HA, Kapur TA, et al. Bone grafts prepared with selective cell retention technology heal canine segmental defects as effectively as autograft. *J Orthop Res*. 2006;24(5):857–866.
7. Bruder SP, Kraus K, Goldberg V, et al. The effect of implants loaded with autologous mesenchymal stem cells on the healing of canine segmental bone defects. *J Bone Joint Surg Am*. 1998;80A:985–996.
8. Fleming JE, Muschler GF. The cell biology of bone tissue engineering. *Semin Arthroplasty*. 2002;13:143–157.
9. Muschler GF, Nitto H, Matsukura Y, et al. Spine fusion using cell matrix composites enriched in bone marrow derived cells. *Clin Orthop*. 2003;407:102–118.
10. Cellect®-Cell Capture Technology. DePuy, Johnson & Johnson Company. 2005–2006.
11. Quarto R, Thomas D, Liang CT. Bone progenitor cell deficits and the age-associated decline in bone repair capacity. *Calcif Tissue Int*. 1995;56:123–129.
12. Muschler GF, Nitto H, Boehm CA, et al. Age- and gender-related change In the cellularity of human bone marrow and the prevalence of osteoblastic progenitors. *J Orthop Res*. 2001;19:117–125.
13. Hernigou P, Beaujean F. Abnormalities in the bone marrow of the iliac crest in patients who have osteonecrosis secondary to corticosteroid therapy or alcohol abuse. *J Bone Joint Surg Am*. 1997;79:1047–1053.
14. Macey LR, Kana SM, Jingushi S, et al. Defects of early fracture-healing in experimental diabetes. *J Bone Joint Surg Am*. 1989;71:722–733.

Bone Grafts Prepared with Selective Cell Retention Technology Heal Canine Segmental Defects as Effectively as Autograft

Darrel Brodke,[1] Hugo A. Pedrozo,[2] Terri A. Kapur,[3] Mohamed Attawia,[3] Karl H. Kraus,[4] Chantal E. Holy,[3] Sudha Kadiyala,[3] Scott P. Bruder[3,5]

[1]Department of Orthopedics, University of Utah, Salt Lake City, Utah

[2]DePuy Inc, Warsaw, Indiana

[3]DePuy Spine Inc., Raynham, Massachusetts

[4]Tufts University School of Veterinary Medicine, North Grafton, Massachusetts

[5]Department of Orthopaedics, Case Western Reserve University, Cleveland, Ohio

Received 19 January 2005; accepted 9 September 2005

Published online 6 April 2006 in Wiley InterScience (www.interscience.wiley.com). DOI 10.1002/jor.20094

ABSTRACT: Using a canine critical-size segmental defect model, a two-phased study was undertaken to evaluate the healing efficacy of demineralized bone and cancellous chips (DBM-CC) enriched with osteoprogenitor cells using a Selective Cell Retention (SCR) technology. The goals of this study were: 1) to determine the bone-healing efficacy of SCR-enriched grafts versus autograft, and 2) to assess the value of clotting SCR-enriched grafts with platelet-rich plasma (PRP). Thirty dogs were included in Phase I: 18 dogs were treated with an SCR-enriched DBM-CC graft clotted with autologous bone marrow, and were compared to 12 autograft controls. In Phase II, 24 animals were divided into 4 groups of 6 animals, each treated with a different bone graft material: 1) iliac crest autograft, 2) DBM-CC alone, 3) DBM-CC saturated with marrow, and 4) SCR-enriched DBM-CC clotted with PRP. All grafts were placed unilaterally in a 21-mm long osteoperiosteal femoral, instrumented, critical-size defect. Radiographs were obtained for all animals postoperatively and every 4–16 weeks; animals were then sacrificed. All femurs were prepared for histology. Femurs in the Phase II study were also analyzed by micro-CT. At 16 weeks, healing—defined by bridging bone across the defects—was observed in 50% of the DBM-CC alone group and 67% of the DBM-CC saturated with marrow group; 100% of the autograft and SCR-enriched DBM-CC groups were healed. Histologically, grafts clotted with PRP showed more mature bone than those implanted with autologous bone, which in turn were similar to those implanted with bone marrow clotted SCR-enriched grafts. These results demonstrated that: 1) SCR-enriched DBM-CC was equivalent to autograft to repair critical-size defects, and 2) while not statistically significant, PRP may have accelerated bone maturation when used to clot osteoprogenitor-enriched DBM-CC grafts—as compared to cell-enriched, DBM-CC grafts without PRP—in large animal models. © 2006 Orthopaedic Research Society. Published by Wiley Periodicals, Inc. J Orthop Res 24:857–866, 2006

Keywords: osteoprogenitor cells; bone; critical-size defect; cell concentration

INTRODUCTION

Open surgical harvesting of autologous bone graft from the ilium is associated with significant post-operative morbidity.[1,2] Consequently, a concerted research and development effort is underway to evaluate alternative graft materials that obviate the requirement for harvesting autologous bone. A composite substrate mimicking the native characteristics and constituents of autologous bone may provide the most promising alternative graft material to harvested autograft. Specifically, autologous bone marrow has considerable appeal from a bone grafting standpoint because it provides live osteogenic cells and has the ability to effect de novo bone formation directly at the graft site.[3,4] More recently, the concept of grafting bone marrow-augmented composites has been refined with focus on concentrating the potent osteogenic precursor cells found in marrow and creating grafts with high concentrations of those specific cells. A novel Selective Cell Retention (SCR) method was developed as a result of these endeavors to enrich graft materials with osteoprogenitors.[5,6]

Correspondence to: Chantal E. Holy (Telephone: 508-828-3020; Fax: 508-828-3731; E-mail: choly@dpyus.inj.com)

The SCR method relies on the physical principles of an affinity column to populate a custom-designed graft matrix with a high proportion of osteoprogenitor cells found in bone marrow. The custom-design graft matrix is engineered to be highly porous and possess a high surface area for cell attachment. When marrow is passed through this matrix at an optimized, controlled flow, nucleated cells attach to the matrix while hematopoietic cells pass through. The result is a graft material that contains an increased concentration of nucleated, and more specifically, osteoprogenitor cells.[7] In this study, the SCR technology was assessed in a canine critical-size femoral defect. Graft materials were prepared by enriching a matrix composed of canine demineralized bone and cancellous chips (DBM-CC) with osteoprogenitor cells from autologous bone marrow. Controls included autograft and DBM-CC implanted alone or saturated with marrow.

MATERIALS AND METHODS

Study Design

Phase I

Thirty animals were divided into two treatment groups: Group I, autograft ($n = 12$); Group II, SCR-enriched DBM-CC clotted with marrow ($n = 18$). Defect sites were analyzed by x-ray at 0, 4, 8, 12, and 16 weeks postoperatively, at which point the animals were sacrificed and the femurs explanted and prepared for histology. The purpose of the Phase I was to evaluate whether SRC-enriched grafts were equivalent to autograft in a critical-size large-animal model. Large sample sizes were included to increase statistical relevance. Clotting was required to enhance the handling properties of the graft. Previous research also demonstrated superiority of clotted versus non-clotted cell-enriched grafts.[7]

Phase II

Twenty-four animals were randomized into four treatment groups ($n = 6$ per group): Group I, autograft; Group II, DBM-CC alone; Group III, DBM-CC saturated with marrow; Group IV, SCR-enriched DBM-CC clotted with platelet-rich plasma (PRP). Defect sites were analyzed by x-ray at 0, 4, 8, 12, and 16 weeks postoperatively, at which point the animals were sacrificed, the femurs were explanted and viewed by micro-CT. Femurs were further prepared for histology. The purpose of Phase II was to investigate the value-added of SCR-enriched technology by looking at whole marrow grafts as well as SCR-enriched grafts. The use of a PRP clot was also evaluated and bone formation using the PRP-clotted SCR-enriched DBM-CC was compared to that obtained using SCR-enriched DBM-CC clotted with bone marrow.

Surgical Procedure

Surgical Preparation

All procedures were performed under strict adherence to AAALAC International guidelines. Purpose-bred, female hounds were received either at Tufts University School of Veterinary Medicine (Phase I) or the Animal Research Center at the University of Utah (Phase II), housed for a minimum of 7 days, and food fasted for 24 h prior to the first procedure. Propofol (approximately 6 mg/kg) was administered via intravenous catheter to the cephalic vein for anesthesia induction. A 75-mcg Duragesic® patch was then applied to provide the animal with up to 72 h of pain relief postoperatively. The dogs were transferred to the surgical suite and positioned in ventral recumbancy. Isoflurane was initiated at approximately 2%. Intravenous fluids (0.9% NaCl) were given at an approximate rate of 10 mL/kg/h. The antibiotic Cefazolin® was added to the first liter of fluid at a dose of 20 mg/kg. An area over the lumbar sacroiliac junction including the iliac crests was shaved and aseptically prepped. An epidural of Duramorph (0.2 mg/kg) was given to provide 24 h of analgesia.

Bone Marrow Aspiration

Bone marrow aspiration on dogs assigned to Group II of Phase I and Groups III and IV of Phase II was performed using disposable Illinois aspiration needle (Kendal, Mansfield, MA) pre-filled with about 1 cc of heparin (1,000 U/mL). Bone marrow was aspirated from distinct locations of each iliac crest in 2-cc increments. Approximately 8–10 mL of marrow was drawn from the dogs in Group III of Phase II, while 20 mL of marrow was drawn from animals in Group II of Phase I and Group IV of Phase II.

Autograft

For dogs assigned to the autogenous study groups (Groups I in Phases I and II), the iliac crest rim was cut from the iliac crest and bone graft was harvested using a curette. The muscle and subcutaneous tissue were then closed over the iliac crest using a simple interrupted suture. The skin was closed using skin staples.

Preparation of Critical-Sized Defect

All dogs were then positioned in dorsal recumbancy. The surgical limb was suspended from an IV pole and aseptically prepped for surgery. A lateral approach to the femur between the biceps femoris muscle and vastus lateralis was made to expose the femur. An 8-hole, 4.5 mm × 135 mm lengthening plate (Synthes, West Chester, PA) was contoured to the bone. A 21-mm full thickness cortical defect was made at the mid-diaphysis of the bone using an oscillating bone saw. The lengthening plate was placed back on the femur and secured with the cortical screws. The defect was then filled with approximately 4 cc of appropriate graft

 DOI 10.1002/jor

materials, per randomization. Upon completion of the procedure, the muscle, fascia, and subcuticular layers were closed using 2–0 Vicryl in a simple continuous pattern. The skin was closed with skin staples.

Graft Preparation

SCR-Enriched DBM-CC (Group II of Phase I and Group IV of Phase II)

A custom-made SCR device was prepared specifically for this study. The device was made of a graft preparation chamber connected via plastic tubing to a syringe pump. Four cubic centimeters of a canine mixture of DBM and CC (obtained from Veterinary Transplant Services, Inc., Kent, WA) were placed in the graft preparation chamber. The cancellous chips were rongeured to sizes smaller than 2.5 mm. The demineralized bone powder was sieved to sizes less than 1,250 μm. The mix contained a 1:1 volume equivalent of dry CC and DBM. The DBM-CC mixtures were hydrated with saline for 1–2 min. The saline was then removed and replaced with the heparinized marrow. Approximately 20 cc of marrow were aspirated twice through the matrices at a rate of 4.3 mL/min. The DBM-CC was then ready for clotting with either marrow or PRP.

PRP Preparation

PRP was prepared as follows: 55 mL of autologous blood was centrifuged using Symphony PCS™ (DePuy Spine, Raynham, MA). Concentrated platelets were resuspended in platelet-poor plasma to create 10 mL of PRP.

Clotting of the Grafts

Clotting was achieved by mixing osteoprogenitor-enriched DBM-CC matrices with 0.4 mL of a $CaCl_2$ clotting solution with 4 mL of either PRP or autologous marrow.

DBM-CC Saturated With Marrow (Group III of Phase II)

Approximately 4 cc of DBM-CC was hydrated with 1–2 mL of saline. The saline was then replaced with 4 mL of marrow. The marrow/DBM-CC mixture was allowed to set for 5 min. Clotting was obtained by mixing the mixture with 1–2 mL of nonheparinized marrow and 0.1 mL of $CaCl_2$ clotting.

DBM-CC Alone

Approximately 4 cc of DBM-CC was hydrated with 5–7 mL of saline for 1–2 min prior to implantation.

肝素稀释六倍

凝块的制备

流速：5ml：33ml/m

骨粉和盐水的浓度：2：1—0.25

Inductivity Testing

DBM-CC was tested for osteoinductivity in an intramuscular athymic rat model. The test material was implanted in the hind limbs of four athymic rats, using protocols validated elsewhere.[8] Approximately 0.1 cc of DBM-CC was placed in between the muscle bands of the bicep femoris. At 6 weeks postsurgery, the rats were euthanized and the implants retrieved. Defect sites were fixed in 10% formalin and processed for histological evaluation.

肌内异位成骨

裸鼠观察指标 6周 组织学 0.1cc材料

Cellularity Testing

Nucleated cell counts were performed on all bone marrow samples after lysing red blood cells with 3% acetic acid, using protocols validated previously.[9] Five million nucleated cells from each marrow sample were then plated in a T-75 culture flask containing 20 mL of osteogenic differentiation media (DMEM + 10% fetal calf serum, 10 mM β-glycerophosphate, 100 nM dexamethasone, 50 μM ascorbic phosphate, and 1% penicillin-streptomycin). The flasks were incubated at 37°C, 5% CO_2, and media was changed every 4 days for 9–12 days or until colonies were visible. Cultures were then fixed and stained for alkaline phosphatase (AP) using Sigma's 86-R Alkaline Phosphatase kit (Sigma, St. Louis, MO). AP-stained colonies were manually counted (Olympus SZ40 dissecting microscope).

Radiographic Analyses

At 4, 8, 12, and 16 weeks, dogs were anesthetized via intravenous injection of Pentothal (approximately 25 mg/kg) in either cephalic vein. Radiographs of the operated leg were taken using a Siemens Mobilette Plus (HP6564020) device. X-ray exposure was maintained constant for all animals at 50 kV for 3.2 mAs. Following the 16-week radiograph, animals were euthanized with an intravenous injection of Beuthanasia D® (1 mL per 10 lb body weight). The implanted femur was harvested and the plate removed and replaced with a PMMA plate; femurs were then placed in 10% neutral buffered formalin.

Computed Tomography

The femurs were scanned with an EVS-R9 micro-CT scanner manufactured by Enhanced Vision Systems Corp (now part of General Electric Medical Systems, London, Ontario, Canada), at 50 kVp and 1 mA maximum tube current. Samples were scanned at an 80-μm voxel resolution with 2 × 2 or 4 × 4 binning in the detector panel.

Histology and Histomorphometric Analyses

Undecalcified samples were embedded in PMMA. Sagittal sections were performed along the fusion sites and through the transverse processes and stained with hematoxylin and eosin (H&E).

Histomorphometry

图像分析系统

Histomorphometry was performed using a Bioquant™ image analysis system. Two measurements were obtained for each slide: 1) percent de novo cortical bone formed; and 2) percent de novo medullary bone formed.

具体分析方法

Histopathology

Each slide was scored from 0 to 4 by an independent blinded pathologist (0 = no tissue; 1 = minimal; 2 = mild; 3 = moderate; and 4 = marked). The parameters evaluated were: 1) cortical bone connectivity within the defect, or the degree of newly formed bone, end-to-end; 2) cancellous bone connectivity, and 3) periosteal callus formation. This last score provided an estimate of the amount of periosteal reaction in the defect sites. These analyses were based on previously published bone histological reviews.[10]

RESULTS

DBM-CC Osterinductivity Testing in Rat Muscle Pouch

Tissue reactions to implants were mild with scattered areas of inflammatory cells and fibrosis. Calcification was observed in approximately 25% of the implant volume. Bone tissue was identified in 20% of the overall implanted volume.

Bone Marrow Cellularity

The nucleated cell content in the marrow samples ranged from 5.0 million cells/cc to 51.8 million cells/cc, with an average of 32.4 ± 14.6 million cells/cc. Osteoprogenitor cells were found at a frequency of 64.6 ± 30.2 cells per million nucleated cells. SCR-enriched graft contained on average 3.6 times more osteoprogenitor cells and 1.4 times more nucleated cells.

富集干细胞量2000个/ml

X-Ray Analyses

Autograft and both SCR-enriched DBM-CC groups resulted in a 100% healing. In contrast, 67% of the defects filled with DBM-CC saturated with marrow and 50% of the defects filled with DBM-CC alone showed evidences of bridging bone (Fig. 1). In the autograft groups, all animals showed radiographic evidences of cortical bone formation and remodeling by 16 weeks. Complete osteointegration of the cut ends with de novo bone tissue was observed in all samples. In some instances, underfill of the grafted area, evidenced by a concave bone formation under the plate was observed and was indicative of stress shielding (Fig. 2a,b). Similarly, all the SCR-enriched DBM-CC samples showed radiographic evidence of cortical bone formation and remodeling at 16 weeks. No difference in bone formation between the SCR-enriched PRP-clotted grafts and the SCR-enriched marrow clotted grafts could be observed by X-ray (Fig. 2c,d). In the DBM-CC saturated with marrow group, four of the six defects healed at 16 weeks. In some of the fused samples, the cut ends of the defects were still clearly visible (Fig. 2e,f). Stress shielding was observed in three of the four healed defects.

Half of the defects filled with DBM-CC alone healed at 16 weeks. Bone formation patterns within the fused samples varied significantly: in one case, radio-opacity was most dense within the medullary canal, with clear stress shielding effect

sion rates for all groups

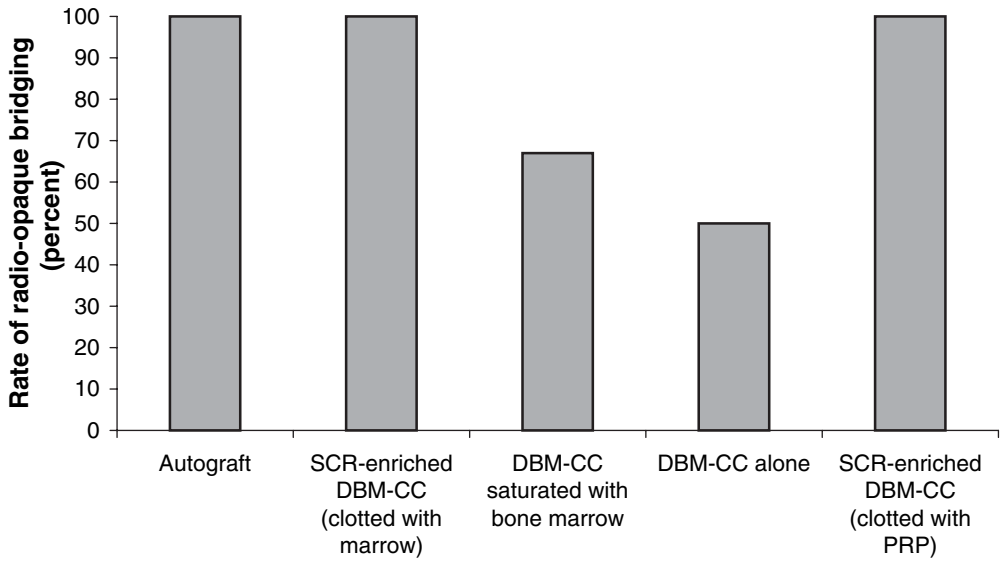

Figure 1. Graph of radiographic bridging rates at 16-weeks postoperative, for all treatment groups.

DOI 10.1002/jor

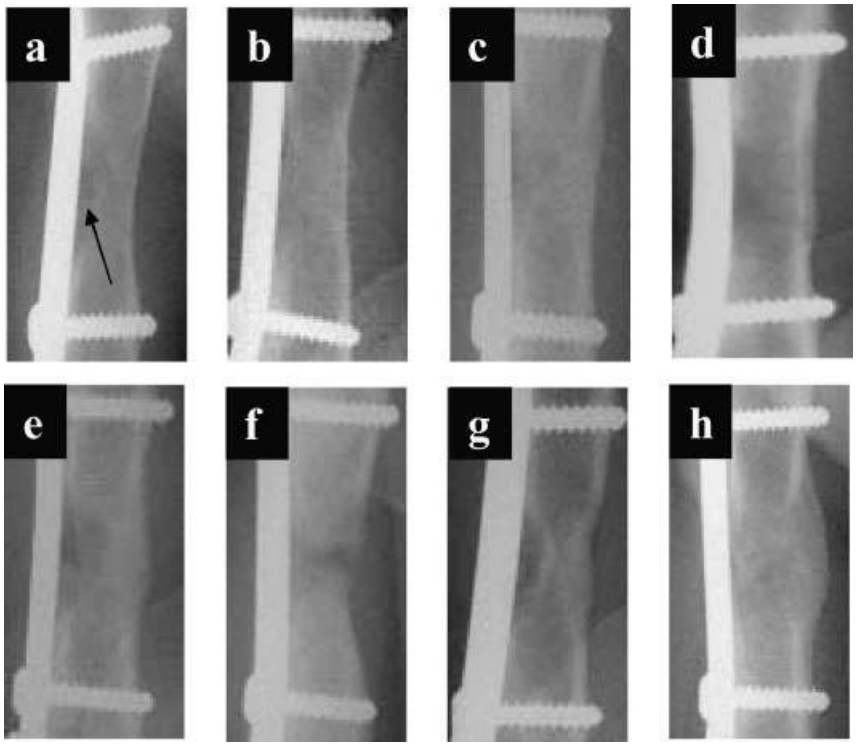

Figure 2. Representative x-rays of defect sites, at 16-weeks postoperative. (a,b) Autograft-treated defects. Stress shielding is indicated by arrow in (a). (c) Defect grafted with SCR-enriched DBM-CC, clotted with PRP. Defect grafted with SCR-enriched DBM-CC, clotted with marrow. (e,f) Defects filled with DBM-CC saturated with marrow. (g) Defect grafted with DBM-CC alone. (h) Defect grafted with DBM-CC alone.

resulting in an underfill of the bone defect under the plate (Fig. 2g). In another fused sample, radio-opaque tissue was observed in both the medullary canal and the cortical area (Fig. 2g,h).

Samples were also analyzed for radio-opaque bridging at the various time points (Fig. 3). All sites filled with autograft showed radio-opacity throughout the defects at 4 weeks. SCR-enriched DBM-CC clotted with PRP followed with 60% bridging sites at 4 weeks and 100% bridging by 8 weeks. A slower rate of bone formation was observed with SCR-enriched DBM-CC clotted with bone marrow, for which 100% bridging was observed at 12 weeks. DBM-CC alone and DBM-CC with bone marrow showed increases in bridging rates between 4 and 8 weeks, with slower increases in bridging rates thereafter.

Micro-CT Analyses

Micro-CT analyses confirmed the x-ray results in terms of overall healing rates for all investigated groups. Micro-CTs were also used to visualize the architecture of the newly formed bone. In the autograft group, bony trabeculae were observed in the medullary cavity of all samples. A denser, cortical rim was also visible in most cases. The stress shielding effect described above was clearly visible in some cases, where the cortical rim on the plated side was relatively thin (Fig. 4a,b). Defects filled with SCR-enriched DBM-CC clotted with PRP showed similar bone architecture as autograft (Fig. 4c,d). In the marrow-saturated DBM-CC group, dense, woven-like bone structure was sometimes observed within the marrow cavity (Fig. 4e,f). In contrast, de novo bone formation in the DBM-CC alone group differed significantly from one femur to another, with scattered, irregular bone fragments spanning the length of the defects (Fig. 4g,h).

Histological Evaluations

While not statistically significant, percent mean cortical bone formation was highest in the PRP-clotted SCR-enriched DBM-CC group, followed by the marrow clotted SCR-enriched DBM-CC group and the autograft groups (Table 1). Similarly, cortical bone connectivity was highest in the PRP-clotted cell-enriched group (Fig. 5).

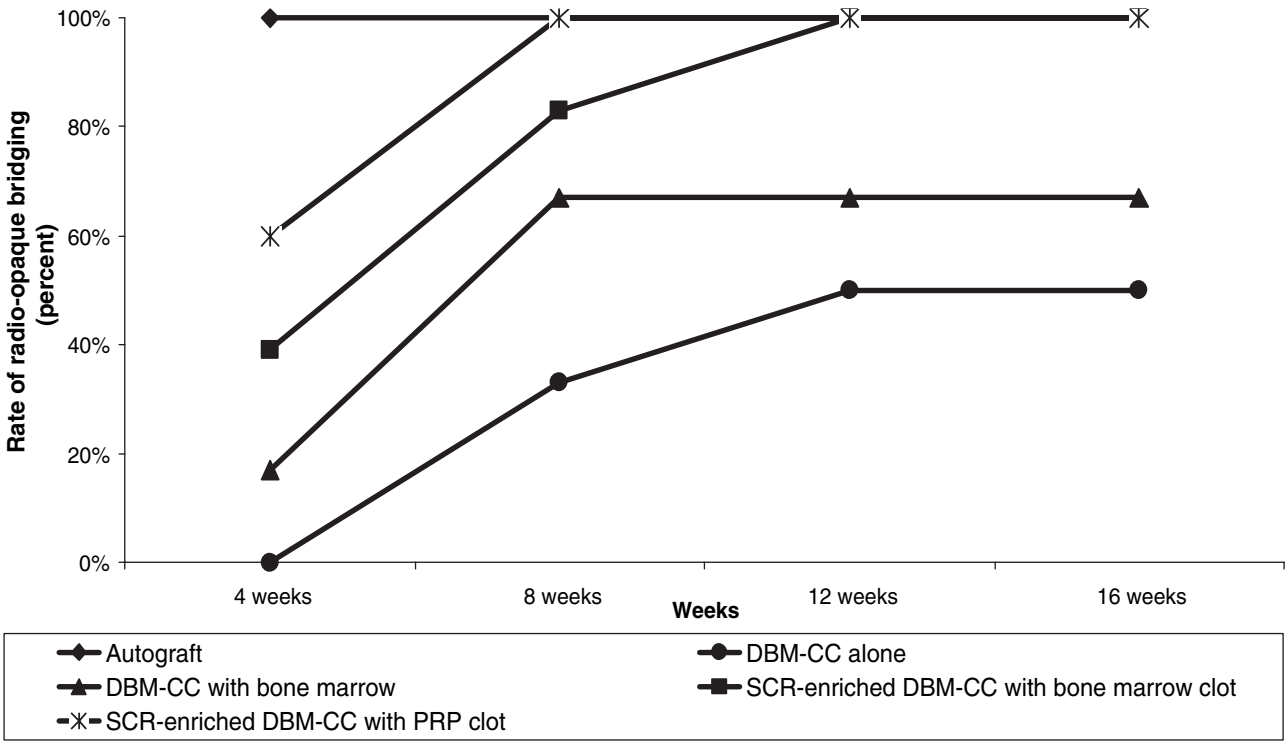

Figure 3. Graph of radio-opaque bridging rates by treatment group, as a function of time. At 4 weeks, some level of radio-opaque bridging was observed in all autograft cases; however, this radio-opacity may be due to implanted material and not to newly formed bone.

DISCUSSION

A canine critical-size femoral segmental defect was used herein to compare the bone-healing efficacy of SCR-enriched graft materials compared to autologous bone. This model provides a challenging environment to evaluate bone grafts in a large defect and therefore mimics clinical conditions where significant volumes of bone tissue are lost. Because of its clinical relevance, this model has been extensively used.[11–13] In this study, graft materials were prepared that simulated the environment provided by autologous bone. Autologous bone was previously shown to present three key attributes: 1) chemical and physical surface properties that favored osteogenic cell attachment and migration, also referred to as osteoconductivity; 2) embedded growth factors and bone morphogens that stimulate cell differentiation into osteoblasts, also referred to as osteoinductivity; and 3) a pool of osteogenic cells, capable of differentiating into mature osteoblasts, also referred to as osteogenicity. These three attributes are currently believed to play key roles in autograft bone healing.[14] It was therefore hypothesized herein that graft materials that would combine all three attributes might have a similar bone-forming potential to autograft.

All test materials contained allogeneic cancellous chips (CC), a proven osteoconductive substrate,[15] with demineralized bone fibers (DBM). These bone fibers played two major roles: 1) to provide osteoinductive agents; and 2) to confer a 3-D geometry to the grafts. The osteoinductivity of the DBM-CC grafts was tested in a rat muscle pouch. New bone formation in these non-orthotopic sites demonstrated that bone morphogens and/or growth factors embedded in the DBM fibers were osteoinductive.

The role of osteogenic cells added to graft materials prior to implantation was tested herein using autologous marrow. The use of marrow to augment grafts was described in numerous preclinical and clinical applications; in all cases, the addition of marrow to graft materials increased the bone-forming efficacy of those graft materials.[4,7,16] Recently, marrow aspiration techniques were also optimized for increased cellular content. These techniques specified that only small (<2 cc) samples of marrow be aspirated from a given site.[5] This technique was utilized in this study to maximize the cellular content of the canine marrow aspirates.

 DOI 10.1002/jor

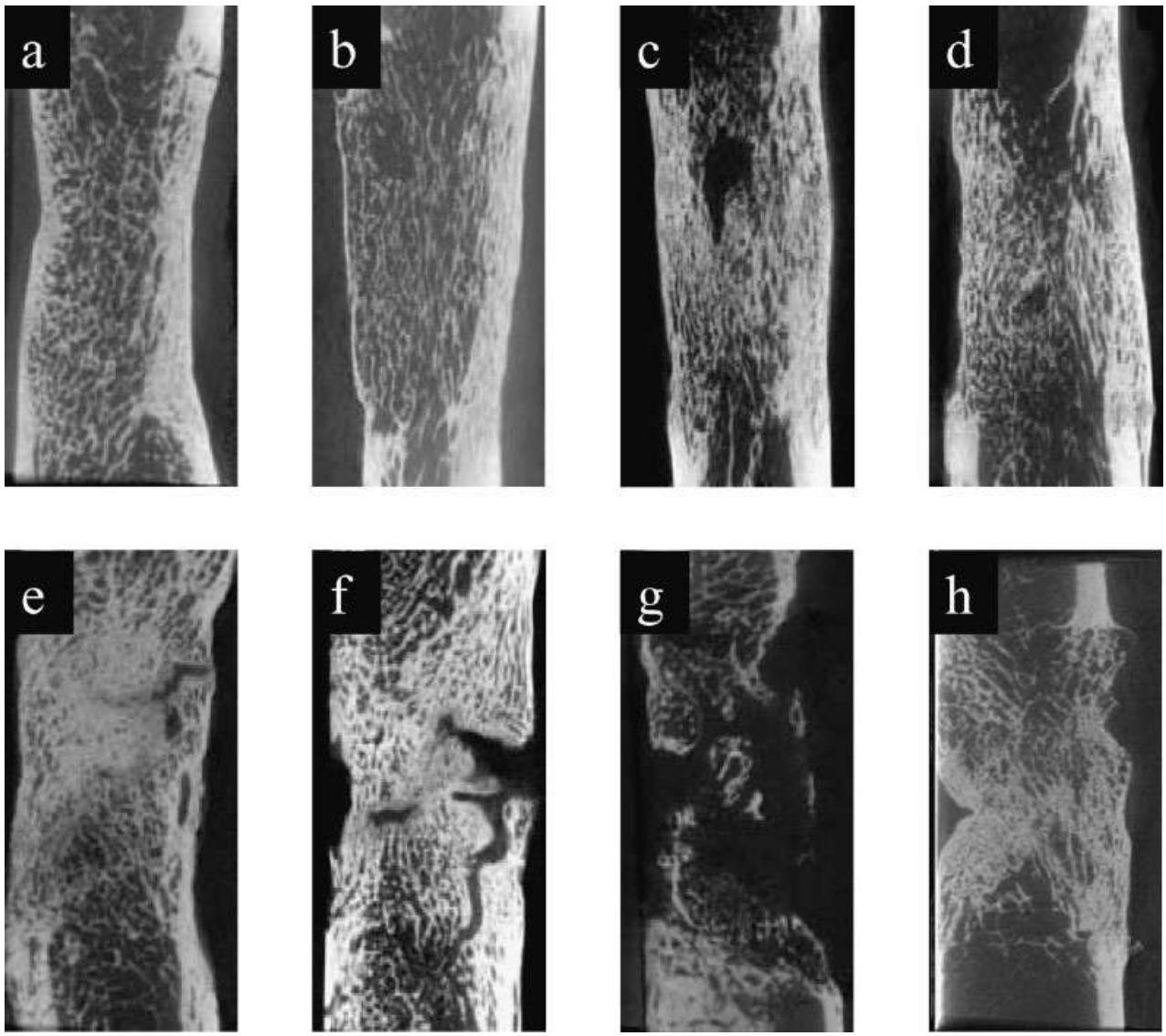

Figure 4. Representative micro-CT sagittal views, at 16-weeks postoperative. (a,b) Defects filled with autograft. (c,d) Defects filled with SCR-enriched DBM-CC, clotted with PRP. (e,f) Defects filled with DBM-CC saturated with marrow, with areas of dense woven bone visible throughout the defect sites. (g,h) Defects filled with DBM-CC alone, showing significant underfill areas due to uneven bone regeneration (g).

The value of augmenting grafts with marrow was tested using the following grafts: 1) DBM-CC alone; and 2) DBM-CC saturated with marrow. Radiographic and micro-CT analyses revealed higher incidences of bridging bone in the marrow group (67%) as compared to the DBM-CC alone group (50%). In addition, micro-CT sections revealed a more uniform bone formation pattern in the marrow group versus DBM-CC alone. These observations were further confirmed by histology, where trends of increased de novo bone volumes were observed in the marrow group as compared to the DBM-CC alone group. These results confirmed previous preclinical studies that demonstrated the benefit of marrow for bone regeneration in large animal models.[16]

While marrow enhanced the bone-forming efficacy of grafts, DBM-CC saturated with marrow was not equivalent to autograft. Two reasons were likely to explain this observation: 1) a lower osteoprogenitor cell density in the DBM-CC with marrow versus autograft; and 2) a lower osteoinductivity of the DBM with marrow versus autograft. Autograft was shown to contain two sources

Table 1. Radiological and Histological Results Obtained for All Treatment Groups

Groups	Percent Fusion		Histological Analyses[a]				
	X-Ray Analyses	Micro-CT Analyses	Percent Cortical Bone	Percent Medullary Bone	Cortical Connectivity Score (1–4)	Cancellous Connectivity Score (1–4)	Periosteal Callus Formation Score (1–4)
Autograft	100	100	29.3 ± 17.5	43.0 ± 16.6	2.8 ± 0.7	2.9 ± 0.8	0.8 ± 1.3
SCR-enriched DBM-CC clotted with PRP	100	100	43.0 ± 8.6	54.4 ± 12.0	3.0 ± 1.2	2.9 ± 1.1	0.7 ± 0.6
SCR-enriched DBM-CC clotted with marrow	100	100	43.5 ± 13.9	46.2 ± 14.4	1.5 ± 1.3	1.6 ± 1.3	2.0 ± 0.8
DBM-CC saturated with marrow	67	67	45.3 ± 18.4	46.7 ± 18.5	2.2 ± 1.3	1.5 ± 1.7	1.6 ± 0.9
DBM-CC alone 50	50	50	30.5 ± 12.7[b]	31.7 ± 15.4[b]	1.4 ± 1.0	1.0 ± 1.5	1.1 ± 1.0

SCR, Selective Cell Retention; DBM-CC, demineralized bone and cancellous chips; PRP, platelet-rich plasma; CT, computed tomography.
[a]Histological evaluations performed on two adjacent slides per bone.
[b]Statistically significant vs. autograft, SCR-enriched DBM-CC clotted with PRP and SCR-enriched DBM-CC clotted with marrow ($p < 0.05$).

of osteoprogenitors, each contributing to de novo bone formation: 1) osteoprogenitors in suspension in the marrow these cells are primarily responsible for new bone formation; and 2) osteoprogenitors attached on bony surfaces, whose efficacy in new bone formation still remains to be demonstrated. As a result, the number of osteoprogenitors in the marrow group was probably lower than that contained in autografts. The difference in osteoinductivity between both groups was not tested herein.

In order to address the difference in osteogenicity between DBM-CC saturated with marrow and autologous bone, the SCR technology was used to increase the osteoprogenitor content of the DBM-CC grafts by three- to fourfold. The effect of enriching grafts with the SCR technology was shown by comparing the grafts: 1) DBM-CC saturated with marrow; 2) SCR-enriched DBM-CC clotted with marrow; and 3) autograft.

Bone marrow-derived cells have mainly been used in two different ways within the scientific literature, as part of a whole bone marrow aspirate, as observed in Group III of Phase II, or isolated and culture-expanded.[11,17] While culture-expansion of mesenchymal stem cells has shown to provide excellent results in vivo, significant cost and safety issues have reduced the market potential for this specific technique. In this article, we therefore focused on cell concentration methods that would be feasible in an operating room setting and would not require costly cell culture conditions.

Overall radiographic evidence showed that, at 16 weeks, all animals treated with the SCR technology healed, while only 67% of the DBM-CC marrow group healed. This fact was confirmed by histological observations that showed more cortical bone formation in the SCR-enriched group versus marrow group. Two major conclusions could be drawn from these facts: 1) enriching the osteoprogenitor content of grafts by three-to-four times increased the bone-forming potential of DBM-CC; 2) enriched grafts performed similarly to autograft, in this model.

Previous work evaluating culture-expanded mesenchymal stem cells in canine defects also resulted in 100% fusion rate, as observed herein. These studies included grafts that may have contained about 3,600 times the native osteoprogenitor cell level (based on total number of cells implanted by Arinzeh et al.[11] versus total number of osteoprogenitor cells found in native levels of bone marrow, as observed in this research). Compared to the SCR-enriched cell grafts, culture-expanded graft contained therefore roughly

DOI 10.1002/jor

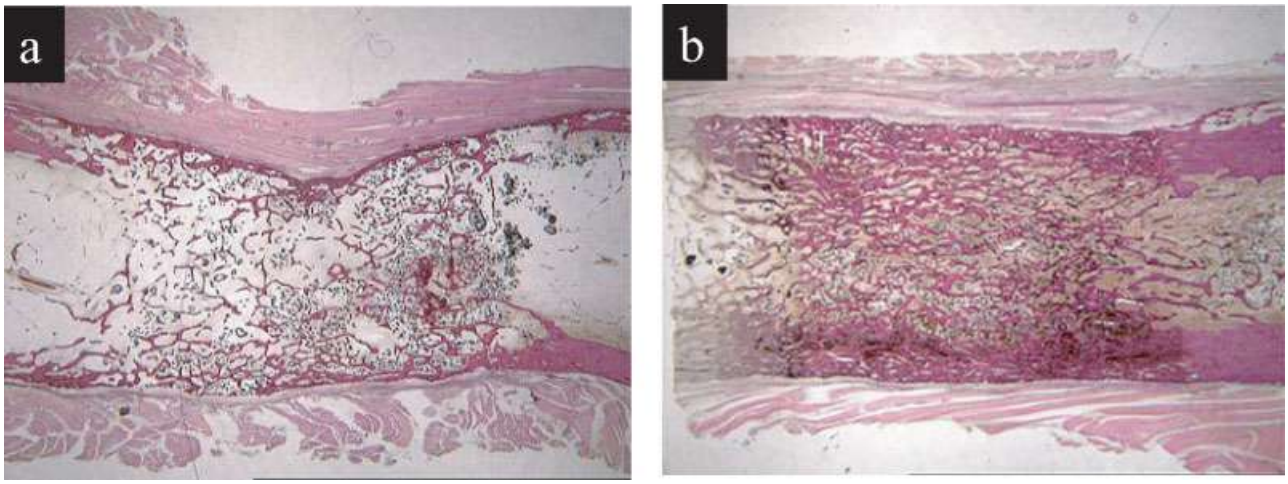

Figure 5. Histological micrograph of defects filled with (a) autograft and (b) SCR-enriched DBM-CC clotted with PRP (original magnification, ×5).

1,000 times more cells. Nevertheless, in this particular animal model, similar bone healing was observed using either a three-to-four times cell concentration or a 3,600-times culture-expanded cell solution. In culture-expanded cell constructs, it is noteworthy to observe that cells are isolated from the native bone marrow environment, which may also influence overall healing. These results indicate that, when preserving the bone marrow environment with all its undefined plasma content on an optimized carrier as used herein, a three-to-four time cell concentration was sufficient to allow for bone healing in this animal model.

Looking at the rate of bone formation, autograft was first seen to show 100% bridging radio-opacity in this model. However, it is very likely that a significant amount of the radio-opacity observed at 4 weeks was due to implanted material and not to de novo bone formation. No meaningful conclusions on the rate of bone formation using autograft versus SCR-enriched grafts could therefore be reached.

Finally, the role of PRP with SCR-enriched matrices was evaluated. Canine PRP, obtained using the Symphony device as described in the Materials and Methods section, was tested for platelet yield, platelet viability, and TGF-β1 content by Kevy and Jacobson, for a different study. Briefly, 76.2 ± 19.4% platelet retention was obtained, containing 75.5 ± 17.9 μg/μL TGF-β1.[18] In this current study, PRP served two roles: 1) it provided a method of clotting the DBM-CC, to increase the handling properties of the final grafts; and 2) it increased growth factor concentrations at the defect sites. Growth factors contained in PRP were shown previously to act as a chemo-attractant,[19] increase cell proliferation, and improve bone matrix formation, but did not affect cell differentiation. The role of PRP was assessed by comparing the following test materials: 1) SCR-enriched DBM-CC clotted with marrow; 2) autograft, and 3) SCR-enriched DBM-CC clotted with PRP. Radiographically, all three groups resulted in 100% healing rate. Histologically, high ratios of cortical bone formation and low levels of fibrous ingrowth were observed in all cases. However, histological observations also revealed a more mature bone formation in the PRP clotted grafts as compared to the autograft group, which was similar to the marrow-clotted SCR-enriched group. While not statistically significant, this result highlighted a potentially favorable effect of PRP on bone healing and is consistent with some of the previously published data that indicated trends of accelerated bone formation in PRP-grafted bone sites.[20] It is important to note that specific care was given herein in the preparation of the PRP to maintain cell viability and ensure a concentration range of growth factor within previously described optimal ranges.[21] This is particularly relevant since recent studies demonstrated that all PRPs are not created equal, and that PRP prepared in systems that may use high mechanical stress and affect platelet viability may not be effective.[22]

In conclusion, this research demonstrated that graft materials could be enriched with osteoprogenitor cells using intraoperative technologies. These cell-enriched grafts were more efficient than grafts saturated with marrow and as efficient as autograft in repairing critical-sized defects in a

血小板滞留问题

large animal model. In addition, while not statistically significant, bone maturation within the defects may have been accelerated when the SCR-enriched grafts were clotted with autologous PRP. These results indicate that SCR-enriched grafts are a viable alternative to autologous bone for the repair of large, critical-sized defects.

ACKNOWLEDGMENTS

This study was funded by DePuy Spine. Dr Brodke is a paid consultant for DePuy. Research funds were provided to Dr Kraus to perform the study. All other authors are DePuy employees. We would also like to acknowledge Dr Manuel Jayo for histomorphometric and histopathological analyses and David Malmstrom for surgical expertise.

REFERENCES

1. Fernyhough JC, Schimandle JJ, Weigel MC. 1992. Chronic donor site pain complicating bone graft harvesting from the posterior iliac crest for spinal fusion. Spine 17:1474–1480.
2. Gupta AR, Shah NR, Patel TC, et al. 2001. Perioperative and long-term complications of iliac crest bone graft harvesting for spinal surgery: a quantitative review of the literature. Int Med J 8:163–166.
3. Burwell RG. 1985. The function of marrow in the incorporation of a bone graft. Clin Orthop 200:125–141.
4. Connolly JF. 1998. Clinical use of marrow osteoprogenitor cells to stimulate osteogenesis. Clin Orthop 355(Suppl): S257–S266.
5. Muschler GF, Boehm C, Easley K. 1997. Aspiration to obtain osteoblast progenitor cells from human bone marrow: the influence of aspiration volume. J Bone Joint Surg [Am] 79:1699–1709.
6. Muschler GF, Midura RJ. 2002. Connective tissue progenitors: practical concepts for clinical applications. Clin Orthop 395:66–80.
7. Muschler GF, Nitto H, Matsukura Y, et al. 2003. Spine fusion using cell matrix composites enriched in bone marrow-derived cells. Clin Orthop 407:102–118.
8. Cole BJ, Bostrom MPG, Pritchard TL, et al. 1997. Use of bone morphogenetic protein 2 on ectopic porous coated implants in the rat. Clin Orthop 345:219–228.
9. Jaiswal N, Haynesworth SE, Caplan AI, et al. 1997. Osteogenic differentiation of purified, culture-expanded human mesenchymal stem cells in vitro. J Cell Biochem 64:295–312.
10. Schmidmaier G, Wildemann B, Cromme F, et al. 2002. Bone morphogenetic protein-2 coating of titanium implants increases biomechanical strength and accelerates bone remodeling in fracture treatment: a biomechanical and histological study in rats. Bone 30:816–822.
11. Arinzeh TL, Peter SJ, Archambault MP, et al. 2003. Allogeneic mesenchymal stem cells regenerate bone in a critical-sized canine segmental defect. J Bone Joint Surg [Am] 85A:1927–1935.
12. Kadiyala S, Young RG, Thiede MA, et al. 1997. Culture expanded canine mesenchymal stem cells possess osteochondrogenic potential in vivo and in vitro. Cell Transplant 6:125–134.
13. Kraus KH, Kadiyala S, Wotton H, et al. 1999. Critically sized osteo-periosteal femoral defects: a dog model. J Invest Surg 12:115–124.
14. Bruder SP, Fox BS. 1999. Tissue engineering of bone. Cell based strategies. Clin Orthop 367(Suppl):S68–S83.
15. Cornell CN, Lane JM. 1998. Current understanding of osteoconduction in bone regeneration. Clin Orthop 355 (Suppl):S267–S273.
16. Den Boer FC, Wippermann BW, Blokhuis TJ. 2003. Healing of segmental bone defects with granular porous hydroxyapatite augmented with recombinent human OP-1 or autologous bone marrow. J Orthop Res 21:521–528.
17. Bruder SP, Jaiswal N, Ricalton NS, et al. 1998. MSCs in osteobiology and applied bone regeneration. Clin Orthop 355(Suppl):S247–S256.
18. Kevy SV, Jacobson MS. 2004. Concentrated autologous bone marrow stem cells and platelets for bone grafting in dogs. Proc ACVS, Denver, CO.
19. Oprea WE, Karp JM, Hosseini MM, et al. 2003. Effect of platelet releasate on bone cell migration and recruitment in vitro. J Craniofac Surg 14:292–300.
20. Marx RE, Carlson ER, Eichstaedt RM, et al. 1998. Platelet-rich plasma: growth factor enhancement for bone grafts. Oral Surg Oral Med Oral Pathol Oral Radiol Endod 85: 638–646.
21. Marx RE. 2001. Platelet rich plasma (PRP); what is PRP and what is not PRP. Implant Dentistry 10:225–228.
22. Weiner BK, Walker M. 2004. Efficacy of autologous growth factors in lumbar intertransverse fusions. Spine 28:1968–1971.

Cell Therapy for Secondary Osteonecrosis of the Femoral Condyles Using the Cellect DBM System

A Preliminary Report

Kevin Lee, MD, FRCS,* and Stuart B. Goodman, MD, PhD*†

Abstract: We describe a novel treatment of secondary osteonecrosis (ON) of the femoral condyles that is relatively simple, has low morbidity, and does not preclude the patient from other more extensive treatments in the event of failure. Three patients with extensive secondary ON of the femoral condyles were treated with decompression and debridement of the area of ON and grafting with the Cellect DBM System (Depuy Spine, Inc., Raynham, Mass), which provided a graft matrix enriched with a 3-fold to 4-fold increase in osteoprogenitor cells. At 2 years, all 3 patients had no complications and had excellent results with near-normal function and activity levels. Our preliminary results demonstrate that this technique is a viable option, at least in the short term, especially in patients with extensive, multifocal lesions.
Key words: secondary osteonecrosis, femoral condyles, osteoprogenitor, stem cells, demineralized bone, matrix.

Osteonecrosis (ON) of the femoral condyle is a well-described condition [1] that refers to 2 separate disorders: spontaneous and secondary ON [2,3]. Secondary ON, in distinction to the spontaneous type, usually occurs in patients younger than 45 years and has a rather insidious onset; and the lesions are usually bilateral, multifocal, and more extensive. There is usually a strong association with conditions such as steroid therapy, alcohol abuse, and systemic lupus erythematosus. Therefore, any treatment of this specific group of patients must take into account their young age, high activity levels, immunosuppression, multifocality, and large size of lesions, as well as probable involvement of other joints. The treatment will most likely be one that "buys time" for the patient and ideally should have minimal morbidity and not preclude the patient from other forms of intervention in case of failure. Our technique combines decompression and debridement of the necrotic lesion with the use of the Cellect DBM System (Depuy Spine, Inc., Raynham, Mass) that enables the mixing of autologous bone marrow harvested from the anterior iliac crest with demineralized bone matrix (DBM) and allograft chips, resulting in a graft matrix enriched with a 3-fold to 4-fold increase in osteoprogenitor cells [4]. Several studies have shown the positive effect of increased cell concentration on bone regeneration [4-7].

*From the *National University Hospital of Singapore; and †Department of Orthopaedic Surgery, Stanford University School of Medicine, Stanford, California.*
Submitted October 4, 2007; accepted January 6, 2008.
No benefits or funds were received in support of the study.
Reprint requests: Stuart B Goodman, MD, PhD, Department of Orthopaedic Surgery #R153, Stanford University Medical Center, 300 Pasteur Drive, Stanford, CA 94305-5326.

0883-5403/08/2401-0008$36.00/0
doi:10.1016/j.arth.2008.01.133

Materials and Methods

This is a preliminary review of the short-term results (2 years) of 3 patients with secondary ON

of the femoral condyles who were treated with decompression, debridement, and grafting with the Cellect DBM System. All 3 patients underwent a diagnostic arthroscopy to exclude loose bodies, chondral lesions, or associated mensical injuries before the grafting procedure. Bone marrow was harvested from the iliac crest via a small stab incision approximately 3 cm posterior to the anterior superior iliac spine and using the bone aspiration needle supplied in the Cellect Graft Preparation Device set from Depuy, Inc. Six syringes containing approximately 12 mL of marrow and 6 mL of heparin (1000 U/mL) each were obtained. Care was taken to aspirate only 2 to 4 mL from each site before the direction of the needle was changed, as it has been shown by Muschler at al [8] that dilution with peripheral blood occurs when the volume of aspirate increases. The aspirated marrow was then syringe-pumped through the prefilled allograft cartridge that incorporates a proprietary formulation of DBM fibers and cancellous bone chips. This enables selective retention and a 3-fold to 4-fold increase in osteoprogenitor cells within the graft material. Attention was then directed to the actual operative site. A direct approach to both condyles

Fig. 1. Typical preoperative plain radiographs and magnetic resonance imaging scans of one patient. Note preservation of the joint space.

was performed under image intensifier guidance. A cortical window was made over the affected condyle. Necrotic bone material was curetted and then irrigated. The defect was then packed with the previously prepared graft material. The patients were placed on toe-touch weight-bearing in a Bledsoe (Bledsoe Brace Systems, Grand Prairie, Tex) brace for the first 6 weeks and then continued on physiotherapy and weight-bearing as tolerated thereafter.

Results

Their mean age at time of surgery was 21 years (range, 18-23), and the mean duration of symptoms before surgery was 18 months. The ON involved both knees in 2 of the 3 patients, and one of the patients with bilateral knee involvement also had bilateral hip involvement. All 3 patients had steroid-induced ON. One had a diagnosis of Crohn disease, another was a heart transplant patient who was also on other immunosuppressant medications, and the last patient was treated with high-dose steroids for severe optic nerve swelling associated with the use of minocycline. The mean preoperative Knee Society Scores and Knee Society Function Scores were 56 and 53, respectively (range, 50-60 and 50-60, respectively). The radiological staging system reported by Aglietti et al [9] was used, and this was a modification of the original staging described by Koshino [10]. All 3 patients had preoperative radiographs and magnetic resonance imaging scans, and the preoperative stage was 3 in all the patients. All 3 patients had involvement of both condyles, with the lateral femoral condyle being more affected. The size of the lesion has important prognostic implications; it can be measured by either the ratio [11] or the area [12] technique, and it has been shown that there is no difference between the two in predicting prognosis [13,14]. We used the ratio method and classified a lesion as being large if it involved more than 0.32 of the involved condyle width. The mean ratio of knees with favorable treatment outcomes was 0.32 [13]. All 3 of our patients had large lesions (Fig. 1).

The operating times ranged from 60 to 75 minutes, and the mean blood loss was 60 mL. The mean duration of hospital stay was 2 days. The mean Knee Society Scores and the Knee Society Function Scores at 2 years were 97 (range, 95-100) and 87 (range, 70-100), respectively. The relatively poorer Knee Society Function Score (70) in one of the patients with bilateral lesions was due to pain in the contralateral knee. Otherwise, the function and satisfaction in the operated knee were rated as excellent in all 3 patients. There were no complications from the operations, and radiographs at 2 years showed good graft integration and no further progression of the ON or subchondral collapse (Fig. 2).

Discussion

All 3 patients shared the unfortunate consequences of steroid-induced [15,16] ON of the distal

Fig. 2. Radiograph at 2-year follow-up showing integration of graft material and no further progression of ON or subchondral collapse.

femoral condyles. In a clinical study of 18 knees [17] with steroid-induced ON of the knee, the authors found that 80% of the cases were bilateral and that the lateral femoral condyle was predominantly involved. This was the exact clinical presentation of our patients. The current treatment options available include conservative management, arthroscopic debridement, osteochondral allografts, high tibial osteotomy, core decompression, and joint arthroplasty (either unicompartmental or total).

In contrast to spontaneous ON, this group of patients fare poorly with conservative treatments in view of their very young age (mean age of 21 years in our series); high activity levels; and extensive, multifocal lesions. Mont et al [18] treated 32 knees conservatively, and only 59% had good outcomes at 2 years of follow-up. In another study [19], Mont and colleagues examined 248 knees in 136 patients with secondary ON. They found that the condition predominantly affects women and was associated with corticosteroid use in 90% of their patients. Only 8 (20%) of 41 initially symptomatic knees treated nonoperatively had a successful outcome at a mean of 8 years. Arthroscopic debridement for secondary ON is not common. It has been used with mixed success mainly for treatment of spontaneous ON [20,21]. A recent report [22] examined the use of arthroscopic microfracture for treating ON in the knee. Although promising results were seen in the spontaneous ON group, an increase in the size of the lesion was seen in 27% of the secondary ON group.

We use arthroscopy as a diagnostic aid before the actual surgical procedure to look for chondral involvement and other mechanical lesions such as meniscal and cruciate ligament injuries and do not believe that microfracturing in a necrotic bed of subchondral bone provides sufficient osteoprogenitor cells to facilitate bone repair in larger lesions.

Osteochondral allografts for steroid-induced ON have had poor results [23]. Bayne at al [24] found that the use of fresh osteochondral allografts in patients with steroid-induced ON did well for the first 6 to 18 months, but there was subsequent graft subsidence. Osteochondral allografting might be an option for young patients with localized ON, but is not suitable for our patients who were on steroids and had diffuse, extensive lesions.

The use of core decompression has had success in the early stages of the disease but only fair to poor outcomes in the later stages. Jacobs et al [25] performed core decompressions for 28 femurs. All 7 cases in stages 1 and 2 had good results; and of the 21 cases in stage 3 disease, less than 50% had good results. Thus, core decompression appears to have low morbidity and relative success in early stages of ON. Koshino [10] reported good results with the use of core decompression or bone grafting combined with proximal tibial osteotomy. The necrotic lesion improved radiographically in 17 of 23 knees. This technique, however, is not applicable to our patients who had involvement of both femoral condyles.

Histopathological examination of the bone around the central necrotic zone in the later stages of ON shows normal growth characteristics with signs of intense perifocal reaction and, occasionally, sclerosis [26]. The appearance is very similar to that of fracture callus. Deeper within the condyle, the deposition of new, immature bone is observed around dead bone. The use of bone graft attempts to aid in the reparative process and provide structural support. Harvesting of autogenous iliac crest bone graft, the criterion standard, is associated with significant morbidity. Patients with ON secondary due to steroid use have been shown to have a decrease in osteogenic stem cells in their bone marrow [27,28].

Steroids have also been shown to stimulate adipogenesis and fat-specific genes [29-31]. Because osteogenic cells and adipocytes share a common stem cell origin, a decrease in the overall number of stem cells and an increase in the proportion of adipocytes lead to insufficient osteogenic cells to effect bone remodeling by creeping substitution. The success of any grafting technique would thus depend on the number of osteoprogenitor cells that could be transplanted. Bone marrow contains connective tissue progenitors (CTPs) [32], which are a heterogenous population of stem cells and progenitor cells in native tissues. The CTPs include osteogenic cells that are key to bone regeneration. Only 0.01% of nucleated cells from human marrow aspirates are glass-adherent or plastic-adherent, but more than 90 % of the adherent colony-forming cells can differentiate along the osteoblast lineage [33,34].

The work of Muschler et al [35-37] showed that bone graft material supplemented with marrow-derived osteogenic CTPs demonstrated better bone formation. The Cellect Graft Preparation System, which was based on their work, was initially designed for use in spine fusion.

It allows a 3-fold to 4-fold increase in osteoprogenitor cell concentration in the graft matrix, which is a combination of allograft and DBM. The increased numbers of cells increase the bone regenerative potential of this graft composite; and the cells secrete growth factors and angiogenic

cytokines [38], which are crucial in bone regeneration in ON. In a study looking at the results of core decompression and grafting with bone marrow, Hernigou and Beaujean [39] found that patients who had the greater number of progenitor cells transplanted had the better outcome.

Our technique of combining decompression, debridement, and grafting with the Cellect DBM System is simple, has low morbidity, and does not preclude the patients from future interventions. The short-term results are promising in this small group of young patients who have extensive, late-stage lesions. A longer-term follow-up in a larger cohort of patients might prove its value as an addition to the armamentarium in the treatment of ON.

References

1. Ahlback S, Bauer GC, Bohne WH. Spontaneous osteonecrosis of the knee. Arthritis Rheum 1968; 11:705.
2. Mont MA, Ragland PS. Osteonecrosis of the knee. In: Scott WN, editor. Insall & Scott Surgery of the Knee. 4th ed. Churchill Livingstone; 2006. p. 460.
3. Narvaez J, Narvaez JA, et al. Osteonecrosis of the knee: differences among idiopathic and secondary types. Rheumatology 2000;39:982.
4. Kadiyala S, et al. Rapid bone regeneration in femoral defects by an autologous osteoprogenitor cell concentrate prepared using an intraoperative selective cell retention technique. Transactions of the 49th Annual Meeting of the Orthopaedic Research Society; 2003.
5. Connolly J, Guse R, Lippiello L, et al. Development of an osteogenic bone-marrow preparation. J Bone Joint Surg Am 1989;71:684.
6. Bruder SP, et al. Mesenchymal stem cells in osteobiology and applied bone regeneration. Clin Orthop Relat Res 1998;344(Suppl):S247.
7. Muschler GF, et al. Spine fusion using cell matrix composites enriched in bone marrow–derived cells. Clin Orthop Relat Res 2003;407:102.
8. Muschler GF, Boehm C, Easley K. Aspiration to obtain osteoblast progenitor cells from human bone marrow: the influence of aspiration volume. J Bone Joint Surg Am 1997;79:1699.
9. Aglietti P, Insall JN, Buzzi R, et al. Idiopathic osteonecrosis of the knee. Aetiology, prognosis and treatment. J Bone Joint Surg Br 1983;65:588.
10. Koshino T. The treatment of spontaneous osteonecrosis of the knee by high tibial osteotomy with and without bone-grafting or drilling of the lesion. J Bone Joint Surg Am 1982;64:47.
11. Lotke PA, Abend JA, Ecker ML. The treatment of osteonecrosis of the medial femoral condyle. Clin Orthop Relat Res 1982:109.
12. Muheim G, Bohne WH. Prognosis in spontaneous osteonecrosis of the knee. Investigation by radionuclide scintimetry and radiography. J Bone Joint Surg Br 1970;52:605.
13. Al-Rowaih A, Bjokengren A, Egund N, et al. Size of osteonecrosis of the knee. Clin Orthop Relat Res 1993:69.
14. Al-Rowaih A, Lindstrand A, Bjokengren A, et al. Osteonecrosis of the knee. Diagnosis and outcome in 40 patients. Acta Orthop Scand 1991;62:19.
15. Abeles M, Urman JD, Rothfield NF. Aseptic necrosis of bone in systemic lupus erythematosus. Relationship to corticosteroid therapy. Arch Intern Med 1978;138: 750.
16. Cruess RL. Steroid-induced osteonecrosis: a review. Can J Surg 1981;24:567.
17. Sasaki T, Yagi T, Monji J, et al. Steroid-induced osteonecrosis of the femoral condyle—a clinical study of eighteen knees in ten patients. J Jpn Orthop Assoc 1986;60:361.
18. Mont MA, Myers TH, Krackow KA. Total knee arthroplasty for corticosteroid associated avascular necrosis of the knee. Clin Orthop Relat Res 1997:124.
19. Mont MA, Baumgarten KM, Rifai A, et al. Atraumatic osteonecrosis of the knee. J Bone Joint Surg Am 2000; 82:1279.
20. Koshino T, Okamoto R, Takamura K, et al. Arthroscopy in spontaneous osteonecrosis of the knee. Orthop Clin North Am 1979;10:609.
21. Miller GK, Maylahn DJ, Drennan DB. The treatment of idiopathic osteonecrosis of the medial femoral condyle with arthroscopic debridement. Arthroscopy 1986;2:21.
22. Akgun I, Kesmezacar H, Ogut T, et al. Arthroscopic microfracture treatment for osteonecrosis of the knee. Arthroscopy 2005;21:834.
23. Ganel A, Israeli A, Horoszowski H. Osteochondral graft in the treatment of osteonecrosis of the femoral condyle. J Am Geriatr Soc 1981;29:186.
24. Bayne O, Langer F, Prtitzker KP, et al. Osteochondral allografts in the treatment of osteonecrosis of the knee. Orthop Clin North Am 1985;16:727.
25. Jacobs MA, Loeb PE, Hungerford DS. Core decompression of the distal femur for avascular necrosis of the knee. J Bone Joint Surg Br 1989;71:583.
26. Lotke PA, Lonner JH. Spontaneous and secondary osteonecrosis of the knee. In: Scott WN, editor. Insall & Scott surgery of the knee. 4th ed. Philadelphia, Penn: Churchill Livingstone; 2006. p. 4389.
27. Hernigou P, Beaujean F. Abnormalities in the bone marrow of the iliac crest in patients who have osteonecrosis secondary to corticosteroid therapy or alcohol abuse. J Bone Joint Surg Am 1997;79:1047.
28. Hernigou P, Beaujean F, Lambotte JC. Decrease in the mesenchymal stem-cell pool in the proximal femur in corticosteroid-induced osteonecrosis. J Bone Joint Surg Br 1999;81:349.
29. Doherty NJ, De Rome M, McCarthy MB, et al. The effect of glucocorticoids on osteoblast function: the effect of corticosterone on osteoblast expression of beta 1 integrins. J Bone Joint Surg Am 1995; 77-A:396.

30. Cui MD, Wang GJ, Dalion G. Steroid-induced adipogenesis in a pluripotential cell line from bone-marrow. J Bone Joint Surg Am 1997;79-A: 1054.
31. Hernigou P, Poignard A, Manicom O, et al. The use of percutaneous autologous bone marrow transplantation in nonunion and avascular necrosis of bone. J Bone Joint Surg Br 2005;87:896 [Review].
32. Ada Au, Boehm CA, Mayes AM, et al. Formation of osteogenic colonies on well-defined adhesion peptides by freshly isolated human marrow cells. Biomaterials 2007;28:1847.
33. Owen M. Marrow stromal stem cells. J Cell Sci Suppl 1988;10:63 [Review].
34. Aubin JE. Bone stem cells. J Cell Biochem Suppl 1998;30-31:73 [Review].
35. Muschler GF, Nakamoto C, Griffith LG. Engineering principles of clinical cell-based tissue engineering. J Bone Joint Surg Am 2004;86-A:1541 [Review].
36. Muschler GF, Negami S, Hyodo A, et al. Evaluation of collagen ceramic composite graft materials in a spinal fusion model. Clin Orthop Relat Res 1996:250.
37. Muschler GF, Nitto H, Matsukura Y, et al. Spine fusion using cell matrix composites enriched in bone marrow-derived cells. Clin Orthop Relat Res 2003; 11:102.
38. Hernigou P. Growth factors released from bone marrow are promising tools in orthopedic surgery. Rev Rhum Engl Ed 1998;65:79 [Review].
39. Hernigou P, Beaujean F. Treatment of osteonecrosis with autologous bone marrow grafting. Clin Orthop Relat Res 2002:14.

SPINE Volume 32, Number 7, pp 720–726

Efficacy of Mesenchymal Stem Cell Enriched Grafts in an Ovine Posterolateral Lumbar Spine Model

Munish C. Gupta, MD,* Thongchai Theerajunyaporn, MD,* Sukanta Maitra, MS,* Mary Beth Schmidt, PhD,† Chantal E. Holy, PhD,† Sudha Kadiyala, PhD,† and Scott P. Bruder, MD, PhD†

Study Design. Four groups of 6 animals underwent single-level noninstrumented posterolateral lumbar fusion (PLF) with one of the following grafts: 1) autograft, 2) cell-enriched β-tricalcium phosphate (TCP), 3) TCP with whole bone marrow, and 4) TCP alone. Plain radiographs were taken after surgery and at death, 6 months after surgery. Explanted spine segments were analyzed by manual palpation, micro-CT, and histology.

Objective. A sheep spine fusion study was undertaken to evaluate the healing performance of a TCP graft enriched with osteoprogenitor cells using Selective Cell Retention technology (SCR), compared with autograft, TCP with whole bone marrow, and TCP alone.

Summary of Background Data. Improved bone healing with previously demonstrated using grafts enriched in osteoprogenitor cells.

Methods. Cell-enriched grafts were obtained by processing 30 mL of bone marrow through 10 mL of TCP. TCP was also used either saturated with bone marrow or alone.

Results. At 6 months, 33% of the SCR-enriched TCP and 25% of the autograft sites were fused, compared with 8% of the TCP plus whole bone marrow and 0% of the TCP alone. Histology of fused samples showed denser bone formation in the SCR-enriched TCP grafts than in the autograft sites.

Conclusions. The use of SCR-enriched TCP and autograft resulted in similar fusion rates in an ovine posterolateral noninstrumented lumbar spine fusion model.

Key words: osteoprogenitors, bone marrow, bone graft, spine fusion model, tricalcium phosphate. **Spine 2007;32: 720–726**

It is well documented that open surgical harvesting of autologous bone graft from the ilium is associated with significant postoperative morbidity.[1] Chronic donor site pain is a frequently reported complication, particularly among patients undergoing bone grafting for multilevel spine fusion procedures where a substantial amount of harvested autograft is needed to facilitate a successful arthrodesis.[1–4] Consequently, significant research and development efforts are underway to evaluate alternative graft materials that obviate the requirement for harvesting autologous bone in a variety of orthopedic and spine procedures.[5–7]

To date, osteoconductive alternative bone grafting materials alone have not consistently produced results equivalent to autologous bone, particularly for challenging clinical applications.[8,9]

Synthetic bone growth factors with osteoconductive grafts have also been investigated, but the costs of these growth factors as well as their high concentration and potential risk of overexuberant bone formation have presently limited their use to very narrow indications.[10]

It is likely that a composite graft that mimics the native characteristics and constituents of autologous bone may provide the most promising alternative graft material to harvested autograft.[11] Specifically, autologous bone marrow has considerable appeal from a bone grafting standpoint because it provides live osteogenic cells and has the ability to effect de novo bone formation directly at the graft site.[12,13] Several studies suggest that aspirated whole bone marrow alone or combined with a biomaterial carrier offers satisfactory clinical results for some grafting applications and avoids the morbidity associated with open surgical harvesting of autograft.[14,15] More recently, the concept of grafting whole bone marrow-augmented composites has been refined with focus on concentrating the osteogenic precursor cells found in marrow and depositing them onto a carrier matrix to provide a more consistent clinical outcome.[16–20]

In this study, a novel Selective Cell Retention (SCR) method was used to enrich a β-tricalcium phosphate (TCP) graft with osteogenic cells. Granular, porous TCP was used to maximize surface areas for cell attachment and *de novo* bone infiltration within the graft material. The SCR method relies on the physical principles of an affinity column to populate grafts with anchorage-dependent cells and has been shown previously to allow osteogenic cells to attach while hematopoietic cells pass through. This process was shown by Muschler *et al* to create grafts with a high proportion of osteoprogenitors.[21]

The objective of this study was therefore to compare cell-enriched TCP grafts against grafts soaked with mar-

From the *Department of Orthopedics, University of California Davis Medical Center, Sacramento CA; and †DePuy Biologics, Raynham, MA.
Acknowledgment date: December 1, 2004. First revision date: March 15, 2005. Second revision date: August 16, 2005. Third revision date: October 6, 2005. Fourth revision date: July 28, 2006. Acceptance date: August 14, 2006.
The device(s)/drug(s) is/are FDA-approved or approved by corresponding national agency for this indication.
Corporate/Industry funds were received in support of this work. Although one or more of the author(s) has/have received or will receive benefits for personal or professional use from a commercial party related directly or indirectly to the subject of this manuscript, benefits will be directed solely to a research fund, foundation, educational institution, or other nonprofit organization which the author(s) has/have been associated. One or more of the author(s) has/have received or will receive benefits for personal or professional use from a commercial party related directly or indirectly to the subject of this manuscript: e.g., honoraria, gifts, consultancies.
Address correspondence and reprint requests to Chantal E. Holy, PhD, 325 Paramount Drive, Raynham, MA 02767; E-mail: choly1@dpyus.jnj.com

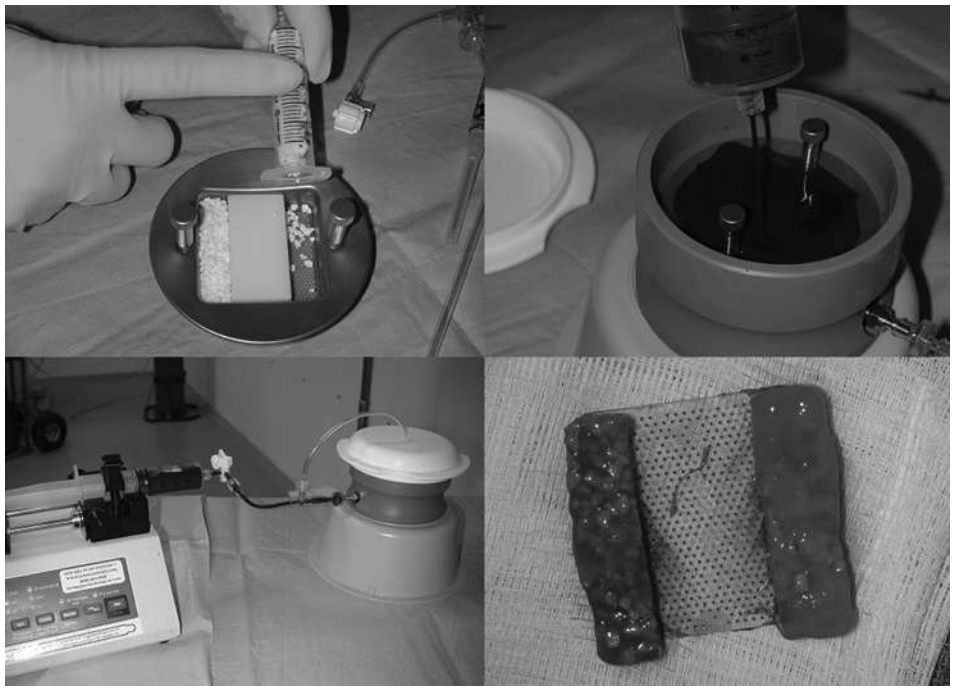

Figure 1. Photographs of the SCR prototype. TCP was placed in a chamber, which was filled with bone marrow; marrow was aspirated through the TCP to produced cell-enriched grafts.

row, TCP alone, and autograft. Tricalcium phosphate enriched with mesenchymal stem cells was compared with TCP soaked with autogenous whole bone marrow, TCP alone, and autograft, in an ovine noninstrumented posterolateral lumbar spine fusion model.

■ Materials and Methods

Overview. Twenty-four skeletally mature Cross female sheep (approx. 150 lb, age 3–4 years) were randomized into 4 groups of 6 animals, each group receiving bilaterally one type of graft (5 mL per side, total of 10 mL per animal) as defined below:

Group 1, Autogenous bone graft from the iliac crest;

Group 2, SCR-enriched TCP;

Group 3, TCP soaked with whole bone marrow;

Group 4, TCP alone.

TCP (Conduit, DePuy Spine) was obtained in granular form. Each granule measured approximately 2 to 3 mm and had a porosity of ~70%.

Surgical Procedure. All animal procedures and surgeries were performed under an approved IACUC protocol at an AAALAC accredited facility (TD Morris, Reistertown, MD). All animals were housed for a minimum of 5 days before the start of the study. Animals were examined by the staff veterinarian, had blood collected for CBC, were vaccinated, checked for fecal ova and parasites, and dewormed within 3 days of arrival. Animals were food fasted for approximately 18 to 24 hours before the treatment procedure. Antibiotic cefazolin (500 mg/kg) was administered to each animal as an intravenous injection. In addition, all animals received an analgesic fentanyl (Duragesic 50 μg/h) transdermal patch. An endotracheal tube was placed and secured, and an area on the abdomen was shaved to accommodate an electrode return patch. The area around the lumbar spine was also shaved in preparation for surgery.

Bone Marrow Aspiration. Immediately before the start of the surgical procedure, animals in Groups 2 had up to 50 mL of bone marrow collected from the iliac crest area using multiple small (2-mL) aspirates. This method was shown by Muschler *et al* to provide highest marrow quality and reduce chances of marrow dilution with peripheral blood.[21] For animals in Group 3, 10 mL of TCP were soaked with approximately 10 mL of bone marrow to form 2 5-mL TCP-marrow grafts to be immediately implanted on each side of the spine.

Preparation of Enriched TCP Grafts. For animals in Group 2, a prototype SCR device was used (Figure 1). This device included a graft chamber, connected to a syringe pump for controlled marrow flow; 30 mL of marrow was passed through 10 mL of TCP, at a controlled flux of 13.5 mL/min/cm^2.

Surgery. The animals were transferred to the operating suite and positioned in ventral recumbence on a warming blanket. An endotracheal tube was attached to an anesthesia machine delivering oxygen, room air, and isoflurane (1%–3%). Replacement fluids (lactated ringers solution or 0.9% NaCl) were administered *via* the intravenous catheter at an approximate rate of 10 mL/kg per hour.

For animals assigned to the autogenous bone graft treatment (Group 1), an epidural injection of morphine (0.05 mg/kg) was administered to provide additional analgesia. An incision was made over the iliac crests, which were exposed. Unicortical harvest of the iliac crest was performed and approximately 10 mL of iliac crest autograft was harvested and morselized into 0.1- to 0.4-mL chips.

Following harvesting, the wound was lavaged and suctioned. The muscle and subcutaneous layer were closed with 2–0 Vicryl in a simple continuous pattern. The lumbar area was then prepared for aseptic surgery. A midline incision was made over the lumbar vertebrae identified as L4 and L5 by manual palpation. Fluoroscopy was then used to identify the correct level for fusion in each animal. In case of sacralization

Figure 2. Photographs of the surgical planes, showing exposed transverse processes and placement of the grafts across the TPs.

or lumbarization, the third motion segment from the sacrum was used. The dorsolumbar fascia was exposed. Two Wiltse-type lateral incisions were made to expose the lateral transverse processes. Attention was given not to disrupt the lamina and facets. The entire area was then thoroughly lavaged and suctioned to remove any residual osseous debris.

The transverse processes were decorticated using a high-speed burr. All shavings from the burr were irrigated out. The appropriate graft was placed in the host bed so that it had complete contact with the decorticated transverse processes (Figure 2). The deep fascial and subcutaneous layers were closed using 2–0 polyglycolic acid sutures in a simple continuous pattern. Radiographs were taken of the lumbar region. Following surgery, each animal was recovered from anesthesia and returned to pen housing.

At 3 months postoperatively, animals were transported to the American Radiology Services (Westminster, MD) for clinical CT scans and anesthetized intravenously with 6 mL of ketamine 100 mg/mL and 3 mL of diazepam 5 mg/mL. Animals were then returned to TD Morris immediately after scanning.

At 6 months after surgery, animals were killed through intravenous injection of Beuthanasia D (1 mL/10 lb of body weight). The lumbar spine segments were explanted, tested by manual palpation for fusion, radiographed, and placed in 10% neutral buffered formalin for fixation. Each spine segment was analyzed as containing 2 distinct fusion sites, one on each side of the vertebral bodies. A total of 12 fusion sites were therefore viewed for each group. All samples were then shipped to Indiana University for micro-CT scanning.

Histology. Undecalcified samples were embedded in PMMA. Sagittal sections were performed along the fusion sites and through the transverse processes. Sections were polished and stained with toluidine blue (T-blue) for histologic evaluation. Similarly, for histologic purposes, each spine segment was analyzed as containing 2 distinct fusion sites. The purpose of the histology was to assess: 1) the overall morphology of *de novo* bone; 2) the maturity of the bone and presence of osteoid and active osteoblasts and osteoclasts; 3) the amount of residual implant material; and 4) the presence of any other cell type in the fusion site.

Computed Tomography. The specimens were scanned with an EVS-R9 micro-CT scanner manufactured by Enhanced Vision Systems Corp. (now part of General Electric Medical Systems, London, Ontario, Canada). The scanner was operated at 50 kVp and 1 mA maximum tube current. Samples were scanned at an 80-μm voxel resolution with 2×2 or 4×4 binning in the detector panel. As for previous analyses, all spine segments were analyzed as containing 2 fusion sites and were assessed as fused or not fused. In addition, each spine segment was rated using Sandhu's fusion rating scale: 0 = no fusion; 1 = bone formation, but no fusion; 2 = unilateral fusion; 3 = bilateral fusion.[22]

■ Results

Overall Fusion Assessments

Fusion assessments are summarized in Table 1. The following fusion assessments were obtained by manual palpation: in the SCR-enriched group, 4 of 6 spine segments seemed fused, while only one spine segment was fused in the autograft group and one in the TCP alone group. Fusion rates and fusion scores were further assessed by clinical and micro-CT, as shown in Figures 3a and 3b, respectively. Three-month clinical CTs were obtained on live animals and indicated that 25% of the autograft sites (3 of 12, one bilateral and one unilateral) and 25% of the SCR-enriched TCP sites (3 of 12, one bilateral and one unilateral) had fused. No fusion was observed in the other groups. Six-month data were obtained on explanted spine segments, using micro-CT analyses. The fusion rate for the autograft group was still at 25% (3 of 12, one bilateral and one unilateral), while 33% of the SCR-enriched TCP sites were fused (2 unilateral and 2 bilateral). No fusions were observed in the TCP alone

Table 1. Fusion Assessment by Manual Palpation, Clinical and Micro-CT as Well as Histology, at 3 and 6 Months

Graft Materials	Manual Palpation by Spine Segment (n = 6 per group)	Fusion Rates by Implant Site (n = 12 per group)		Fusion Scores by Implant Site (n = 12)	
		3 Months (clinical CT) (%)	6 Months (micro-CT and histology) (%)	3 Months (clinical CT)	6 Months (micro-CT and histology)
Autograft	1	25	25	1.3	1.3
SCR-enriched TCP	4	25	33	1.3	1.5
TCP whole bone marrow	1	0	8	0.5	0.3
TCP alone	1	0	0	0.2	0.0

Scores: 0, no bone; 1, bone but no bridging bone; 2, unilateral fusion; 3, bilateral fusion.

group, and an 8% fusion rate was reached within the TCP and whole marrow group (one unilateral).

Fusion scores were further used to evaluate bone formation, with or without fusion. At 3 months, both the autograft and the SCR-enriched TCP group showed similar fusion scores, indicative of both, presence of *de novo* bone tissue as well as fusion. In contrast, the TCP with whole bone marrow only showed presence of *de novo* bone tissue but no fusion. No bone tissue was found in the TCP alone group. At 6 months, similar scores were observed with slightly higher scores in the SCR-enriched TCP group. In all cases, results were not statistically significant.

Radiographs and Micro-CT

Three-dimensional reconstructions of series of 30 μm-thick micro-CT sections were reviewed for all samples (Figure 4). At 6 months, fused sites showed high volumes of bone across the lateral processes; the edges of the lateral processes were often difficult to distinguish from newly formed bone within fusion sites, indicating a high level of osteointegration and remodeling. While implants were consistently placed laterally, away from the gutter, *de novo* bone mass was seen in one of the autograft fusion sites along the gutter as well as far laterally, indicating partial migration of one of the grafts postimplantation. All other fusion masses were seen laterally, away from the gutter.

Histology

Histology was performed using 50-mm-thick, undecalcified, toluidine blue stained sagittal sections (Figure 5). Low-magnification micrographs are shown in Figures 5a and b, while high-magnification radiographs are shown in Figures 5c and d. Fusion rates observed by histology were similar to those obtained by micro-CT.

1. At 6 months, 25% autograft sites fused, containing mild to marked newly formed woven and lamellar bone trabeculae in a cancellous organization, with evidence of remodeling, as seen by secondary osteons near the cortical bone surfaces of the transverse processes. Evidence of endochondral ossification was also observed, with chondrocytic cells involved in endochondral cartilage-to-bone formation. Cancellous bone was surrounded mostly with hematopoietic and fatty marrow tissue.
2. In the TCP and whole bone marrow group, only 8% of the samples fused. No samples from the TCP alone group fused. Fibrovascular tissues bridging the transverse processes were present in 60% of the TCP alone longitudinal samples.
3. In contrast to the autograft group, at the 6-month time point, the TCP alone group had minimal bone surface or soft tissue activity. No fusion was observed in the TCP alone group.
4. In the SCR-enriched TCP group, bone fusion between transverse processes was present in 33% of all longitudinal sections. In general, and similar to autograft, fused SCR-enriched TCP samples showed mild to marked newly formed woven and lamellar bone trabeculae in a cancellous organization with evidences of remodeling; however, in

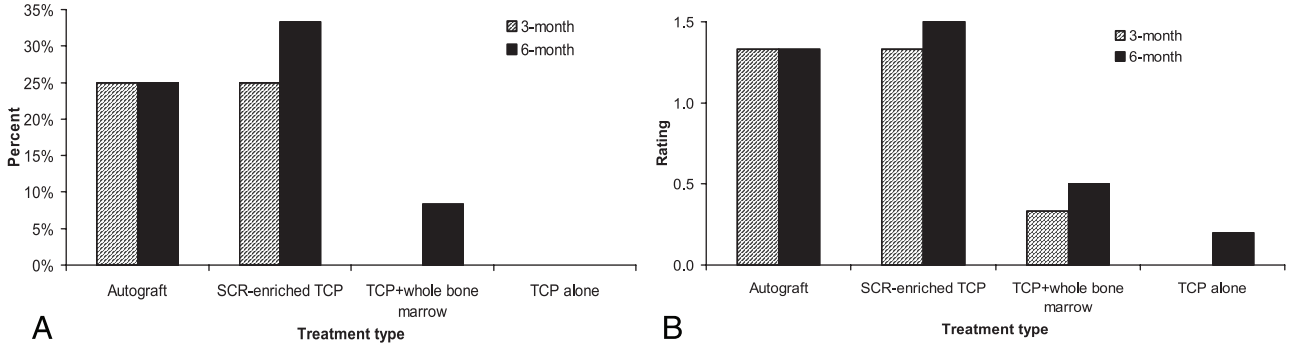

Figure 3. Graphs indicating the fusion rates and fusion scores observed at 3 and 6 months. **A**, Determined by micro-CT analyses using a simple fused/nonfused assessment. **B**, Determined using a 4-point scaled first described by Sandhu *et al*[26]: 0 = no fusion; 1 = bone formation, but no fusion; 2 = unilateral fusion; 3 = bilateral fusion.

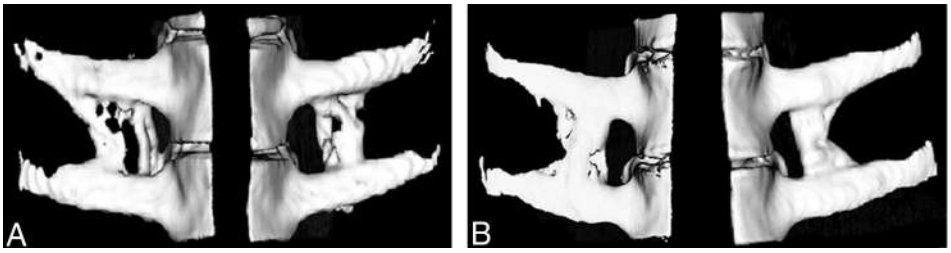

Figure 4. Examples of micro-CT reconstructions of fused samples, 6 months postsurgery, with the following graft materials: **A**, autograft; **B**, SCR-enriched TCP.

contrast to autograft, the cancellous trabeculae present in the cell-enriched TCP group appeared to be more numerous, highly interconnected, with less separation among trabeculae, and thus, denser per unit area of bone tissue. TCP fragments were still visible at high resolution. Hematopoietic and fatty marrow tissue was also found surrounding the cancellous bone, as seen in the autograft samples.

■ Discussion

This study was aimed at investigating the benefit of implanting cells, either from whole bone marrow or using concentration methods, on *de novo* bone formation, using a specific graft volume. Results demonstrated similar performance of SCR-enriched TCP and autograft in an ovine posterolateral lumbar spinal fusion model. This model was chosen initially for its inherently low autograft fusion rate. This model was previously validated, and a 2-level version of a similar type of fusion was recently published.[21] Several factors could contribute to the overall low fusion rates observed here. For example, it is known that graft volume affect fusion rates; a greater graft volume may have resulted in greater fusion success. The challenging aspect of this model was also made possible by carefully preventing any disruption to the lamina or facets, thereby preventing migration of osteoprogenitor cells from these bony sites to the graft material. In addition, grafts were placed away from the posterior elements, as shown in Figure 2. As a result, fusion sites observed in this study were mainly located far laterally with minimal *de novo* bone masses against the posterior elements. Decorticating the transverse processes with a high-speed burr may have also contributed to reducing the migration of the cells from the transverse processes to the graft material by superficially burning the exposed bone surfaces and thus potentially creating a layer of scar tissue. While no specific markers were used to identify the origin of the cells within the newly formed bone, the osteogenicity of the grafts may therefore, in most part, have been dependent on cells added to the TCP before implantation.

No fusion was observed with TCP alone. It was not expected that TCP alone, being only an osteoconductive graft, would achieve fusion in this challenging model. While osteoconduction is key to bone formation, purely osteoconductive grafts rely on osteoprogenitor cells that either migrate from the local bone or are added to the grafts before implantation for new bone formation. In this study, the potential migration of cells from local bone sites was significantly restricted, as described in Materials and Methods. This surgical technique therefore allowed us to specifically evaluate the osteogenicity of those cells added to the grafts before implantation. It was found that TCP alone could not serve as an effective graft in the absence of an available local supply of osteoprogenitor cells.

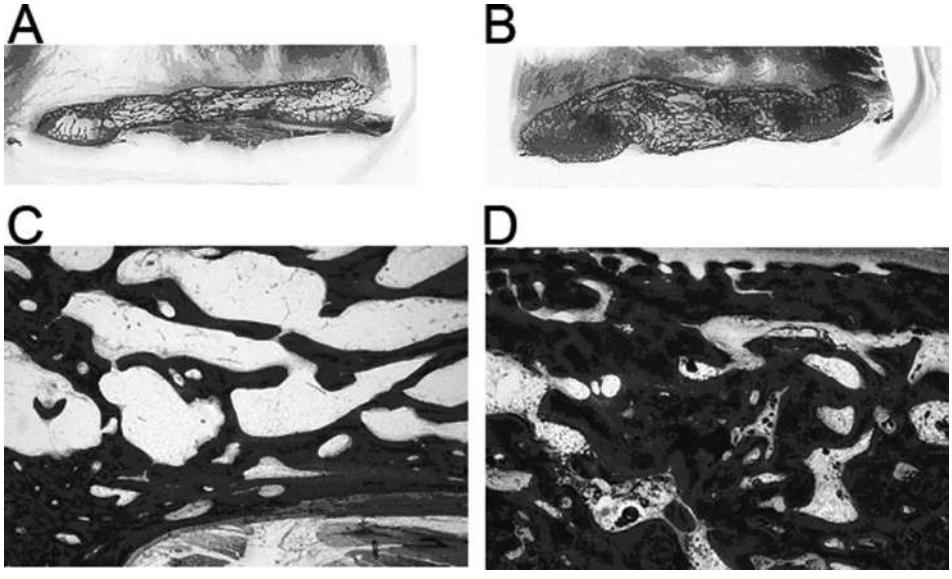

Figure 5. Histologic views of autograft (**A** and **C**) and SCR-enriched TCP (**B** and **D**) sites, showing newly formed woven and lamellar bone trabeculae in a cancellous organization. Original magnifications: A and B, ×4; C and D, ×15.

Using autologous bone marrow with TCP increased bone formation and overall fusion, due to the osteogenic nature of bone marrow. As demonstrated in prior research, bone marrow serves as a repository for mesenchymal stem cells and thereby provides osteogenicity to graft materials.[11–13,16–20,23–25] However, the bone marrow plus TCP group did not perform as well as the autograft group did. This is most likely due to the fact that bone marrow typically contains fewer osteoprogenitor cells than iliac crest autograft. In addition, while both groups (TCP and bone marrow and autograft) contained osteoconductive and osteogenic elements, only autograft contained osteoinductive molecules, such as native bone morphogens, that affect bone regeneration. The osteogenicity of the bone marrow plus TCP group was therefore lower than that of iliac crest autograft.

In this study, the marrow was collected from the iliac crest of the sheep to mimic clinical situations. No preliminary trials were performed to determine whether the sheep iliac crest was indeed the optimal site to collect marrow. Marrow cellularity was shown to vary from one bony site to another and with age. For example, previous studies have shown that, in the rabbit, marrow from the iliac crest is suboptimal compared with marrow from the long bones.[24,25] In humans, bone marrow cellularity was shown to decrease with age[25] and to be highest in the vertebral bodies and the iliac crest.[25] It is possible therefore that, in sheep, using long bone or any other site for marrow harvesting would have resulted in greater marrow cellularity and, hence, higher fusion rates.

At the 6-month endpoint, remains of TCP were still visible by histology. While resorption of graft is critical to optimize *de novo* bone formation, the rates at which these biomaterials degrade need to be concomitant with rates of new bone formation. TCP, being designed for human use, degrades therefore within 12 months, a time period most often required for spinal fusion with autograft. It was therefore anticipated that TCP would still be present in the graft sites after 6 months.

The osteogenic potential of concentrated osteoprogenitor cells was shown in this study, as the effectiveness of the SCR-enriched TCP graft was: 1) improved compared with TCP plus whole marrow and 2) similar to autograft. While the results were not statistically significant, they indicated trends of increased osteogenicity with increased bone cell density. This further supports the hypothesis that an increased concentration of osteoprogenitor cells within a graft matrix, even a purely osteoconductive matrix, creates an environment within the graft material that supports bone formation similar to autologous bone.[26–28]

A recent clinical report by Hernigou *et al* further confirmed these findings.[29] In this recent study, bone marrow-derived cells were centrifuged from autologous bone marrow and injected into nonunion sites. Only those nonunions injected with more than 1500 cells/mL went on to heal, while others did not heal. While the Hernigou *et al* method included injecting cells without an osteoconductive matrix, their conclusions similarly demonstrated that cell concentrates, above a specific threshold, could result in significant healing.[29]

■ Conclusion

In this large animal, noninstrumented, posterolateral lumbar spine fusion model, the fusion rates obtained from using a purely osteoconductive graft material, enriched with autologous mesenchymal stem cells, were similar to those obtained from using autograft. Bone graft substitutes obtained using bone marrow-based technologies provide a safe and efficacious alternative to iliac crest autograft.

■ Key Points

- Autologous bone marrow contains osteoprogenitor cells that can be concentrated using a Selective Cell Retention system (SCR) to form grafts with a threefold to fourfold increase in osteoprogenitor cells.
- The bone-forming potential of SCR-enriched tricalcium phosphate (TCP) grafts was compared with that of autograft and TCP saturated with whole bone marrow in an ovine noninstrumented posterolateral fusion model.
- SCR-enriched and autograft resulted in 33% and 25% fusion rate, respectively, while only 8% fusion was observed in the TCP saturated with whole bone marrow. No fusion was observed in the TCP alone sites.
- SCR-enriched grafts were equivalent to autograft in a challenging, large-animal spine fusion model.

References

1. Russell JL, Block JE. Surgical harvesting of bone graft from the ilium: point of view. *Med Hypotheses* 2000;55:474–9.
2. Fernyhough JC, Schimandle JJ, Weigel MC, et al. Chronic donor site pain complicating bone graft harvesting from the posterior iliac crest for spinal fusion. *Spine* 1992;17:1474–80.
3. Gupta AR, Shah NR, Patel TC, et al. Perioperative and long-term complications of iliac crest bone graft harvesting for spinal surgery: a quantitative review of the literature. *Int Med J* 2001;8:163–6.
4. Summers BN, Eisenstein SM. Donor site pain from the ilium: a complication of lumbar spine fusion. *J Bone Joint Surg Br* 1989;71:677–80.
5. Bauer TW, Muschler GF. Bone graft materials: an overview of the basic science. *Clin Orthop* 2000;371:10–27.
6. Fleming JE Jr, Cornell CN, Muschler GF. Bone cells and matrices in orthopedic tissue engineering. *Orthop Clin North Am* 2000;31:357–74.
7. Lane JM, Tomin E, Bostrom MP. Biosynthetic bone grafting. *Clin Orthop* 1999;367(suppl):107–17.
8. Block JE, Thorn MR. Clinical indications of calcium-phosphate biomaterials and related composites for orthopedic procedures. *Calcif Tissue Int* 2000; 66:234–8.
9. Cornell CN, Lane JM. Current understanding of osteoconduction in bone regeneration. *Clin Orthop* 1998;355(suppl):267–73.
10. Howes R, Bowness JM, Grotendorst GR, et al. Platelet-derived growth factor enhances demineralized bone matrix-induced cartilage and bone formation. *Calcif Tissue Int* 1988;42:34–8.
11. Lowery GL, Kulkarni S, Pennisi AE. Use of autologous growth factors in lumbar spinal fusion. *Bone* 1999;25(suppl 2):47–50.

12. Marx RE, Carlson ER, Eichstaedt RM, et al. Platelet-rich plasma: growth factor enhancement for bone grafts. *Oral Surg Oral Med Oral Pathol Oral Radiol Endod* 1998;85:638–46.
13. Edwards SL, Hendrix R, Schafer MF, et al. Radiographic assessment of posterolateral spine fusion with and without platelet rich plasma. *ISSLS* 2003;117.
14. Weiner BK, Walter M. Efficacy of autologous growth factors in lumbar intertransverse fusion. *Spine* 2003;28:1968–71.
15. Lane JM, Yasko AW, Tomin E, et al. Bone marrow and recombinant human bone morphogenetic protein-2 in osseous repair. *Clin Orthop* 1991;361: 216–27.
16. Bruder SP, Fox BS. Tissue engineering of bone: cell based strategies. *Clin Orthop* 1999;367(suppl):68–83.
17. Burwell RG. The function of bone marrow in the incorporation of a bone graft. *Clin Orthop* 1985;200:125–41.
18. Connolly JF. Clinical use of marrow osteoprogenitor cells to stimulate osteogenesis. *Clin Orthop* 1998;355(suppl):257–66.
19. Chapman MW, Bucholz R, Cornell C. Treatment of acute fractures with a collagen-calcium phosphate graft material: a randomized clinical trial. *J Bone Joint Surg Am* 1997;79:495–502.
20. Tiedeman JJ, Garvin KL, Kile TA, et al. The role of a composite, demineralized bone matrix and bone marrow in the treatment of osseous defects. *Orthopedics* 1995;18:1153–8.
21. Muschler GF, Boehm C, Easley K. Aspiration to obtain osteoblast progenitor cells from human bone marrow: the influence of aspiration volume. *J Bone Joint Surg Am* 1997;79:1699–709.
22. Bruder SP, Jaiswal N, Ricalton NS, et al. Mesenchymal stem cells in osteobiology and applied bone regeneration. *Clin Orthop* 1998;355(suppl):247–56.
23. Muschler GF, Midura RJ. Connective tissue progenitors: practical concepts for clinical applications. *Clin Orthop* 2002;395:66–80.
24. Connolly J, Guse R, Lippiello L, et al. Development of an osteogenic bone-marrow preparation. *J Bone Joint Surg Am* 1989;71:684–91.
25. Muschler GF, Nitto H, Matsukura Y, et al. Spine fusion using cell matrix composites enriched in bone marrow-derived cells. *Clin Orthop* 2003;407: 102–18.
26. Spiro RC, Thompson AY, Poser JW. Spinal fusion with recombinant human growth and differentiation factor–5 combined with a mineralized collagen matrix. *Anat Rec* 2001;263:388–95.
27. Tay BK, Le AX, Heilman M, et al. Use of a collagen-hydroxyapatite matrix in spine fusion. *Spine* 1998;23:2276–81.
28. Sharp TG, Sachs DH, Matthews JG, et al. Harvest of human bone marrow directly from bone. *J Immunol Methods* 1984;69:187–95.
29. Hernigou P, Poignard A, Beaujean F, et al. Percutaneous autologous bone-marrow grafting for nonunions: influence of the number and concentration of progenitor cells. *J Bone Joint Surg Am* 2005;87:1430–7.

Biomaterials 35 (2014) 5689–5699

Contents lists available at ScienceDirect

Biomaterials

journal homepage: www.elsevier.com/locate/biomaterials

A composite demineralized bone matrix – Self assembling peptide scaffold for enhancing cell and growth factor activity in bone marrow

Tianyong Hou [a,b,c,*,1], Zhiqiang Li [a,b,c,d,1], Fei Luo [a,b,c,*], Zhao Xie [a,b,c], Xuehui Wu [a,b,c], Junchao Xing [a,b,c], Shiwu Dong [a,b,c,e], Jianzhong Xu [a,b,c,*]

[a] National & Regional United Engineering Lab of Tissue Engineering, Department of Orthopaedics, Southwest Hospital, the Third Military Medical University, Chongqing, China
[b] Center of Regenetive and Reconstructive Engineering Technology in Chongqing City, Chongqing, China
[c] Tissue Engineering Laboratory of Chongqing City, Chongqing, China
[d] Department of Orthopedics, General Hospital of Chengdu Military Commanding Region, Chengdu, China
[e] Department of Biomedical Materials Science, College of Biomedical Engineering, Third Military Medical University, Chongqing, China

ARTICLE INFO

Article history:
Received 3 March 2014
Accepted 27 March 2014
Available online 20 April 2014

Keywords:
Tissue-engineered bone
Nanoscale biomaterials
Self-assembling peptide
Demineralized bone matrix
Selective cell retention

ABSTRACT

The need for suitable bone grafts is high; however, there are limitations to all current graft sources, such as limited availability, the invasive harvest procedure, insufficient osteoinductive properties, poor biocompatibility, ethical problems, and degradation properties. The lack of osteoinductive properties is a common problem. As an allogenic bone graft, demineralized bone matrix (DBM) can overcome issues such as limited sources and comorbidities caused by invasive harvest; however, DBM is not sufficiently osteoinductive. Bone marrow has been known to magnify osteoinductive components for bone reconstruction because it contains osteogenic cells and factors. Mesenchymal stem cells (MSCs) derived from bone marrow are the gold standard for cell seeding in tissue-engineered biomaterials for bone repair, and these cells have demonstrated beneficial effects. However, the associated high cost and the complicated procedures limit the use of tissue-engineered bone constructs. To easily enrich more osteogenic cells and factors to DBM by selective cell retention technology, DBM is modified by a nanoscale self-assembling peptide (SAP) to form a composite DBM/SAP scaffold. By decreasing the pore size and increasing the charge interaction, DBM/SAP scaffolds possess a much higher enriching yield for osteogenic cells and factors compared with DBM alone scaffolds. At the same time, SAP can build a cellular microenvironment for cell adhesion, proliferation, and differentiation that promotes bone reconstruction. As a result, a suitable bone graft fabricated by DBM/SAP scaffolds and bone marrow represents a new strategy and product for bone transplantation in the clinic.

1. Introduction

Suitable bone grafts are needed to treat a considerable number of disorders, such as bone defects and nonunion resulting from bone tumor excision or trauma, as well as for surgical procedures such as spinal and joint fusion [1,2]. The current gold standard for bone repair is the use of autologous bone grafts, but their availability is limited and the harvesting procedure is associated with significant comorbidities [3]. Although xenogenic bone grafts are widely available, immunogenicity, potential pathogenicity, and the ethical issues associated with their use are difficult to overcome. To date, synthetic biomaterials for bone repair have shown limited osteoinductive potential and do not mimic the biodegradable properties of newly formed bone tissue [4–6]. Demineralized bone matrix (DBM) has been widely used as an allogenic bone graft for bone reconstruction; however, studies have shown that DBM possesses few osteoinductive [7,8].

Tissue engineering is a promising method for bone reconstruction, with the potential for the implantation of a living tissue to promote bone repair. However, the proliferation of harvested cells can take several weeks *in vitro*, which increases the possibility of genetic mutations and oncogenicity [9]. The high cost and the number of procedures required also affect the application of tissue-engineered bone. Compared with conventional tissue-

* Corresponding authors. National & Regional United Engineering Lab of Tissue Engineering, Department of Orthopaedics, Southwest Hospital, the Third Military Medical University, Chongqing, China. Tel.: +86 023 68754164; fax: +86 023 65340297.
E-mail addresses: tianyonghou@126.com, tianyonghou@tmmu.edu.cn (T. Hou), luofly1009@hotmail.com (F. Luo), jianzhong_xu@126.com (J. Xu).
[1] These authors equally contributed to this article.

http://dx.doi.org/10.1016/j.biomaterials.2014.03.079
0142-9612/

engineered materials, some biomaterials containing embedded factors [10,11] or enriched bone marrow [12–15] and platelet-rich plasma [12,16,17] have been shown to promote bone formation and can be easily fabricated for a specific application. Furthermore, bone marrow is the most common source of mesenchymal stem cells (MSCs) for tissue engineering [18]. Because it contains cells and growth factors, bone marrow has been known to magnify osteoinductive properties during bone formation. Bone marrow alone or in combination with an osteoconductive matrix has been reported to promote bone regeneration, particularly when combined with DBM [19–23]. In these studies, selective cell retention (SCR) technology used negative pressure to facilitate the permeation of the biomaterials by bone marrow under conditions of aspiration. As a result, the osteogenic stem cells are concentrated, thereby enriching the material with osteogenic stem cells and growth factors. When using this procedure, it is important to consider the pore size of the biomaterials that are being enriched, as the available pore size can significantly affect cell retention.

The pore size of DBM, approximately 200–500 μm, is larger than the size of cells, which is on the order of tens of micrometers. To improve cell retention, DBM was modified by the introduction of RADA16-I. RADA16-I, a type of nanoscale self-assembling peptide (SAP), is a synthetic matrix that is used to create defined three dimensional (3D) microenvironments for a variety of cell culture experiments. Under physiological conditions, RADA16-I self-assembles into a 3D hydrogel that exhibits a nanometer scale fibrous structure with an average pore size of 50–200 nm. The hydrogel can be readily formed within and outside of the DBM scaffold. RADA16-I has been used to promote bone regeneration in calvarial bone defects [24] and in femur bone defects [2] because of its favorable bone conduction properties, its ability to provide support for various cell types and growth factors, and its minimal infection risk compared to materials of animal origin such as extracellular matrix (ECM). Despite the use of SCR techniques and more aspirates, the cellular density in scaffold was not comparable to those obtained using the traditional cell culture methods [2]. Therefore, some factors that promote bone formation may be involved in this process.

To improve the adhesive properties of DBM, a nanoscale self-assembling peptide was used to modify DBM. Numerous properties of DBM/RADA16-I were analyzed and compared to those of unmodified DBM, including surface properties, the inner structure of them, pore size, and stability. The differences in the number and type of enriching cells were also determined to evaluate the adhesive properties of the scaffolds. The proliferation and differentiation of enriched MSCs in the DBM/RADA16-I scaffolds was analyzed using laser scanning microscopy and real-time RT-PCR analysis. In this study, the enriching factors were detected to explore a new potential osteogenic mechanism that has not been described in previous research. Finally, the enriched composites were transplanted into athymic mice to evaluate their osteogenic potential.

2. Materials and methods

2.1. Preparation of RADA16-I modified DBM

DBM (BIO-GENE®) was purchased from Datsing Biological Technology Co., Ltd. Before fabrication, the DBM scaffolds were submerged in deionized ultrapure water overnight at 4 °C. The scaffolds were then removed from the water and air dried [25]. The RADA16-I peptide ([COCH3]-RADARADARADARADA-[CONH2], molecular weight 1712) was commercially synthesized and purified (BD™ PuraMatrix™ Peptide Hydrogel, BD Biosciences, MA, USA). Each DBM (0.5 cm × 0.5 cm × 0.2 cm) was submerged in 400 μl of 0.5% RADA16-I deionized ultrapure water solution and maintained under ultrasonication conditions for 5 min. Supernumerary 400 μl phosphate-buffered saline (pH = 7.4) was added to the DBM scaffold to trigger RADA16-I gel formation.

2.2. Evaluating DBM/SAP

2.2.1. Surface observation

For morphological observation, a DBM/RADA16-I (DBM/SAP) scaffold was fabricated and immediately examined using environmental scanning electron microscope (ESEM) (Quanta™ 450 FEG, FEI, Netherlands). As a control, an unmodified DBM scaffold was also observed.

2.2.2. X-ray photoelectron spectroscopy (XPS)

To analyze its chemical composition and RADA16-I gel formation within the DBM scaffolds, samples were characterized using XPS (ESCALAB 250, ThermoFisher, USA) with a focused monochromatic Al Ka source (300 W, 15 kV) for excitation. An area of 0.125 mm^2 and depth of 5 nm was used in the constant analyzer energy mode for all measurements. XPS survey spectra over a binding energy (BE) range of 0–1200 eV were acquired. The degree of vacuum was 1×10^{-8} PamB (10 BPa), and the criterion of nuclear potential calibration was Cls = 285.0 eV. Data analysis was carried out with the Multipak software provided by the manufacturer. The BE scale was set by nitrogen only bound to nitrogen at 400 eV. For inner observation, the DBM and DBM/SAP samples were cut in half. Two samples from each group were acquired, and the survey scans were performed in two different areas on each sample.

2.2.3. Fibrilla of SAP and pore size of scaffold

RADA16-I was fabricated on mica slides and imaged to analyze the fibrilla property by atomic force microscopy at gaseous phase (SPI3800N-SPA400, Seiko, JAPAN). The spring constant of the cantilever was 200 N/m, and the length was 115 μm. A 200 nm triangular cantilever was applied in a 100 μm scanner (X: 115 μm, Y: 115 μm, Z: 29.97 μm). The pore size was detected by 3D video microscopy (KH-3000 VD, HIROX, Japan). After water was removed from the DBM/SAP samples using adsorbent paper, the samples were observed from 360°. The pore size of both the DBM and DBM/SAP scaffolds was detected (10 samples per group and 10 pores per sample) and compared. Pore size was determined by the mean of the maximal and minimal transverse diameters.

2.2.4. Stability analysis

The stability of the DBM/SAP samples was analyzed using an elution test. According to the process of enriching marrow, the DBM/SAP samples (n = 12) were immerged in phosphate-buffered saline solution and processed for four enriching cycles. Elution solution was analyzed by ultraviolet light absorbance (ultrospec4300 pro, GE, USA) compared with the DBM elution solution or 0.5% RADA16-I solution alone. This process was repeated for all 12 samples.

2.3. Bone marrow aspirate harvest and fabrication of the enriched composites

The iliac marrow of 12 adult volunteers was aspirated according to the regulation of Southwest Hospital Medical Ethical Committee, the Third Military Medical University (Chongqing, China). The volunteers were sufficiently informed of the experimental goals. For each volunteer, 20 ml of marrow (including 600 U/ml heparinate) was collected from several sites (4 ml from each site). One milliliter of marrow was used to detect the concentration of karyocytes, monocytes, and hemopoietic stem cells (HSCs) as a concentration of influent marrow (M1) using flow cytometry (FACSCalibur, BD, USA). Antibodies, including CD34-PE, CD45-Per CP, and nucleic acid dye (BD, USA), were used to detect karyocytes, monocytes, and HSCs. The samples were diluted 1:10, and 50 μl of the diluted sample was mixed with 10 μl of the staining liquid (CD34-PE, CD45-Per CP, and nucleic acid dye) (BD FACS™, USA) and incubated for 15 min. Finally, 10 μl of erythrocytolysin (BD FACS™) and 440 μl of transparent liquid (BD FACS™) were added to the staining solution and incubated for 30 min, and the samples were analyzed by flow cytometry. Two equal parts marrow (6 ml) for DBM alone and DBM/SAP was used as the influent volume (V1). The 2 samples of DBM/SAP (or DBM alone) were laid abreast in the sample box of BONE GROWTH PROMOTER (FUWOSI, Chongqing, China) to enrich the marrow for 4 cycles. The final effluent volume was labeled V2, and the concentration of karyocytes, monocytes, and HSCs in the effluent of the DBM alone or DBM/SAP samples were detected as a concentration of effluent marrow (M2) by flow cytometry. The enriched cell concentration (C), adherence rate (R) and enriching multiple (E) in scaffolds were calculated as follows: $C = (M1 \times V1 - M2 \times V2)/(V1 - V2)$, $R = (M1 \times V1 - M2 \times V2)/(M1 \times V1)$, and $E = C/M1$.

2.4. Observation of the enriching DBM/SAP

For morphological observation, enriched DBM/SAP and DBM samples were examined using ESEM (Quanta™ 450 FEG, FEI, Netherlands). A subset of samples were fixed in 10% neutral-buffered formalin for 48 h, dehydrated in graded alcohol solutions, and embedded in paraffin. The samples were sectioned (thickness = 5 μm), and the sections were stained with hematoxylin and eosin. Photomicrographs of the sections were taken using an Olympus BX-60 light microscope. The remaining samples were embedded in Tissue-Tek O.C.T., and 10 μm thick sections were incubated in a 1:200 dilution of anti-CD73 goat polyclonal antibody (SANTA CRUZ BIOTECHNOLOGY, INC., USA), 1:200 dilution of anti-CD90 goat polyclonal antibody (SANTA CRUZ BIOTECHNOLOGY, INC., USA), 1:100

Table 1
Primers used for real-time RT-PCR.

Target gene	Oligonucleotide sequence	Expected product (bp)
GAPDH forward	5′-CTTCAACAGCGACACCCACT-3′	226 bp
GAPDH reverse	5′-GTGGTCCAGGGGTCTTACTC-3′	
ALP forward	5′-GACCTCCTCGGAAGACACTC-3′	137 bp
ALP reverse	5′-TGAAGGGCTTCTTGTCTGTG-3′	
OPN forward	5′-CTGAACGCGCCTTCTGATTG-3′	103 bp
OPN reverse	5′-ATCTGGACTGCTTGTGGCTG-3′	
OCN forward	5′-AGCAAAGGTGCAGCCTTTGT-3′	63 bp
OCN reverse	5′-GCGCCTGGGTCTCTTCACT-3′	

Abbreviation: alkaline phosphatase (ALP), Osteopontin (OPN), and Osteocalcin (OCN).

dilution of anti-CD14 Rabbit polyclonal antibody (Abcam, England), or 1:100 dilution of anti-CD34 goat polyclonal antibody (SANTA CRUZ BIOTECHNOLOGY, INC., USA) overnight at 4 °C. Specimens were visualized using the DAB Horseradish Peroxidase Color Development Kit (Beijing ZSGB-BIO INC., China) and observed using an Olympus BX-60 light microscope.

2.5. Enriching rate of mesenchymal stem cells

MSCs derived from bone marrow were isolated using a density gradient solution (Histopaque, Sigma) and seeded at a concentration of 2×10^5 cells/cm^2 in a monolayer in standard medium (1:1 Dulbecco's modified Eagle's medium (DMEM)/Hamm's nutrient mixture F12, Hyclone, Logan, UT) with 15% fetal bovine serum (FBS, Hyclone, Logan, UT) as reported previously [26]. The medium was changed every 2–3 days based on the color, and the adherent cells were trypsinized, washed, and subcultured at a density of 1×10^4 cells/cm^2 in a new flask. The cultures were incubated at 37 °C in a humidified atmosphere containing 5% CO_2. Passage 3 cells were used for the experiments. To mimic the concentration of MSCs in bone marrow, 0.4×10^6 cells/ml MSCs were used to analyze the enriching rate of DBM/SAP scaffolds using SCR technology. The enriching process was the same as described above. The enriched cell concentration, adherence rate and enriching multiple in scaffolds were calculated as described above.

The enriched composites were cultured for 14 days in osteogenic medium (DMEM/F12 (Hyclone, Logan, UT) with 10% FBS (FBS, Hyclone, Logan, UT), 100 nM dexamethasone (Sigma, St. Louis, MO), 50 mM ascorbic acid 2-phosphate (Sigma, St. Louis, MO), and 10 mM b-glycerophosphate (Sigma, St. Louis, MO)). Cell distribution and osteogenic gene expression were detected by laser scanning microscope (LSM 780, ZEISS, Germany) and real-time RT-PCR. On days 3, 7, and 14, the specimens were washed twice with PBS and fixed with 4% paraformaldehyde for 20 min. Next, the specimens were permeabilized using 0.1% Triton X (Amresco, Solon, USA). The cytoskeletons and nuclei of the MSCs were stained with 25 mg/ml rhodamine-labeled phalloidin (Biotium, CA, USA) and 10 mg/ml 4,6-diamidino-2-phenylindole hydrochloride (DAPI; Sigma, St. Louis, MO), respectively.

RNA was extracted from the composites using Trizol (Invitrogen, Carlsbad, CA). Total RNA was isolated and purified using a RNeasy mini kit (Qiagen, Valencia, CA) with the addition of RNase-free DNase I (Qiagen). Purified RNA was quantified using a spectrophotometer, aliquoted, and stored at −20 °C. The two-step SYBR_ExScript_RT-PCR kit (Perfect Real Time, TaKaRa, Dalian, China) for real-time RT-PCR was used to analyze the expression of the following osteogenic genes: alkaline phosphatase (ALP), osteopontin (OPN), and osteocalcin (OCN). GAPDH was used as the housekeeping gene. Gene expression was quantified from standard curves and normalized to the level of GAPDH gene expression. The primers are described in Table 1.

2.6. Detecting factors in the enriched composites

After weighing and calculating the volume, 5 ml of each marrow-enriched DBM/SAP and DBM scaffolds was processed for protein extraction according to the manual of the protein array (Ray Biotech, Inc., USA). Briefly, the marrow was centrifuged to collect the supernatant for analysis. The enriched DBM/SAP and DBM samples were cut into small pieces, lysed in RIPA buffer containing 0.1 M PBS, 1% NP40, 0.1% sodium dodecyl sulfate, 5 mM EDTA, 0.5% sodium deoxycholate, 1 mM sodium orthovanadate, 1% PMSF and homogenized at 0–4 °C. After centrifugation, the supernatant was analyzed. The custom Quantibody human cytokine array was used. This assay is a multiplex sandwich enzyme-linked immunosorbent assay (ELISA)-based system that includes a membrane spotted with 22 selected cytokine- or chemokine-specific antibodies (Supplement 1). The procedure was performed according to the operations manual. Each antibody against a specific cytokine, together with the positive, negative and internal controls, was arrayed in quadruplicate. Data were extracted and analyzed using the RayBio QAM-TH17-1 software (RayBiotech, Inc.). For cytokine levels below the assay sensitivity threshold, a value of 0 was used when comparing the levels.

2.7. Transplantation of the enriched composites

For modeling and graft implantation studies, 8 athymic mice (33.5–38.5 g, 4–6 weeks old) were anesthetized by intraperitoneal injection of 0.5% sodium pentobarbital (45 mg/kg). The bilateral ilia were exposed using a posterolateral approach. The periosteum was erased using a knife, and an enriched DBM/SAP or DBM scaffold was implanted into the site of the right or left defective periosteum, respectively. Next, the grafts were fixed using a monofilament polypropylene suture (6-0, Urgalloy, Japan). After implantation, the muscle and skin were closed. Postoperatively, all mice were allowed to move freely without external support. The incision was disinfected, and antibiotics were administered intramuscularly once per day for 3 days after surgery.

2.8. Observation of bone regeneration

All mice were euthanized 56 days post-operation. The grafts were excised for imaging in air using micro-CT (Viva CT40, Scanco Medical AG, Bassersdorf,

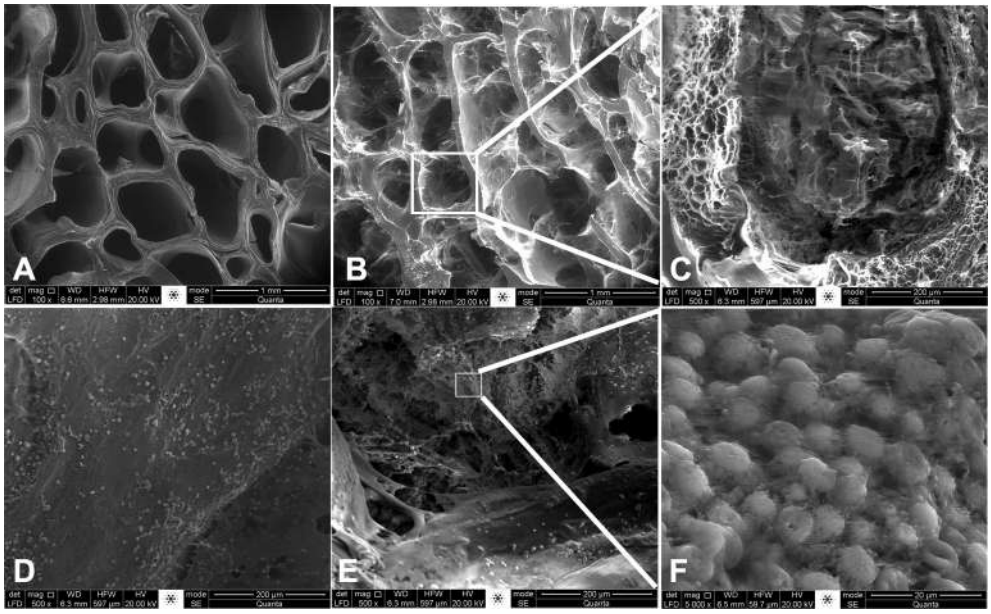

Fig. 1. Observation of DBM and DBM/SAP composite pre-enriching and post-enriching, respectively. A, the inner wall of the DBM alone scaffold was smooth; B, the pore of the DBM/SAP scaffold was filled with Sapeptide and had a net-like appearance, which is enlarged in C; D, a few cells were adhered to the DBM scaffold wall post-enriching; E, a large number of cells were adhered in the DBM/SAP composite post-enriching, and an enlarged image is shown in F.

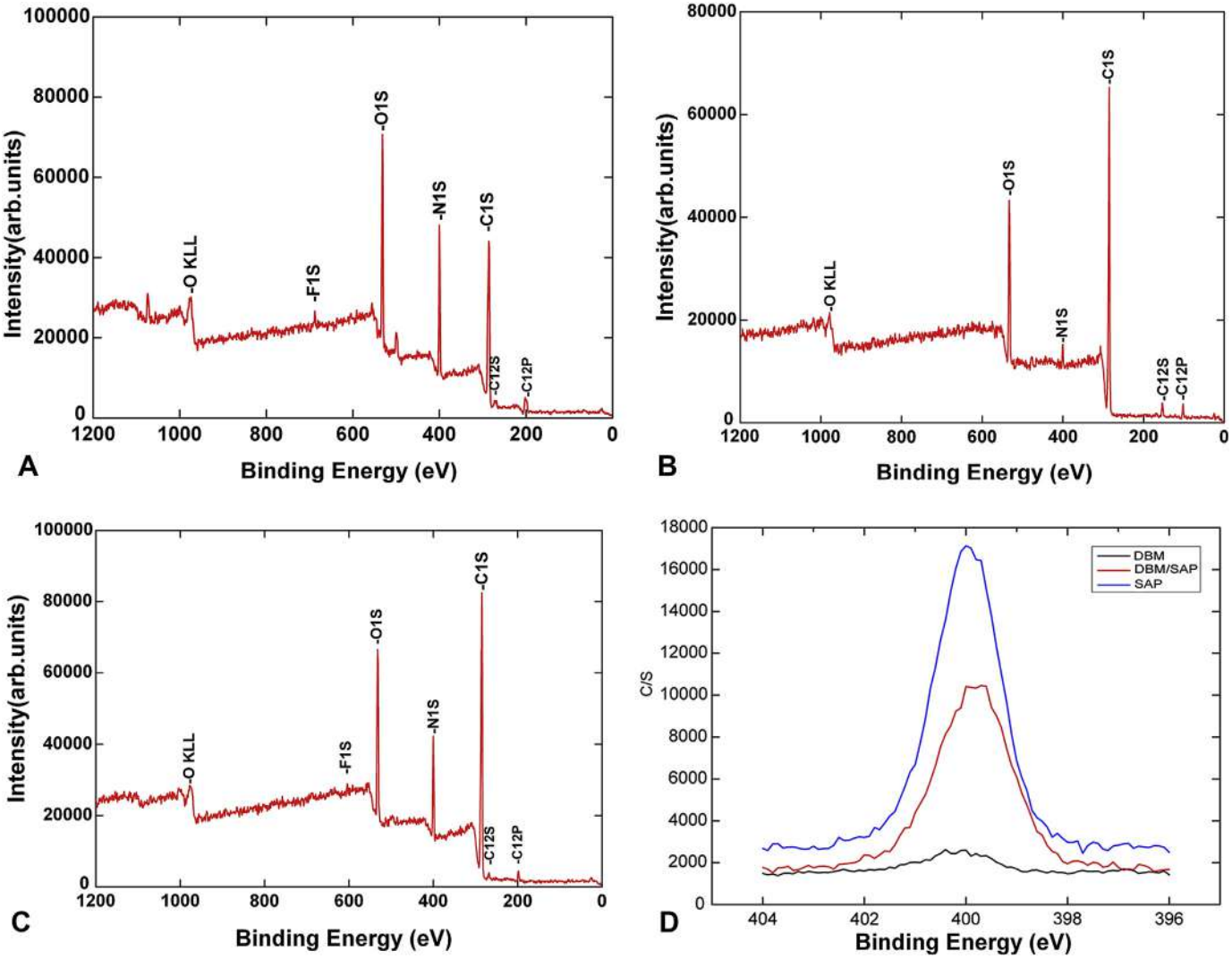

Fig. 2. The nitrogen, oxygen, and carbon contents of SAP (A), DBM (B), and DBM/SAP composite (C) were analyzed by XPS. The nitrogen content in SAP, DBM, and DBM/SAP composite was compared in D.

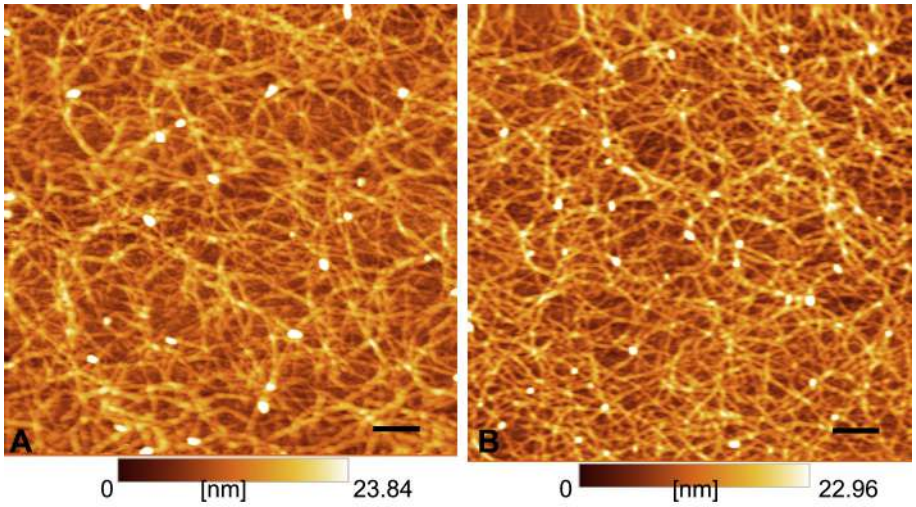

Fig. 3. AFM images of RADA16-I nanofiber at various time points after fabrication. The observations were made using AFM after sample preparation: 30 min (A) and 24 h (B).

Switzerland). The volume of new bone was derived from the CT images by delineating the areas of the contrast-enhanced regions of interest (ROI) in the *X*, *Y*, and *Z* planes. Images were obtained by adjusting the micro-CT data window display to enhance the edge delineation of the new bone mass. The 3D images of the grafts were reconstructed using a middle-frequency kernel. The quantitative measurements of the new bone were used to calculate bone volume per tissue volume (BV/TV) and bone mean density (BMD).

The grafts were sectioned into small bone blocks for histology and histomorphometry according to the procedures described below. Samples were fixed in 10% neutral-buffered formalin for 48 h, subjected to decalcification, dehydrated in graded alcohol solutions, and embedded in paraffin. Samples were then sectioned (thickness = 5 μm) and stained with hematoxylin and eosin and Masson's trichrome stains. Photomicrographs of the sections were taken using an Olympus BX-60 light microscope.

2.9. Statistical analysis

All data are presented as the mean ± SD and were subjected to a paired Student's *t*-test using the SPSS version 10.0 software package (SPSS Inc., Chicago, IL USA). The differences were considered significant if $p < 0.05$.

3. Results

3.1. Character of DBM/SAP

Observation by ESEM (Fig. 1) revealed that the surface along the inner wall of the DBM was smooth (Fig. 1A), and there were a few cells adhered to the DBM scaffold wall post-enrichment (Fig. 1D). In contrast, the pores of the nanoscale DBM/SAP composite scaffolds were filled with SAP and had a net-like appearance (Fig. 1B and C). This suggests that a large number of cells were adhered within the DBM/SAP composite scaffolds post-enrichment, particularly in the surface of the net formed by the nanoscale SAP (Fig. 1E and F).

XPS is a surface-sensitive analysis technique that is capable of providing both qualitative and quantitative information about the presence of different elements. The BE scale at 400 eV was used to detected the element nitrogen. The XPS analysis showed that, compared to the DBM scaffolds alone (Fig. 2B), an additional element, F (BE of 700 ev), was present in the DBM/SAP scaffolds (Fig. 2C), which is a result of the surface modification with the nanoscale SAP (Fig. 2A). The results of BE scale at 400 eV further demonstrated that the curve of the DBM/SAP scaffolds was located between that of the SAP and DBM scaffolds (Fig. 2D), confirming that the DBM/SAP scaffolds were fabricated from both DBM and SAP.

The net of the DBM/SAP scaffolds, formed by the nanoscale SAP, was further observed by AFM. The results showed that the diameter of the SAP was 12.03 ± 1.50 nm, and the pore size was 5–200 nm pore. Samples were observed using AFM between 30 min and 24 h after sample preparation, and the character of the SAP did not changed during this time (Fig. 3A) to 24 h (Fig. 3B). The pore diameters in the DBM and DBM/SAP scaffolds were 396.24 ± 121.65 μm and 20.22 ± 6.73 μm ($n = 100$), respectively.

After the DBM scaffolds were modified by SAP, the elution solution was analyzed to determine the stability of the DBM/SAP scaffolds. The absorbance values of the elution solutions from the DBM and DBM/SAP scaffolds were traced into a curve at wavelengths from 200 to 260 (Supplement 2A). As a positive control, 0.5% SAP solution alone was also analyzed. The curves of the DBM and DBM/SAP scaffolds were nearly coincident, whereas that of the SAP solution was higher. There was no significant difference between the mean maximum absorbance values for the DBM and DBM/SAP scaffolds; however, when compared to 0.5% SAP, the maximum absorbance values of both the DBM and DBM/SAP scaffolds were significantly lower ($p < 0.05$) (Supplement 2B). The results showed that the binding of SAP to the DBM scaffolds was stable, and the SCR process could not cause defluxion of the SAP from the DBM/SAP composite scaffolds.

3.2. Enriching cells by DBM/SAP and DBM

Four cycles of the SCR process were performed (Supplement 3). ESEM showed that numerous cells were adherent to the inner net of the DBM/SAP scaffolds and that these cells were uniformly distributed; however, only a few cells were adhered to the wall of

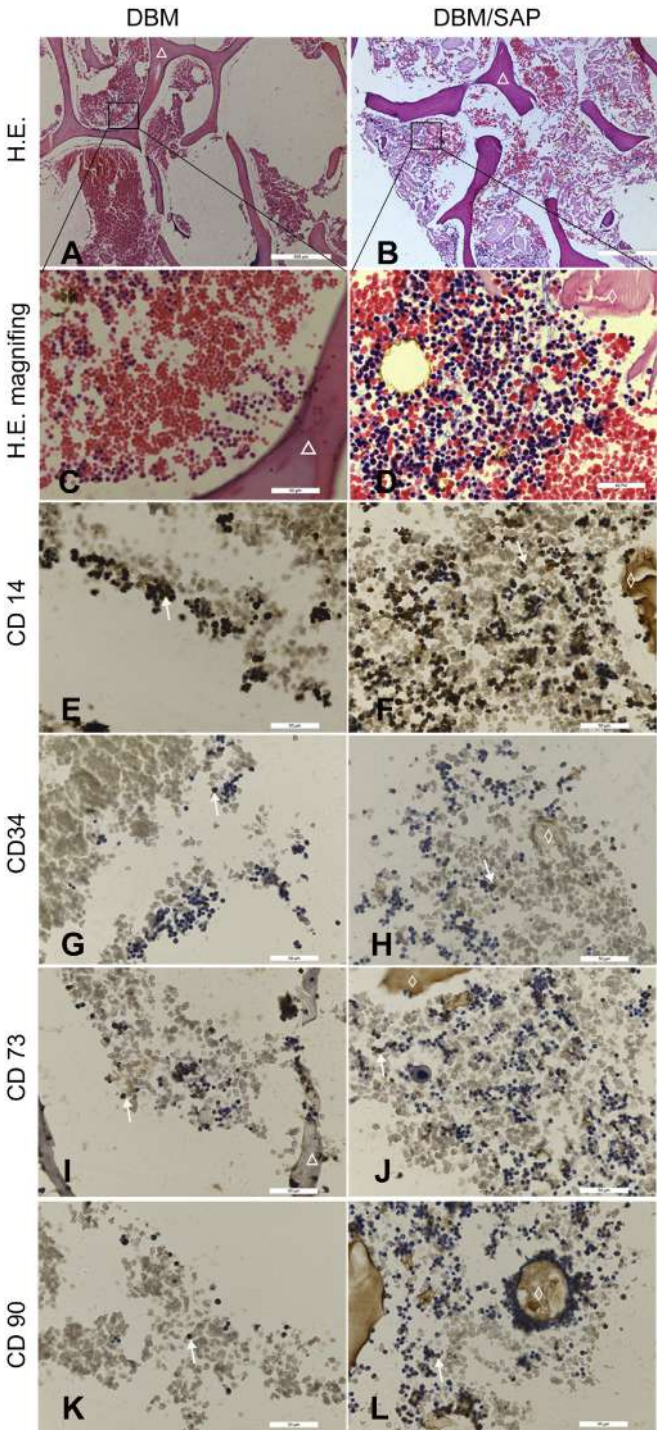

Fig. 4. H&E staining (A–D) for morphological observation and immunohistochemistry staining for cellular identification (E–L) were practiced after the DBM or DBM/SAP and bone marrow were fabricated and immediately sliced. The positive expression of CD73 (MSCs), CD105 (MSCs), CD14 (monocytes), and CD34 (hemopoietic stem cells) were demonstrated (arrows) in the DBM scaffold (triangle) and SAP modified materials (rhombus). Bar scales are 500 μm in A and B and 50 μm in C–L.

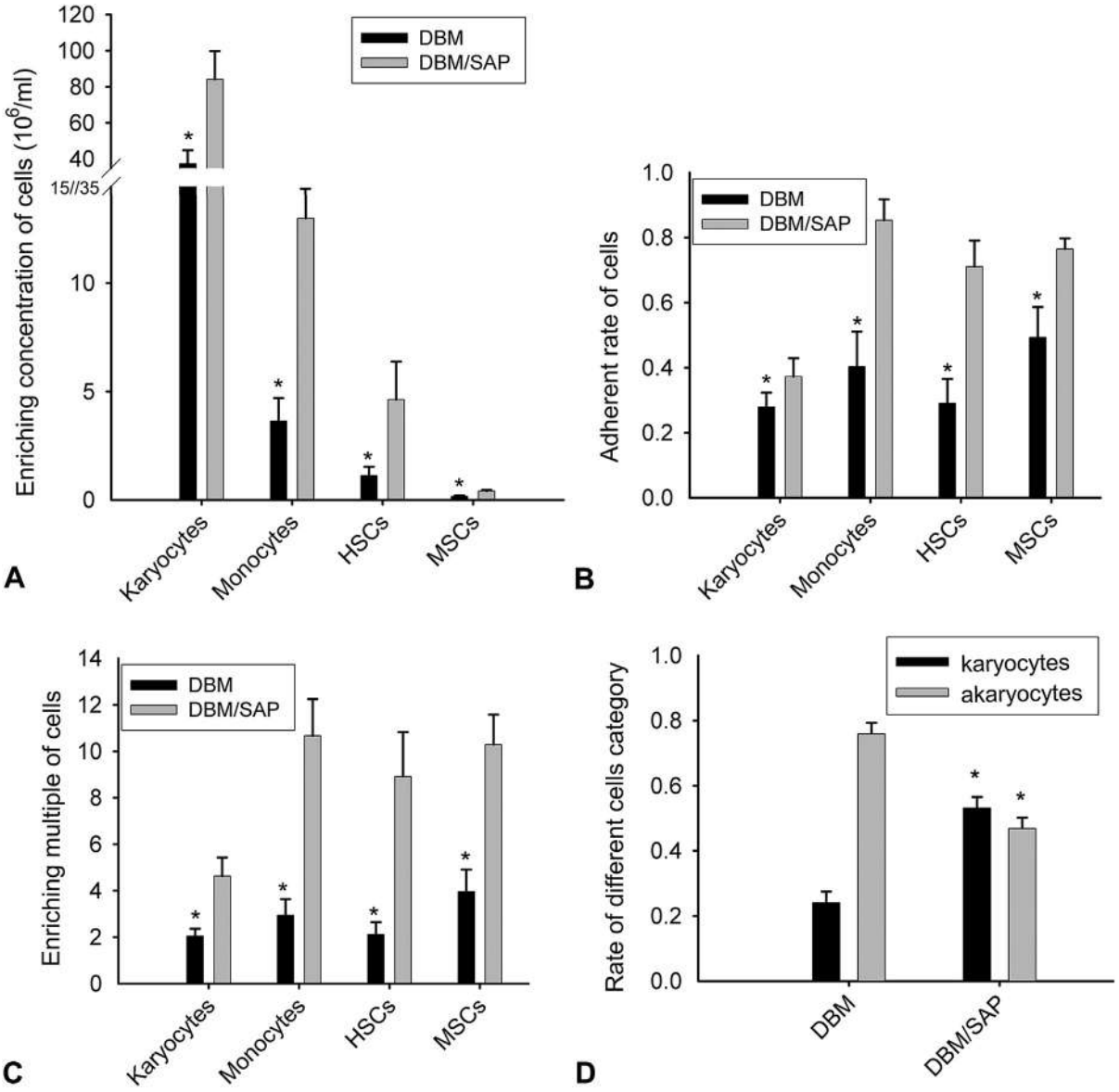

Fig. 5. The enriched concentration (A), adherence rate (B), enriching multiple (C), and rates of different cell categories (D) in the DBM or DBM/SAP scaffolds were detected after bone marrow or MSC solution (passage 3, 0.4×10^6/ml) was used for enrichment. The karyocytes, akaryocytes, monocytes, and hemopoietic stem cells (HSCs) were derived from bone marrow. *There was a significant difference between DBM and DBM/SAP ($p < 0.05$).

the DBM alone scaffolds, and these cells were irregularly distributed (Fig. 1). Further H&E staining demonstrated that red blood cells were a major portion of the enriched cells in the DBM alone scaffolds (Fig. 4A–D), with over 50% being akaryocytes (Fig. 5D). The number of karyocytes was significantly increased in DBM/SAP scaffolds, and slightly higher than the number of akaryocytes (Fig. 5D). There was a large amount of SAP biomaterial in the pores of the DBM scaffolds, and the enriched cells were located in the spaces among this biomaterial. Immunohistological staining revealed that monocytes (CD14 positive), HSCs (CD34 positive), and MSCs (CD73 or CD90 positive) were also included in the enriched cell population (Fig. 4E–L), but these cells were present in only small numbers. However, these cells types were present in higher numbers in the DBM/SAP scaffolds compared with the DBM alone scaffolds. FACS analysis precisely measured the enriched cell concentration (C), adherence rate (R) and enriching multiple (E) of the enriched cells, including karyocytes, monocytes, and HSCs, in the DBM/SAP and DBM alone scaffolds (Fig. 5 and Supplement 4). The enriched concentration, adherence rate, and enriching multiple of the DBM/SAP scaffolds were superior to those of the DBM alone scaffolds. This trend was consistent among the different cell types, including karyocytes, monocytes, and HSCs. The ratio of karyocytes and akaryocytes was determined by FACS (Fig. 5D). Karyocytes included monocytes, HSCs, MSCs, and additional cell types. The rate of karyocytes in the DBM/SAP scaffolds was significantly higher than that in the DBM alone scaffolds ($p < 0.05$). To detect the enriching ability of the DBM/SAP scaffolds, MSCs isolated from bone marrow and cultured for 3 passages were dissolved in medium at a physiological concentration. The MSC solution infiltrated into the DBM/SAP or DBM alone scaffolds using BONE GROWTH PROMOTER, similar to the procedure for bone marrow. The enriching results were consistent with those of bone marrow, and the enriched concentration, adherence rate, and enriching multiple of the DBM/SAP scaffolds surpassed those of the DBM alone

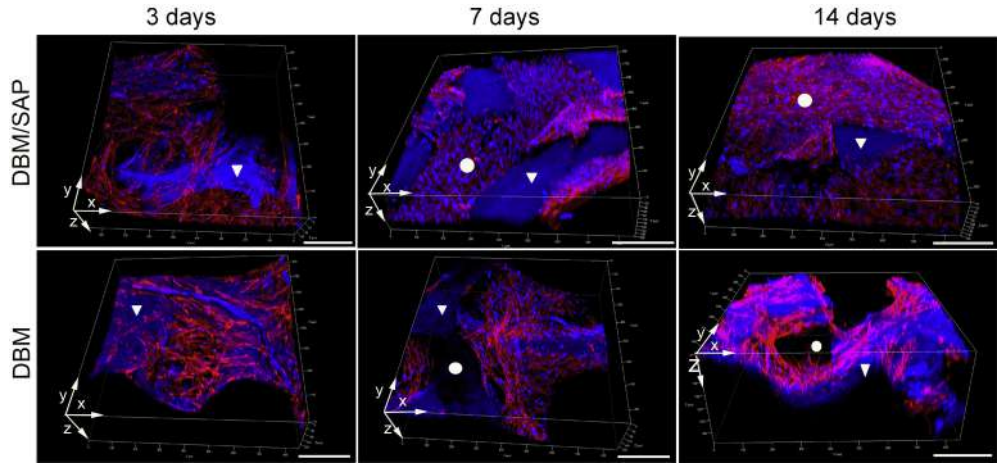

Fig. 6. Proliferation and distribution of MSCs in the DBM and DBM/SAP scaffolds after retention. MSCs was stained using phalloidin (red), and the cell nucleus and DBM scaffold (triangle) were visualized using DAPI (blue). More cells were observed in the DBM/SAP scaffold. Unlike the DBM alone scaffold, DBM/SAP could supply cell adhesion sites in the pores of the DBM due to the RADA16-I modification. In the DBM/SAP group, the cells proliferated on surface of the DBM and in the interior of the pores (round). Bar scale is 200 μm. (For interpretation of the references to color in this figure legend, the reader is referred to the web version of this article.)

scaffolds (Fig. 5). There was a significant difference between the DBM/SAP and the DBM alone scaffolds ($p < 0.05$).

3.3. Proliferation and osteogenic differentiation of enriched MSCs in DBM/SAP

MSC proliferation was observed during subsequent culture after the cells were retained within the scaffolds. Higher numbers of MSCs were observed in the DBM/SAP scaffolds (Fig. 6) compared to the DMB alone scaffolds. Unlike the DBM alone scaffolds, the DBM/SAP scaffolds provided cell adhesion sites were provided by the RADA16-I peptide, which was located in the interior of the pores within the DBM scaffolds. Therefore, MSCs proliferated not only on the surface of the DBM scaffolds but also in the interior of the pores in the DBM/SAP group. The enriched MSCs underwent osteogenic differentiation after induction with osteogenic medium. Analysis of the real-time RT-PCR results showed that the MSCs within the DBM/SAP scaffolds displayed higher levels of alkaline phosphatase (ALP), osteopontin (OPN), and osteocalcin (OCN) compared to the MSCs enriched in the DBM scaffolds. There was a significant difference between the DBM and DBM/SAP scaffolds ($p < 0.05$, Fig. 7).

3.4. Enriched factors by DBM/SAP and DBM

Three marrow samples were used to detect the factors enriched by the DBM/SAP and DBM scaffolds. Bone morphogenetic protein-6 (BMP-6), platelet-derived growth factor-BB (PDGF-BB), vascular endothelial growth factor (VEGF), and epidermal growth factor (EGF) were selected from 22 detected cytokines or chemokines (Supplement 1) because their concentrations were more than

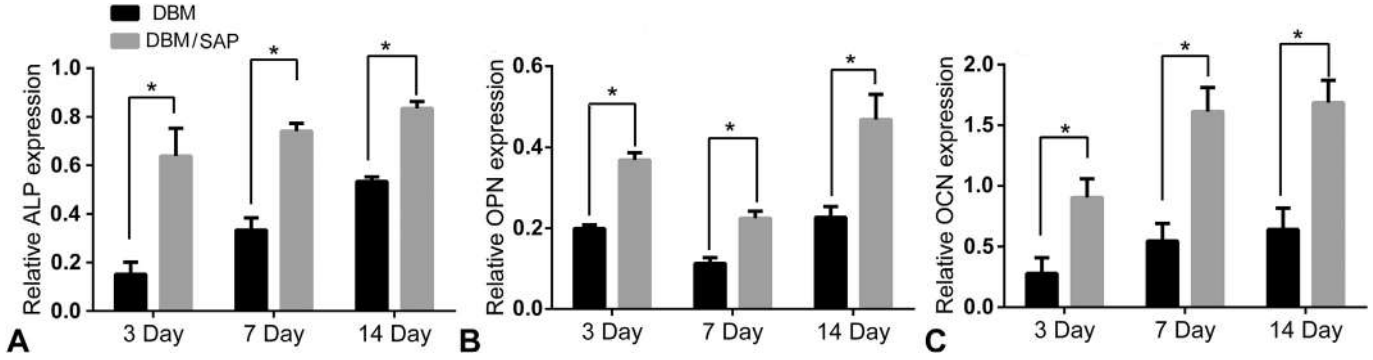

Fig. 7. Enriched MSCs underwent osteogenic differentiation following induction with osteogenic medium, as detected by real-time RT-PCR. Expression of osteogenic genes showed that MSCs enriched in the DBM/SAP scaffold displayed higher levels of alkaline phosphatase (ALP), osteopontin (OPN), and osteocalcin (OCN) than the MSCs enriched in the DBM scaffold. *There was a significant difference between DBM and DBM/SAP ($p < 0.05$).

Table 2
Analysis of enriching yield of different factors from bone marrow in DBM/SAP or DBM alone.

Factors (pg/ml)	DBM	Bone marrow sample 1			Bone marrow sample 2			Bone marrow sample 3		
		M alone	DBM+M	DBM/SAP+M	M alone	DBM+M	DBM/SAP+M	M alone	DBM+M	DBM/SAP+M
BMP-6	0.00	3288.43	325.87	7738.26	1804.05	2241.97	3218.87	751.25	0.00	0.00
PDGF-BB	0.00	570.82	424.36	1118.88	560.30	411.65	747.07	282.14	79.60	168.71
VEGF	0.00	28.79	22.45	25.15	15.30	25.10	62.55	32.84	0.00	0.00
EGF	0.00	17.02	40.64	85.93	13.61	33.48	77.11	10.59	10.60	12.00

10 pg/ml in bone marrow (Table 2). The concentrations of factors in the DBM/SAP enriched composite scaffolds were typically the highest and were higher than those in either the marrow alone or in the DBM enriched composite scaffolds, but the difference was not large, as determined for BMP-6, PDGF-BB, and VEGF in marrow sample 3 and VEGF in marrow sample 1. The maximal enriching multiple was 5.67 for EGF of sample 2. The mean enriching multiples of BMP-6, PDGF-BB, VEGF, and EGF were 1.38, 1.30, 1.65, and 3.95, respectively; however, DBM only exhibited an enriching effect on EGF, and not on the other factors.

3.5. Osteogenesis of DBM/SAP enriching composites

The morphology of the newly formed bone in the transplanted site was reconstructed using micro-CT, which showed that the new bone formation in the DBM/SAP group was greater than that in the

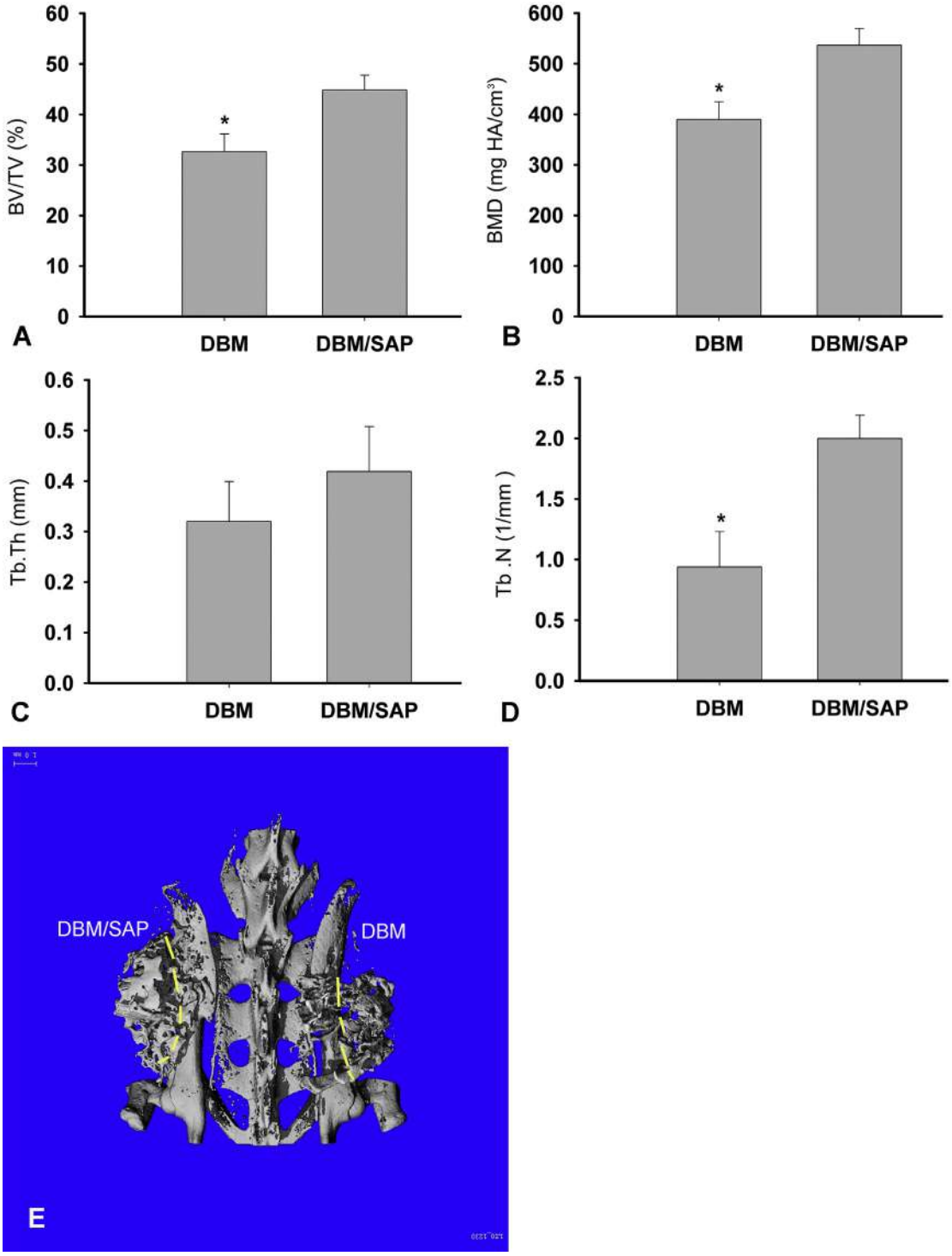

Fig. 8. Osteogenic observation of the grafts 56 days after implantation. DBM or DBM/SAP and bone marrow were fabricated using BONE GROWTH PROMOTER and were immediately transplanted into the latero-ilium of mice for 56 days. The morphology of the newly formed bone in the graft was reconstructed using micro-CT (E). Morphometric analysis of the BV/TV (A), BMD (B), Tb.Th (C), and Tb.N (D). *There was a significant difference between DBM and DBM/SAP ($p < 0.05$).

DBM alone group 56 days post-operation (Fig. 8E). Morphology measures were used to calculate the amount of newly formed bone in the transplanted sites. The calculated parameters showed that BV/TV in the DBM/SAP group was significantly greater than that in the DBM alone group (Fig. 8A). Additionally, BMD, Tb.Th, and Tb.N were also increased in the DBM/SAP group (Fig. 8B–D). There were significant differences in BV/TV, BMD, and Tb.N between the DBM/SAP and DBM groups, but not Tb.Th ($p < 0.05$). H&E (Fig. 9A and B) and Masson's (Fig. 9C and D) staining demonstrated that more newly formed bone tissue and mature bone tissue were present in the DBM/SAP group compared with the DBM alone group.

4. Discussion

It is well-known that bone marrow is osteogenic by virtue of its rich source of osteogenic stem cells. Some research and clinical applications have demonstrated that bone marrow can promote bone repair [12–15]. However, because bone marrow is fluid, when it is applied alone or with biomaterials as a graft composite through simple soaking, the osteogenic effect is not strong enough. It is difficult to retain bone marrow at the defect site for an adequate duration of time to allow for osteogenesis or to enrich enough osteogenic stem cells into the biomaterials through simple soaking to promote osteogenesis. Furthermore, osteogenic stem cells make up a very small percentage (e.g., MSCs <0.005%) of nucleated cells in healthy adult bone marrow [27]. Improved osteogenesis requires a higher quantity of cells and bone marrow. In all cases, bone marrow was limited to aspirates from the ilium (3–5 ml per site) to minimize peripheral blood dilution [28]. Therefore, valid bone marrow can be only harvested in limited amounts. To improve osteogenesis, SCR technology has been introduced to increase the enrichment of osteogenic stem cells [19–23]; however, the current research on enriching biomaterials for the promotion of osteogenic mechanisms is insufficient, even though SCR technology increases the osteogenic effect of some biomaterials. Physical interception through suitable pore size of scaffolds is the key mechanism to enriching cells from bone marrow. RADA16-I, a type of nanoscale SAP, was used to modify the DBM scaffolds and shrink the pore size. As a result, the mean pore size of the DBM/SAP scaffolds decreased to 20.22 μm after SAP modification compared to 396.24 μm for the DBM scaffolds. XPS and ESEM showed that nanoscale SAP could modify the surface and interior of the DBM scaffold. AFM revealed that RADA16-I SAP instantly formed nanoscale gel following triggering, and there was no change until 30 min post-triggering. Imitating SCR processes, the mean maximum absorbance values from the DBM/SAP scaffold elutant did not appear the same as the wave of SAP, which suggested that the interaction between the SAP and the DBM scaffolds was tight and stable. All of these findings demonstrated that the SAP could efficiently bind to the DBM scaffolds and modify its structure. The cellular counting results demonstrate that the decrease in pore size elevated the enriching yield of cells. Although previous studies have shown similar results [21], these studies did not describe the categories of the enriched cells or their present rates in the whole enriched population.

As peripheral blood, bone marrow also includes karyocytes and akaryocytes. The number of karyocytes (including monocytes, MSCs and HSCs) is relatively less than that of akaryocytes; however, their detection is easy, and the osteogenic effect mainly depends on them. Therefore, karyocytes, monocytes, and HSCs have been analyzed for enriching yield, but MSCs had not been studied because of their very low concentration in bone marrow. As a different method, MSC enrichment was performed with isolated MSCs in a manner that mimicked the physiological concentration. Compared with the DBM alone scaffolds, the DBM/SAP scaffolds can significantly increase all types of karyocytes, as demonstrated by the results of the flow cytometry analysis. This analysis showed that the DBM/SAP scaffolds could significantly increase the rate of karyocytes in the enriched cells. Morphological observations showed that more karyocytes were retained in the DBM/SAP scaffolds than in the DBM alone scaffolds. Immunohistochemistry staining confirmed the existence of monocytes (CD14 positive), MSCs (CD73 and CD90 positive), and HSCs (CD34 positive). As an analog of ECM, RADA16-I can not only decrease the pore size of the scaffolds but also build an extracellular microenvironment [29]. As a ligand for cell adhesion receptors, oligopeptides of RADA16-I also can promote cellular adhesion, especially that of karyocytes [30]. All of these properties are potentially beneficial to karyocyte enrichment, just as monocytes, MSCs, and HSCs. As an ECM-like substance, RADA16-I can also promote bone regeneration by supporting various different cell types and growth factors [2,21]. Compared with the DBM alone scaffolds, RADA16-I in DBM/SAP scaffolds can supply more sites for cell adherence. RADA16-I can also produce an ECM-like microenvironment and direct mineralization [31], which may promote the osteogenic differentiation of MSCs. Therefore, DBM/SAP scaffolds can elevate the osteogenesis of the bone marrow composite compared with the DBM alone scaffolds.

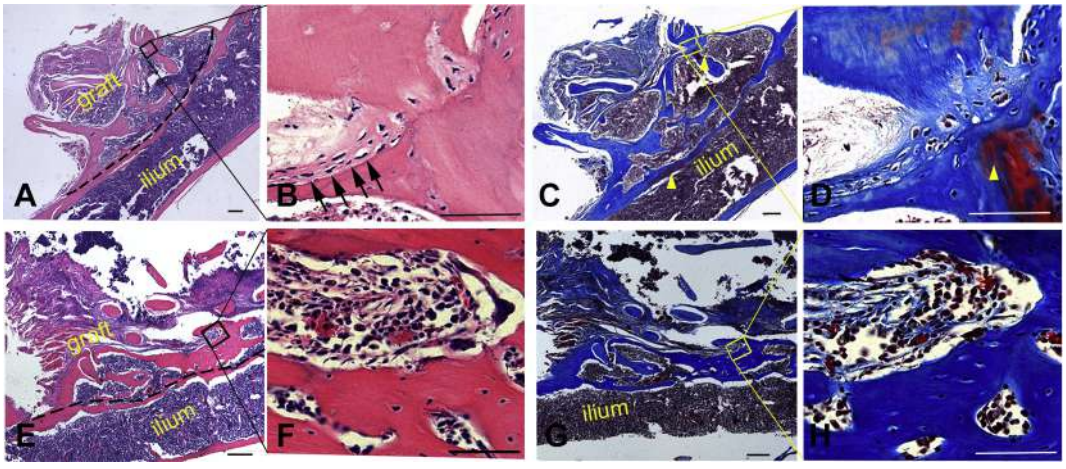

Fig. 9. The osteogenic observation of DBM/SAP (A–D) and DBM (E–H) were shown by H&E (A, B, E, and F) and Masson's (C, D, G, and H) staining after they underwent selective cell retention in bone marrow and were transplanted into mice for 56 days. The newly formed bone was more obvious in the DBM/SAP group than in the DBM alone group, and osteoblasts were observed in the grafts of the DBM/SAP group (black arrow). Mature bone tissue (yellow triangle) was also visible in the DBM/SAP group. Bar scale is 200 μm. (For interpretation of the references to color in this figure legend, the reader is referred to the web version of this article.)

One challenge to this approach is that the rate of osteogenic stem cells is low in the enriched cells; however, retained factors possibly contribute to osteogenesis. Twenty two cytokines or chemokines that can promote osteogenesis were selected, and their concentrations in bone marrow were detected according to a standard. The factors were analyzed for their enriching ability of the scaffolds if their concentrations were more than 10 pg/ml in bone marrow. Finally, BMP-6, PDGF-BB, VEGF, and EGF were chosen for evaluation. Except for EGF, the DBM alone scaffolds did not display any essential enriching effect on other factors. In contrast, the DBM/SAP scaffolds had increased enriching concentrations for all 4 factors. The cytokines enriched by the DBM/SAP were possibly due to both the physical presence of the nanofibers and the charge of SAP. RADA16-I SAP has been used as a vehicle for controlled release of factors based on the above mechanisms [29,32]. As is well known, most factors have positive charges or negative charges [32]. For example, VEGF has net negative charges at pH 7.4. SAP also has some charges. Although RADA16-I has no residual charge at pH 7.4 [32], SAP has regular repeating units of positively charged residues (arginine) and negatively charged residues (aspartic acid) compared with hydrophobic residues (alanine) [33]. In fact, factors with positive charges possibly interact with aspartic acid and then adhere to RADA16-I SAP. In contrast, factors with negative charges may interact with the arginine of RADA16-I SAP. This may explain why the DBM/SAP scaffolds can enrich more factors than the DBM alone scaffolds.

DBM/SAP enriched composites were transplanted into peri-ilia to evaluate their osteogenic capabilities compared to those of the DBM alone enriched composites. The histological observation and micro-CT showed more newly formed bone in the DBM/SAP group. The potent ingredients include nanoscale SAP as well as more enriched osteogenic stem cells and factors. RADA16-I SAP can promote bone reconstruction [24] through its interaction with cells and its regulation of cellular functions such as adhesion, migration, proliferation, and differentiation [29]. Additionally, the enriching osteogenic stem cells (MSCs) and factors (BMP-6, PDGF-BB, VEGF, and EGF) can also accelerate bone formation.

5. Conclusion

RADA16-I, a nanoscale SAP, was used to modify DBM scaffolds to improve their enriching ability. Compared with DBM alone scaffolds, the DBM/SAP scaffolds had a smaller and more suitable pore size and more available charged group. Through physical and charge interactions, the DBM/SAP scaffolds can be enriched with more osteogenic stem cells and factors from bone marrow. As a similar structure and effect of ECM, RADA16-I SAP can further reinforce the osteogenesis of the DBM scaffolds by creating an osteogenic microenvironment that promotes the interaction of the DBM with the cells and regulates cellular functions. In brief, DBM/SAP enriched composites may be a useful new supply of suitable bone grafts for clinical use.

Acknowledgments

This work was supported by the Foundation of Southwest Hospital (SWH2013JS07), CSTC (2010BB5163), the National High Technology Research and Development (863) Program of China (2012AA020504), and the Military Foundation (BWS11C040).

Appendix A. Supplementary data

Supplementary data related to this article can be found at http://dx.doi.org/10.1016/j.biomaterials.2014.03.079.

References

[1] Ye S, Seo KB, Park BH, Song KJ, Kim JR, Jang KY, et al. Comparison of the osteogenic potential of bone dust and iliac bone chip. Spine J 2013;13:1659–66.
[2] Nakahara H, Misawa H, Yoshida A, Hayashi T, Tanaka M, Furumatsu T, et al. Bone repair using a hybrid scaffold of self-assembling peptide PuraMatrix and polyetheretherketone cage in rats. Cell Transplant 2010;19(6):791–7.
[3] Sen MK, Miclau T. Autologous iliac crest bone graft: should it still be the gold standard for treating nonunions? Injury 2007;38(Suppl. 1):S75–80.
[4] LeGeros RZ. Properties of osteoconductive biomaterials: calcium phosphates. Clin Orthop Relat Res 2002;395:81–98.
[5] Conz MB, Granjeiro JM, Soares Gde A. Hydroxyapatite crystallinity does not affect the repair of critical size bone defects. J Appl Oral Sci 2011;19(4):337–42.
[6] LeGeros RZ. Calcium phosphate-based osteoinductive materials. Chem Rev 2008;108(11):4742–53.
[7] Schubert T, Lafont S, Beaurin G, Grisay G, Behets C, Gianello P, et al. Critical size bone defect reconstruction by an autologous 3D osteogenic-like tissue derived from differentiated adipose MSCs. Biomaterials 2013;34(18):4428–38.
[8] Urist MR. Bone: formation by autoinduction. Science 1965;150:893–9.
[9] Rubio D, Garcia-Castro J, Martín MC, de la Fuente R, Cigudosa JC, Lloyd AC, et al. Spontaneous human adult stem cell transformation. Cancer Res 2005;65(8):3035–9.
[10] Ko IK, Ju YM, Chen T, Atala A, Yoo JJ, Lee SJ. Combined systemic and local delivery of stem cell inducing/recruiting factors for in situ tissue regeneration. FASEB J 2012;26(1):158–68.
[11] Song G, Habibovic P, Bao C, Hu J, van Blitterswijk CA, Yuan H, et al. The homing of bone marrow MSCs to non-osseous sites for ectopic bone formation induced by osteoinductive calcium phosphate. Biomaterials 2013;34(9):2167–76.
[12] Zhong W, Sumita Y, Ohba S, Kawasaki T, Nagai K, Ma G, et al. In vivo comparison of the bone regeneration capability of human bone marrow concentrates vs. platelet-rich plasma. PLoS One 2012;7(7):e40833.
[13] Siwach RC, Sangwan SS, Singh R, Goel A. Role of percutaneous bone marrow grafting in delayed unions, nonunions and poor regenerates. Indian J Med Sci 2001;55(6):326–36.
[14] Niedźwiedzki T. Effect of bone marrow on healing of fractures, delayed unions and pseudoarthroses of long bones. Chir Narzadow Ruchu Ortop Pol 1993;58(3):194–204.
[15] Connolly JF, Guse R, Tiedeman J, Dehne R. Autologous marrow injection as a substitute for operative grafting of tibial nonunions. J Clin Orthop 1991;266:259–70.
[16] Nather A, Wong KL, David V, Pereira BP. Allografts with autogenous platelet-rich plasma for tibial defect reconstruction: a rabbit study. J Orthop Surg (Hong Kong) 2012;20(3):375–80.
[17] Messora MR, Nagata MJ, Pola NM, de Campos N, Fucini SE, Furlaneto FA. Effect of platelet-rich plasma on bone healing of fresh frozen bone allograft in mandibular defects: a histomorphometric study in dogs. Clin Oral Implants Res 2013;24(12):1347–53.
[18] Friedenstein AJ, Piatetzky-Shapiro II, Petrakova KV. Osteogenesis in transplants of bone marrow cells. J Embryol Exp Morphol 1966;16:381–90.
[19] Muschler GF, Nitto H, Matsukura Y, Boehm C, Valdevit A, Kambic H, et al. Spine fusion using cell matrix composites enriched in bone marrow-derived cells. Clin Orthop 2003;407:102–18.
[20] Muschler GF, Matsukura Y, Nitto H, Boehm CA, Valdevit AD, Kambic HE, et al. Selective retention of bone marrow-derived cells to enhance spinal fusion. Clin Orthop Relat Res 2005;432:242–51.
[21] Brodke D, Pedrozo HA, Kaput TA, Attawia M, Kraus KH, Holy CE, et al. Bone grafts prepared with selective cell retention technology heal canine segmental defects as effectively as autograft. J Orthop Res 2006;24(5):857–66.
[22] Lee Kevin, Stuart B. Cell therapy for secondary osteonecrosis of the femoral condyles using the Cellect DBM System: a preliminary report. J Arthroplasty 2009;24(1):43–8.
[23] Fitzgibbons TC, Hawks MA, McMullen ST, Inda DJ. Bone grafting in surgery about the foot and ankle: indications and techniques. J Am Acad Orthop Surg 2011;19(2):112–20.
[24] Misawa H, Kobayashi N, Soto-Gutierrez A, Chen Y, Yoshida A, Rivas-Carrillo JD, et al. PuraMatrix facilitates bone regeneration in bone defects of calvaria in mice. Cell Transplant 2006;15(10):903–10.
[25] Hou T, Li Q, Luo F, Xu J, Xie Z, Wu X, et al. Controlled dynamization to enhance reconstruction capacity of tissue engineered bone in healing critically sized bone defects: an in vivo study in goats. Tissue Eng Part A 2010;16(1):201–12.
[26] Xing J, Hou T, Luobu B, Luo F, Chen Q, Li Z, et al. Anti-infection tissue engineering construct treating osteomyelitis in Rabbit Tibia. Tissue Eng Part A 2013;19(1–2):255–63.
[27] Muschler GF, Boehm C, Easley K. Aspiration to obtain osteoblast progenitor cells from human bone marrow: the influence of aspiration volume. J Bone Jt Surg Am 1997;79:1699–709.
[28] Garg NK, Gaur S. Percutaneous autogenous bone-marrow grafting in congenital tibial pseudarthrosis. J Bone Jt Surg Br 1995;77:830–1.
[29] Luo Z, Zhang S. Designer nanomaterials using chiral self-assembling peptide systems and their emerging benefit for society. Chem Soc Rev 2012;41(13):4736–54.

[30] Zhang S, Holmes TC, DiPersio CM, Hynes RO, Su X, Rich A. Self-complementary oligopeptide matrices support mammalian cell attachment. Biomaterials 1995;16(18):1385–93.
[31] Hartgerink JD, Beniash E, Stupp SI. Self-assembly and mineralization of peptide-amphiphile nanofibers. Science 2001;294(5547):1684–8.
[32] Gelain F, Unsworth LD, Zhang S. Slow and sustained release of active cytokines from self-assembling peptide scaffolds. J Control Release 2010;145(3):231–9.
[33] Holmes TC, de Lacalle S, Su X, Liu G, Rich A, Zhang S. Extensive neurite outgrowth and active synapse formation on self-assembling peptide scaffolds. Proc Natl Acad Sci U S A 2000;97:6728–33.

TISSUE ENGINEERING: Part A
Volume 21, Numbers 7 and 8, 2015

DOI: 10.1089/ten.tea.2014.0294

The Osteogenetic Efficacy of Goat Bone Marrow-Enriched Self-Assembly Peptide/Demineralized Bone Matrix *In Vitro* and *In Vivo*

Zhiqiang Li, PhD,[1–4] Tianyong Hou, PhD,[1–3] Moyuan Deng, PhD,[1–3] Fei Luo, PhD,[1–3] Xuehui Wu, PhD,[1–3] Junchao Xing, PhD,[1–3] Zhengqi Chang, PhD,[1–3] and Jianzhong Xu, PhD[1–3]

In clinical practice, the prolonged duration, high cost, critical technique requirements, and ethical issues make the classical construction method of tissue-engineered bones difficult to apply widely. The major essentials in tissue engineering strategies include seed cells, growth factors, and scaffolds. This study aimed to incorporate these factors in a rapid and cost-effective manner. A self-assembly peptide/demineralized bone matrix (SAP/DBM) composite was artificially established and used for bone marrow enrichment via a selective cell retention approach. Then, goat mesenchymal stem cells (gMSCs) were seeded onto the SAP/DBM or DBM. The proliferation status of gMSCs in different scaffolds was analyzed, and the osteogenetic efficacy was evaluated after osteogenic induction. Bilateral critical-sized femoral defects (20-mm in length) were created in goats, and then the defects were implanted with the postenriched composite or DBM. Then, bone scan imaging, micro-computed tomography (CT) analysis and histological examination were performed to assess the reparative effects of the different implants. Compared with the DBM scaffolds, the growth of gMSCs in the postenriched SAP/DBM composite was faster and the expression levels of the osteo-specific genes (i.e., alkaline phosphatase, osteocalcin, osteopontin, and runt-related transcription factor 2) were significantly higher after 14 days of osteogenic induction. More importantly, the postenriched SAP/DBM composite significantly enhanced bone metabolic activity in the defect area compared with DBM at 2 and 4 weeks postoperation. Moreover, bone reconstruction was complete in marrow-enriched SAP/DBM composite, but not in the DBM. In addition, all of the osteo-related parameters, including the ratio of bone volume to total bone volume, bone mineral density, new trabecular number, and new trabecular thickness, were significantly higher in the marrow-enriched SAP/DBM than those in the DBM. These results indicated that the SAP/DBM composite held great potential for clinical applications; immediate implantation after marrow enrichment could be a new and effective strategy for treating bone defect.

Introduction

The classical strategy for tissue-engineered bones involves roughly four steps: (i) collection of seed cells; (ii) *in vitro* expansion and induction of seed cells; (iii) seeding cells into the scaffolds and coculturing; and (iv) *in vivo* transplantation. Despite the excellent efficacy, this strategy is limited by high manufacturing costs and possible security issues.[1] In the field of bone tissue engineering, bone marrow is one of the most important source of seed cells, as mesenchymal stem cells (MSCs) derived from bone marrow have been universally recognized for their multi-lineage differentiation potentials and reliable reparative capacity.[2,3] Bone marrow contains various types of cells and growth factors.[4] During the process of bone tissue engineering, only MSCs in marrow are collected, while other compositions with important roles in osteogenesis, such as hematopoietic stem cells, platelets and growth factors, are discarded. The injection of bone marrow into the lesion site can avoid such drawbacks and has been proven to have benefits.[5,6] However, this strategy was greatly constrained by the tremendous amount of marrow required, multiple doses of marrow required, and low marrow concentrations in the local transplantation site. Therefore, this study focused on the osteogenic efficacy of concentrated marrow. Within a special self-assembly peptide microenvironment (RADA16-I), the marrow was concentrated using the selective cell retention (SCR) strategy. This strategy could be accomplished

[1]National & Regional United Engineering Lab of Tissue Engineering, Department of Orthopaedics, Southwest Hospital, The Third Military Medical University, Chongqing, China.
[2]Center of Regenerative and Reconstructive Engineering Technology in Chongqing City, Chongqing, China.
[3]Tissue Engineering Laboratory of Chongqing City, Chongqing, China.
[4]Department of Orthopedics, Chengdu Military General Hospital, Chengdu, China.

directly during the surgery, without any manufacturing courses.

Peptide RADA16-I (AcN-RADARADARADARADA-$CONH_2$) consists of a 16 amino acid sequence and in physiological solutions, it can assemble into a three-dimensional (3D) interweaving nano-fiber scaffold by itself.[7–9] The low biomechanical strength is the main obstacle to its application as a bone scaffold. In the present stage, it is difficult to balance bioactivity with biomechanics in one single bone graft. Like autologous bones, demineralized bone matrix (DBM) is one of the most common materials used for bone grafts.[10,11] However, the mean pore size of DBM is so large that flowing marrow cannot be detained for enrichment. Thus, we tried to create a compound microenvironment to enrich marrow in DBM with inlaid self-assembly peptide (SAP). Various essentials related with osteogenesis, including stem cells, growth factors, artificial extracellular matrix (ECM), and mechanical support, were integrated into the compound's microenvironment.[12] Moreover, the fabricated method was simple, safe, and rapid. To the best of our knowledge, treating critical-sized femoral defects in goats with bone marrow-enriched SAP/DBM composite is original in the field of tissue engineering applications. It proposes a promising method for clinical application.

Materials and Methods

DBM modification with SAP

Goat allogeneic DBMs were prepared as previously described.[13] These DBMs were cut into blocks ($10\times10\times5$ mm) and slices ($5\times5\times1$ mm) for grafting and cell culture, respectively. RADA16-I with purity over 95% (China peptides Co., Ltd., Shanghai, China) was dissolved with a 20% sucrose solution to a final concentration of 0.5% (w/v). DBMs were immersed in the peptide solution for 5 min and then were washed with phosphate-buffered saline (PBS, $1\times$). The microscopic structures of different materials were observed with an Environmental Scanning Electron Microscope (ESEM) (Quanta™ 450 FEG; FEI, Eindhoven, The Netherlands).

Evaluation of SAP morphology

Ten microliters of the peptide solution was dropped onto a freshly cleaved mica surface for 10 s and then rinsed with 100 μL of distilled water to induce self-assembling. The samples were dried in air. Images were acquired by Atomic Force Microscope (AFM) (SPI3800N-SPA400; Seiko, Japan).

Postenrichment morphological observation

The morphological characteristics of bone marrow-enriched SAP/DBM and DBM were revealed by histological staining. A subset of samples were fixed in 4% paraformaldehyde for 48 h and embedded in paraffin. Then, sections (5 μm thick) were prepared from samples and stained with hematoxylin and eosin (H&E). Photomicrographs were taken with a light microscope (LEICA DM 6000B, Stuttgart, Germany).

Cell proliferation assay

Cell proliferation status was analyzed using the commercial Cell Counting Kit-8 (CCK-8; Beyotime, Shanghai, China). Ten thousand cells were suspended in a total of 80 μL of medium, and were seeded on one side of DBM or RAD/DBM scaffolds (length × width × height: $5\times5\times1$ mm, $n=6$/group) without spillage of cells. After incubation 2 h for cell attachment, the opposite side was seeded in the same way. Then, the scaffolds were transferred to 48-well culture plates and cultured in Dulbecco's modified Eagle's medium (Hyclone, South, Logan, UT) at 37°C and 5% CO_2. At 3, 7, and 14 days, 20 μL of CCK-8 solution was added to each scaffold with a total of 200 μL medium, and samples were incubated for 2 h at 37°C. One hundred microliters of incubated cell suspension from each scaffold was transferred to a 96-well plate, and the optical density (OD) was measured at 450 nm using a microplate reader (Varioskan; Thermo, Waltham, MA).

Cell distribution after osteogenic differentiation

Using a bone marrow concentrator device (FWS Co., Ltd., Chongqing, China), 5 mL of goat iliac marrow was enriched with a SAP/DBM or DBM scaffold. Goat mesenchymal stem cells (gMSCs) were harvested as previously described.[14] Sixty to 80 μL of cell suspension was slowly instilled onto one side of the postenriched SAP/DBM or DBM. After incubation for 2 h, the opposite side was seeded in the same way. The resulting composites were cultured with osteogenic medium containing 0.1 mM dexamethasone, 50 mM ascorbic acid phosphate (Wako Chemicals USA, Richmond, VA), and 10 mM β-glycerol phosphate. The media were changed twice a week. After 7 and 14 days, the composites were collected, rinsed with PBS twice, fixed with 4% paraformaldehyde for 20 min, and then permeabilized with 0.1% Triton X (Amresco, Solon, OH). The cytoskeletons of gMSCs were stained with 25 μg/mL rhodamine-labeled phalloidin (Biotium, Hayward, CA) for 30 min. The nuclei were stained with 10 μg/mL 4′,6′-diamidino-2-phenylindole hydrochloride (DAPI; Beyotime) for 5 min. Subsequently, the specimens were visualized using a confocal laser scanning microscope (LSM 780; Zeiss, Jena, Germany).

Quantitative real-time reverse transcription–polymerase chain reaction assay

To evaluate the osteogenic differentiation of gMSCs in the bone marrow-enriched SAP/DBM composite, the mRNA expression levels of alkaline phosphatase (*ALP*), osteocalcin (*OCN*), osteopontin (*OPN*), and runt-related transcription factor 2 (*Runx2*) were assessed at days 7 and 14 of culture. Total RNA was extracted with TRIzol reagent (Invitrogen, Carlsbad, CA) and an RNeasy Mini kit (Qiagen, Valencia, CA) according to the instruction. cDNA was synthesized as follows: 37°C for 15 min and 85°C for 10 s. Then, polymerase chain reaction (PCR) assays were performed in a CFX96 Thermocycler (Bio-Rad, Hercules, CA) using the following parameters: 95°C for 2 min followed by 40 cycles of 95°C for 10 s, 60°C for 10 s, and 72°C for 20 s. mRNA expression levels were measured via PrimeScript™ RT reagent Kits (TaKaRa, Shiga, Japan) and SYBR® Green Realtime PCR Master Mix according to the manufacturer's instructions. All primer sequences (Sangon Biotech Co., Ltd., Shanghai, China) were designed using primer 5.0 software and were summarized in Table 1. All assays were repeated thrice in duplicate. The relative expression level of

Table 1. Primers for Real-Time Polymerase Chain Reaction in This Study

Gene	*GenBank ID*		*Sequence*	*Size (bp)*
ALP	XM_005677026	Forward primer	5′ CCACCTTTCCCAGCCACATC 3′	70
		Reverse primer	5′ CATGGCGTACTCCAAGACCT 3′	
OCN	AY661470.1	Forward primer	5′ GGTGGTGAAGAGACTCAGGC 3′	95
		Reverse primer	5′ GCTCACACACCTCCCTCTTG 3′	
OPN	EU295699.1	Forward primer	5′ CCTGTTAATACCTGTCAGCCC 3′	213
		Reverse primer	5′ TTAACATTCGGACAAGTAATC 3′	
Runx2	XM_005696518	Forward primer	5′ AAGATGCTTCCGGTCCAGTC 3′	259
		Reverse primer	5′ CTCCTCTTTCGTTCCACCCC 3′	
GAPDH	AJ431207	Forward primer	5′ TGTTTGTGATGGGCGTGAAC 3′	137
		Reverse primer	5′ CATAAGTCCCTCCACGATGC 3′	

ALP, alkaline phosphatase; GAPDH, glyceraldehyde-3-phosphate dehydrogenase; OCN, osteocalcin; OPN, osteopontin; Runx2, runt-related transcription factor 2.

the target gene was normalized against GAPDH using the $2^{-\Delta\Delta Ct}$ method.

Bone marrow aspiration and creation of critical-sized femoral defect

All procedures were performed in strict compliance with the recommendations in the Guide for the Care and Use of the Third Military Medicine University (TMMU). Twelve adult male goats (purchased from the animal center of TMMU, Chongqing, China) were used for modeling and implantation. The goats were anesthetized by inhalation of 2% isoflurane. Then, venous channels were established and saline solution was given at a rate of ~10 mL/kg/h. A preoperative prophylactic antibiotic (penicillin G, 800,000 units) was also administered intravenously. General anesthesia was implemented by Zoletil 50 (mixture of Tiletamine and Zolezepam, 1:1, 10 mg/kg) with atropine sulfate (0.1 mg/kg, subcutaneous injection 15 min before anesthesia), and was maintained via inhalation of a mixture of oxygen and halothane. Using syringes containing sodium heparin solution (1000 units/mL), bone marrow was aspirated from bilateral iliac crests using multipoint paracentesis and the mixed liquids (bone marrow: anticoagulant solution = 2:1, v/v; 30 mL in total) were collected.[15] The surgery was performed according to the approach previously described by our group.[13] The goat was positioned in left lateral recumbency first, and the right hind limb was draped using sterile procedures. The intramedullary pin was fixed on the location device *in vitro*, and the intramedullary pin was locked in with screws when it was inserted into the marrow cavity of the femur; a 20 mm osteoperiosteal critical-sized defect was made in the mid-diaphysial of the femur with a wire saw. Two pieces of bone marrow-enriched SAP/DBM were implanted to fill up the defect from one direction, and eight pieces of composites in total were fixed using adsorbable thread from four directions and were covered with muscle. In the same way, the left defect was implanted with bone marrow-enriched DBM, which served as a control. Postoperatively, Meloxicam (0.5 mg/kg) was intramuscularly injected daily for analgesia and early functional exercise,[16] and a special soft pocket device, consisting of lifting cords on the hindlimb and traction cords on the forelimb, was used to assist limb movements. All goats showed favorable surgical tolerance and postoperative recovery was uneventful.

Radionuclide bone imaging

Bone metabolism in the reconstructed area (REC) was assessed by serial radionuclide bone imaging. The goats were generally anesthetized with the aforementioned method at 2 and 4 weeks postoperatively. Then, they were fixed, and the defect areas were scanned.[13] For each goat, technetium-99m methylene diphosphonate (2 mCi/kg; Beijing Atom-Hitech Company, Beijing, China) was administered through the ear vein, and after 2 h, bone scan images (BSI) were acquired by the eNTEGRA workstation of the Millennium/MPR SPECT (GE, Piscataway, NJ). The count uptake ratio in the REC was calculated by the eNTEGRA workstation and compared with that in the adjacent knee joint (normal area [NOR]).

Micro-CT analysis

At 8 and 16 weeks postoperation, all femurs were excised and scanned with a micro-CT system (μCT 40; Scanco, Brüttisellen, Switzerland) to measure the bone volume and degree of calcification in the defect area. Samples were scanned with a voxel size of 20 μm. The X-ray tube was operated at 70 kV and 120 μA. The image matrix size was 1024 × 1024 pixels. A two-dimensional image in the sagittal view and 3D reconstruction was performed by Scanco version 5.0. The ratio of bone volume to total bone volume (BV/TV), bone mineral density (BMD), new trabecular number (Tb.N), and new trabecular thickness (Tb.Th) within the defects were quantified by Scanco software.

Histological examination

Histological examination was conducted to assess the process of new bone formation. Femurs were fixed with 4% neutral paraformaldehyde for 2 weeks, decalcified with 10% nitric acid solution for ~5 days, and embedded in paraffin. Samples were cut lengthwise using a slicer (RM2235; Leica, Wetzlar, Germany) to prepare serial sections (5 μm thick). Then, the slices were stained with H&E and Masson's trichrome. Photomicrographs were taken with a LEICA DM 6000B light microscope.

Statistical analysis

Data were expressed as the mean ± standard deviation, Statistical analysis was carried out using a two-tailed

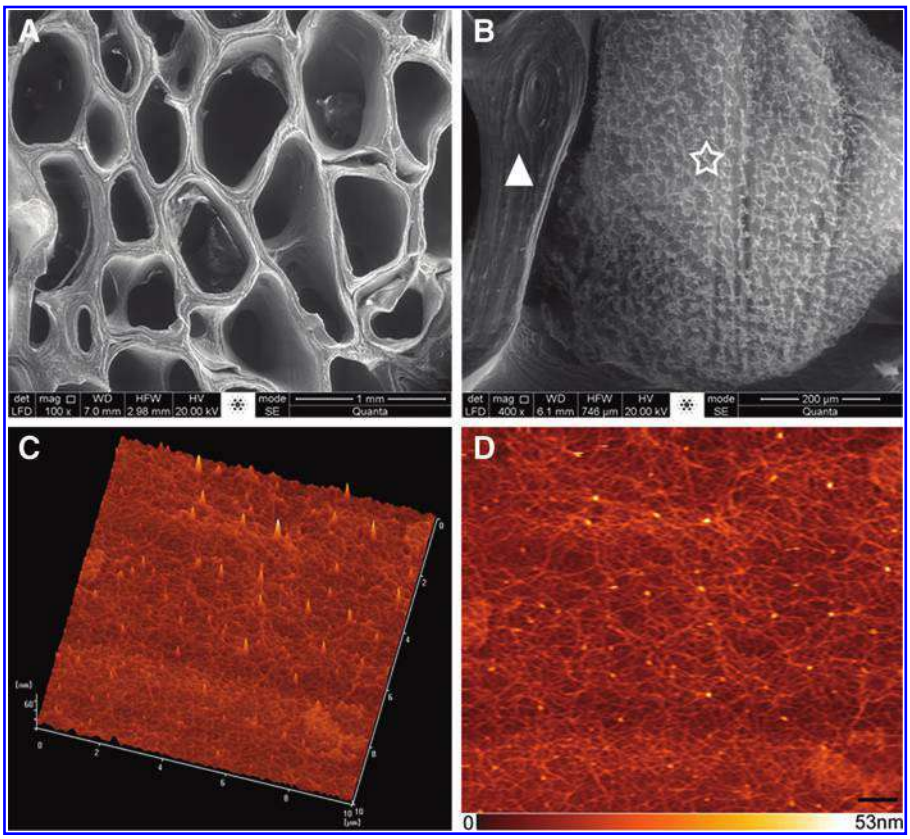

FIG. 1. Characterization of DBM and SAP/DBM. The morphological observations of DBM **(A)** and SAP/DBM scaffolds **(B)** were made using ESEM. The aperture was about 200–900 μm in the DBM scaffolds; SAP was attached to the inner walls of DBM and interwoven to form a 3D retiform structure in the SAP/DBM scaffolds. AFM images showed the 3D structure **(C)** and 2D nano-fiber structure **(D)** of RADA16-I SAP after fabrication. DBM, demineralized bone matrix (▲); SAP, self-assembly peptide (★). Scale bar is 1 mm, 200, 10 and 1 μm in **(A–D)**, respectively. AFM, Atomic Force Microscope; 2D, two-dimensional; 3D, three-dimensional; DBM, demineralized bone matrix; ESEM, Environmental Scanning Electron Microscope; SAP, self-assembly peptide. Color images available online at www.liebertpub.com/tea

Student's *t*-test (SPSS 13.0). A p-value < 0.05 was considered statistically significant.

Results

Morphological characterization

As revealed by ESEM, SAP was attached to the inner walls of DBM and interwoven to form a 3D retiform structure (Fig. 1A, B). Such a nano-fiber structure could promote physical retention for marrow cells and growth factors. The self-assembly process of SAP was successfully realized as the nano-fibers had a uniform long appearance, as detailed by AFM (Fig. 1C, D). The postenrichment observation showed that marrow cells retained in the DBM scaffolds were distributed along the inner walls of the DBM, and most of the pores were empty (Fig. 2A, B). However, in

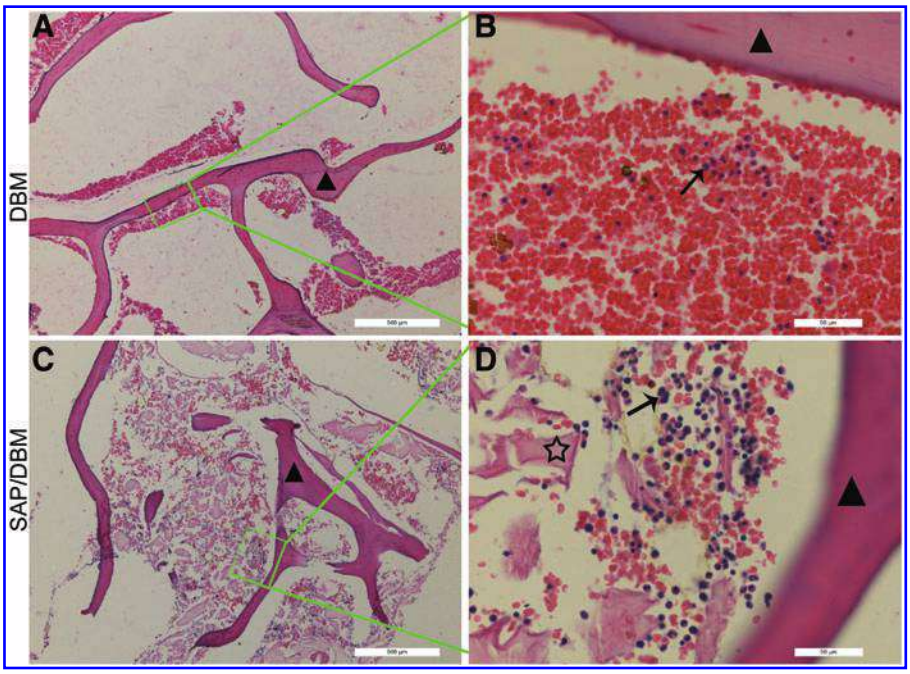

FIG. 2. H&E staining of marrow-enriched DBM and SAP/DBM. The marrow cells retained in the DBM were distributed along the inner walls of DBM, and most of the pores were empty in the DBM **(A)**; SAP/DBM showed marrow cells were uniformly distributed throughout the scaffolds and filled up most of the pores **(C)**. **(B, D)** Were the magnifying image of *rectangular part* in **(A, C)**, respectively. DBM (▲), SAP (★), karyocyte (→). *Green line* indicates the correspondence magnifying image of green rectangular part. Scale bar is 500 μm **(A, C)** and 50 μm **(B, D)**. H&E, hematoxylin and eosin. Color images available online at www.liebertpub.com/tea

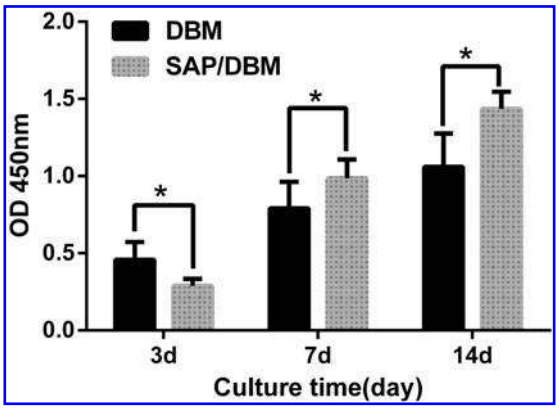

FIG. 3. Proliferation status of gMSCs. Cell cultured in the DBM and SAP/DBM scaffolds was analyzed using CCK-8 at 3, 7, and 14 days ($n=6$). The data were expressed as the mean ± SD. * There was a significant difference between the two groups ($p<0.05$). CCK-8, Cell Counting Kit-8; gMSCs, goat mesenchymal stem cells; SD, standard deviation.

the SAP/DBM scaffolds, marrow cells were uniformly distributed throughout the scaffolds and filled up most of the pores (Fig. 2C, D).

Cell proliferation status and distribution after osteoinduction

The CCK-8 assay was employed to compare the proliferation status of gMSCs in different scoffolds (Fig. 3). The OD was 0.45 ± 0.11 and 0.29 ± 0.05 in the DBM and SAP/DBM scaffolds, respectively, after 3 days of culture. The results demonstrated that cell proliferation in the DBM scaffolds was significantly higher than that in the SAP/DBM scaffolds. In contrast, as time extended to 7 and 14 days, cell proliferation in the SAP/DBM scaffold was significantly higher than that in the DBM scaffolds ($p<0.05$, $n=6$).

Three-dimensional images revealed that after culture with osteogenic medium for 7 days, gMSCs retained in the scaffold were distributed along the inner walls of the DBM (Fig. 4A); furthermore, it was visible that cells had stretched into the nano-fiber mesh of the SAP/DBM (Fig. 4B). At 14 days, more cells were observed within the nano-fibers. This implied that gMSCs could fill the entire inner space of the SAP/DBM scaffold after a certain period of culture (Fig. 4D). In contrast, the cytoskeletons of gMSCs only appeared on the pore surfaces of the DBM scaffold (Fig. 4C).

mRNA expression of osteogenic genes

The gene expression levels of *ALP*, *OPN*, *OCN*, and *Runx2* were detected by quantitative real-time reverse transcription–polymerase chain reaction (qRT-PCR) at 7 and 14 days after osteogenic induction (Fig. 5). At 7 days, *ALP* expression was significantly higher in the SAP/DBM scaffolds, compared with that in the DBM ($p<0.05$), whereas no significant difference existed in *OPN* expression ($p=0.28$). Moreover, both *OCN* and *Runx2* expressions were significantly lower in the SAP/DBM scaffolds. At 14 days, *OCN*, *OPN*, and *Runx2* expression levels were

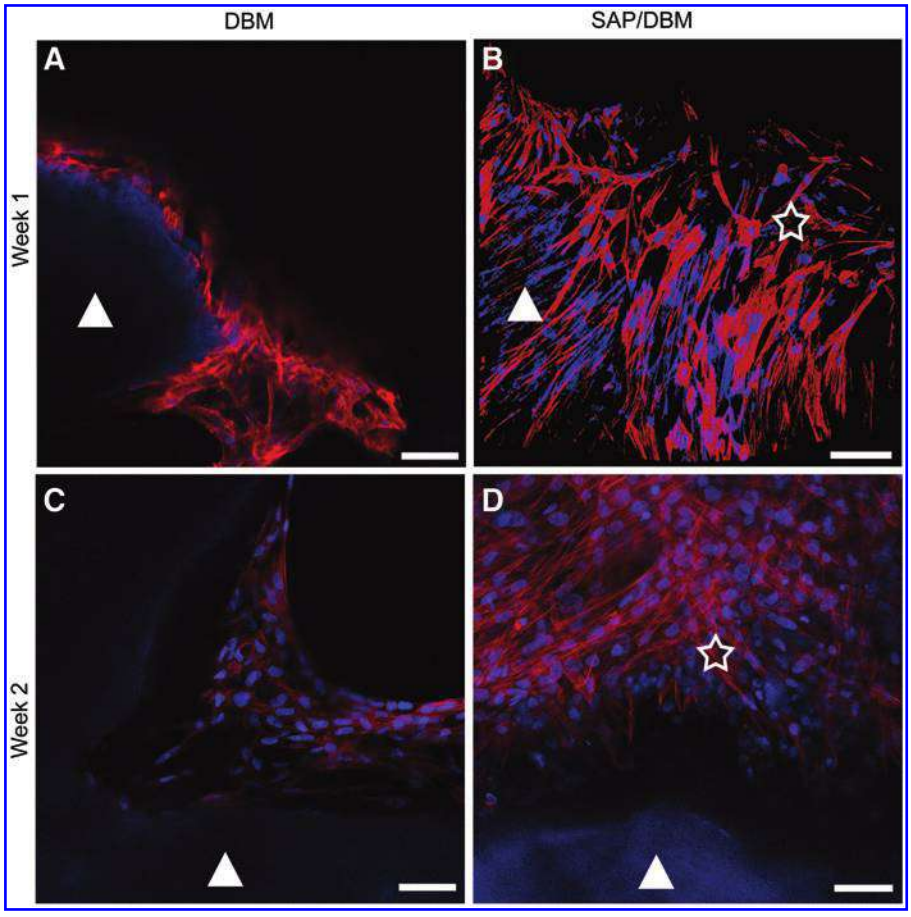

FIG. 4. Differentiation and osteoinduction of gMSCs in marrow-enriched DBM and SAP/DBM scaffolds. The cytoskeleton of gMSCs were stained *red* using phalloidin, and nucleus were stained *blue* using DAPI. More cells were observed in the SAP/DBM **(B, D)** than that in the DBM **(A, C)** at 7 and 14 days, respectively. Moreover, the direction of cell distribution in the DBM was along the inner wall of DBM, and more cells stretched into the nano-fiber mesh of SAP in the SAP/DBM. DBM (▲), SAP (★). Scale bar is 50 μm. Color images available online at www.liebertpub.com/tea

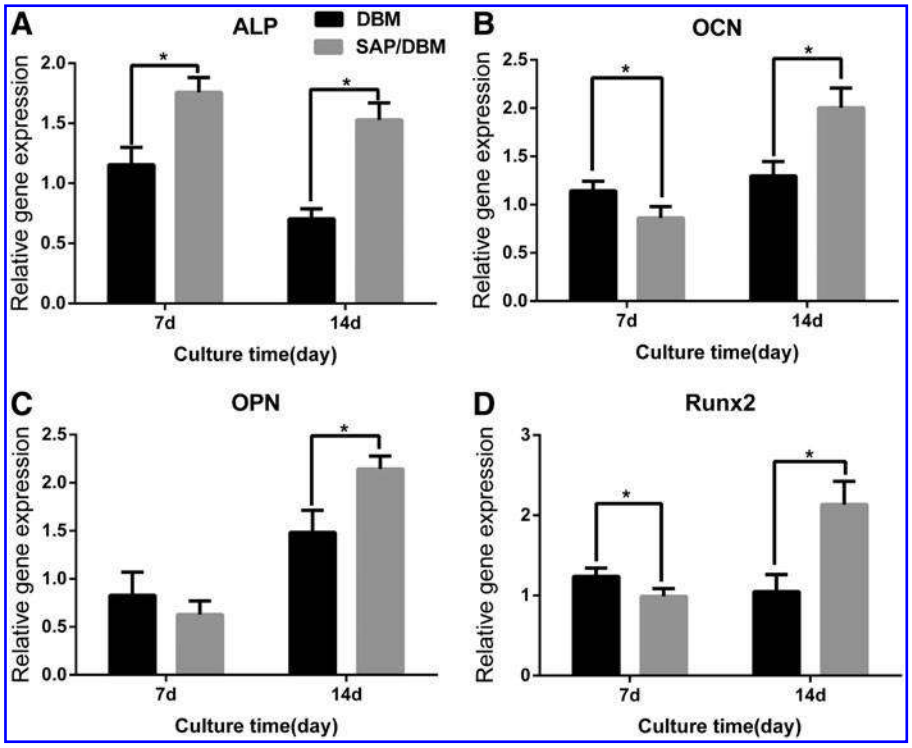

FIG. 5. The expression levels of osteo-specific marker genes. gMSCs in marrow-enriched DBM and SAP/DBM scaffolds underwent osteogenic differentiation following induction with osteogenic medium, gene expression of *ALP* **(A)**, *OCN* **(B)**, *OPN* **(C)** and *Runx2* **(D)** were assessed by qRT-PCR at 7 and 14 days. The levels of these genes expression in the SAP/DBM were higher compared with that in the DBM at 14 days. *ALP*, alkaline phosphatase; *OCN*, osteocalcin; *OPN*, osteopontin; qRT-PCR, quantitative real-time reverse transcription–polymerase chain reaction; *Runx2*, runt-related transcription factor 2. Data were expressed as the mean ± SD. All assays were repeated three times in duplicates. * There was a significant difference between marrow-enriched DBM and SAP/DBM ($p < 0.05$).

upregulated in the SAP/DBM scaffolds and were significantly higher than those in the DBM scaffolds.

Bone scan images

The activity of bone metabolism could be represented by the BSI.[17] All of the BSIs of the REC exhibited a count ratio over 1.0, indicating that the grafts were undergoing a healing process (Fig. 6). The count uptake ratio in the REC implanted with the SAP/DBM composite was significantly higher than that in the DBM (3.86 ± 1.58 vs. 2.51 ± 1.08 at 2 weeks, 11.82 ± 4.04 vs. 7.54 ± 2.10 at 4 weeks, $p < 0.05$, $n = 6$).

Micro-CT assessments

For each group, micro-CT data were obtained from six independent replicates ($n = 6$) and were quantified to assess the osteogenic efficacy. At 8 weeks postoperation, complete bone union was observed in the defect implanted with the marrow-enriched SAP/DBM (Fig. 7C, D), whereas nonunion was still apparent in the defect filled with the marrow-enriched DBM (Fig. 7A, B). Consistently, quantitative analysis showed that BV/TV in the SAP/DBM was significantly greater than that in the DBM (Fig. 7I). Moreover, both Tb.N and Tb.Th exhibited a significant difference between the SAP/DBM and DBM (Fig. 7K, L). However, no significant difference in BMD was detected (640.33 ± 84.01 vs. 599.30 ± 79.74, $p = 0.105$, Fig. 7J). At 16 weeks, the SAP/DBM displayed high homogeneity and complete bone remodeling (Fig. 7G, H), whereas, the bone remodeling level remained low and the architecture of the trabecula bone was not homogenous in the DBM (Fig. 7E, F). Consistently, all of the BV/TV, BMD, Tb.N, and Tb.Th in the SAP/DBM

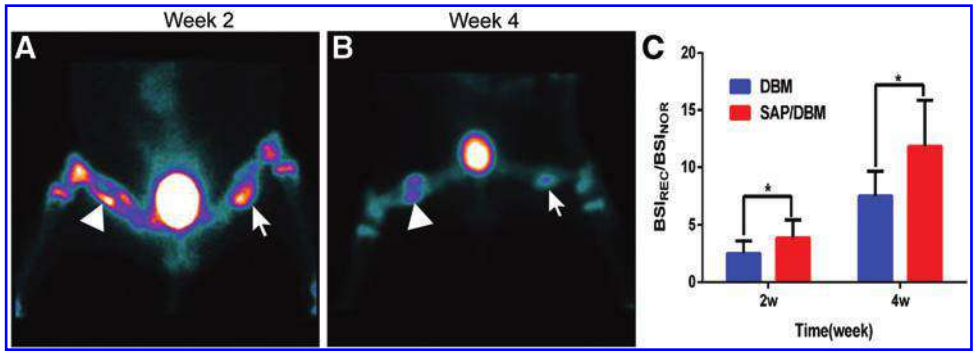

FIG. 6. The image of bone scan (BSI) and quantitative assay. The bone metabolism of REC was evaluated by radionuclide bone imaging at 2 weeks **(A)** and 4 weeks **(B)** postoperation. The count uptake ratio (BSI_{REC}/BSI_{NOR}) **(C)** was collected by SPECT, and the NOR of knee joint in homonymy was selected respectively as the comparison area. The bone metabolism in the REC of marrow-enriched SAP/DBM was higher than that of DBM at 2 and 4 weeks, respectively. The REC of marrow-enriched SAP/DBM (▲), The REC of marrow-enriched DBM (→). * There was a significant difference between marrow-enriched DBM and SAP/DBM ($p < 0.05$). NOR, normal area; REC, reconstructed area. Color images available online at www.liebertpub.com/tea

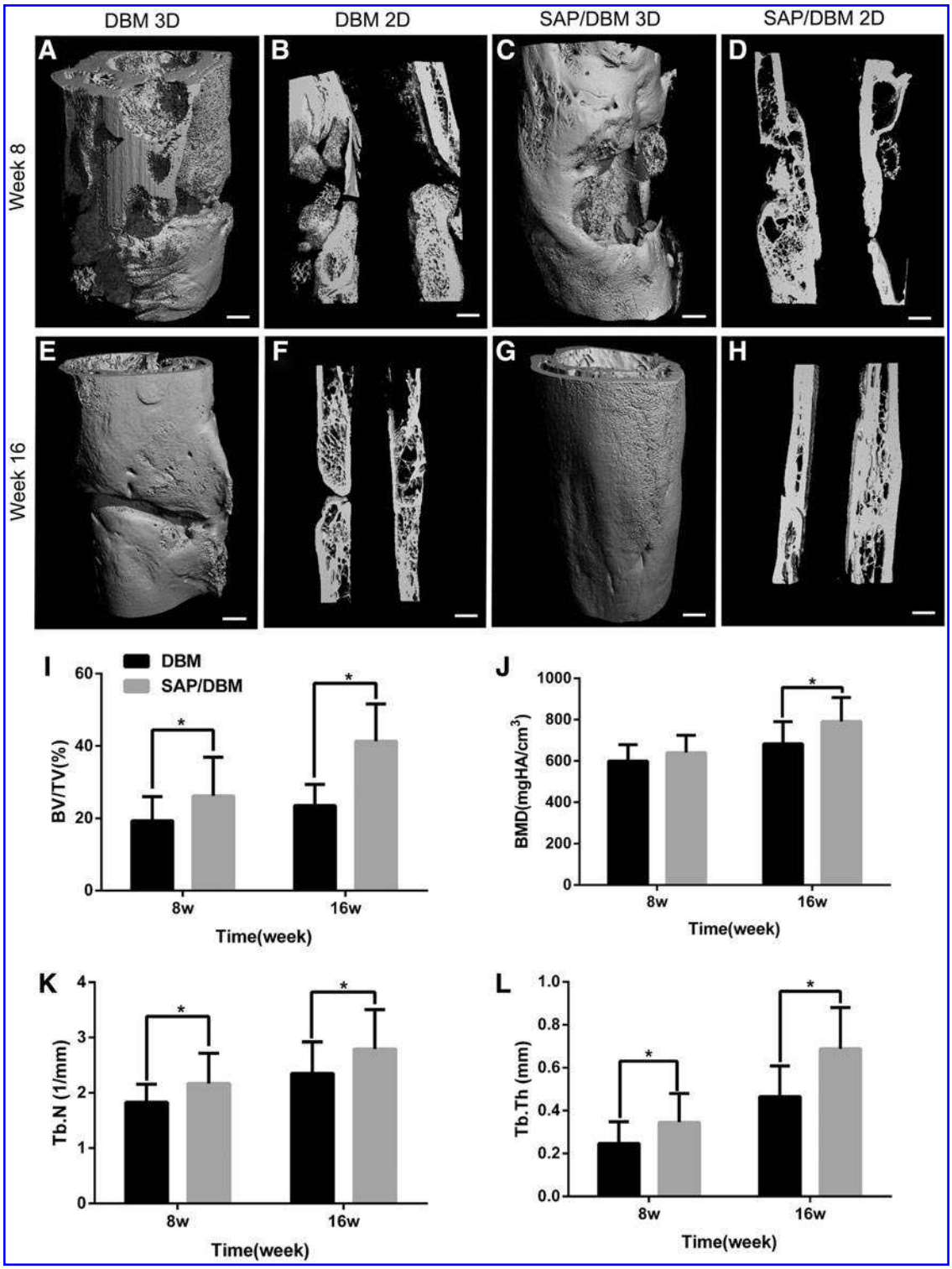

FIG. 7. Micro-CT observation and quantitative evaluation of bone repair and osseointegration. The 3D **(C)** and 2D center-sagittal view images **(D)** for marrow-enriched SAP/DBM showed superior reunion in reconstruction areas at 8 weeks postoperation, compared with that of DBM **(A, B)**. At 16 weeks, the reconstruction areas of marrow-enriched SAP/DBM displayed high homogeneity and bone remolding was complete **(G, H)**, and marrow-enriched DBM showed imperfect union and bone remodeling level was still low from 3D image **(E)**, and the architecture of trabecula bone was leptos from 2D image **(F)**. Morphometric analysis of BV/TV **(I)**, BMD **(J)**, Tb.N **(K)**, and Tb.Th **(L)** showed the quantify of reconstruction area in SAP/DBM was significantly greater than that of DBM except BMD at 8 weeks. BMD, bone mineral density; BV/TV, bone volume to total bone volume ratio; Tb.N, the new trabecular number; Tb.Th, new trabecular thickness. * There was a significant difference between marrow-enriched DBM and SAP/DBM ($p < 0.05$). Scale bar is 5 mm.

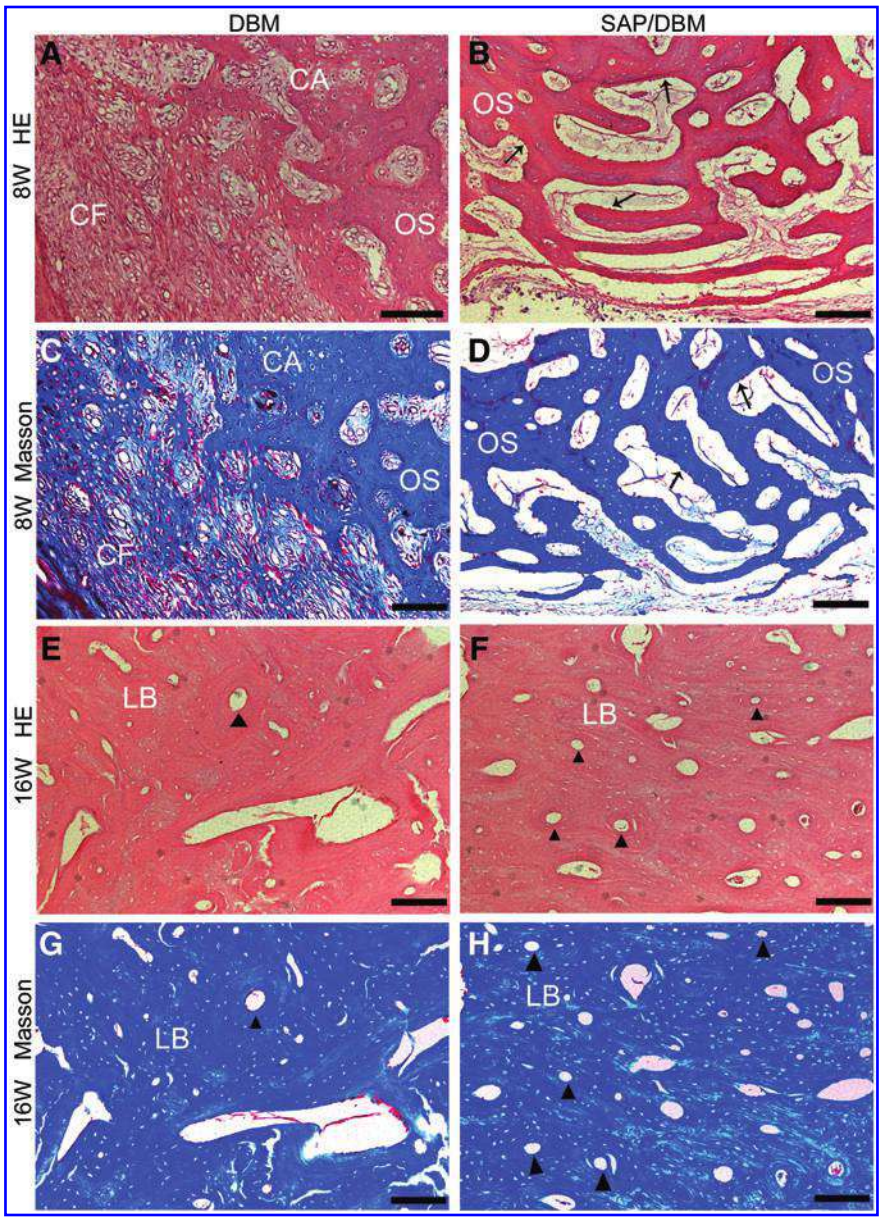

FIG. 8. Histological observation of the new bone formation. At 8 weeks postoperation, H&E **(B)** and Masson-Trichrome **(D)** staining in marrow-enriched SAP/DBM showed extensive newly osteoids as compared with abundant of cartilage-like fiber in marrow-enriched DBM **(A, C)**, which suggested endochondral bone formation. At 16 weeks postoperation, the number of osteons was relatively small in the DBM, and the collagen fibers of lamellar bones were massive and mussy **(E, G)**; abundant osteons and ordered collagen fibers were evident in the SAP/DBM **(F, H)**, suggested bone remodeling was superior. CA, cartilage; CF, cartilage-like fiber; LB, lamellar bone; OS, osteoid; osteon (▲), osteoblasts (→). Scale bar: 100 μm. Color images available online at www.liebertpub.com/tea

were significantly higher than those in the DBM (Fig. 7I–L, $p < 0.05$, $n = 6$).

Histological examination

For assessing new bone formation, histological findings were consistent with the results of the micro-CT analysis. At 8 weeks postoperation, the defect areas implanted with marrow-enriched DBM were still visible and were surrounded by cartilage-like fibers and osteoids (Fig. 8A, C), suggesting ongoing endochondral bone formation. However, mature and circuitous trabecular structures were observed in marrow-enriched SAP/DBM, and the defected areas implanted with marrow-enriched with SAP/DBM were almost invisible and replaced with Masson-Trichrome-positive collagen (Fig. 8B, D). At 16 weeks, the number of osteons was relatively small in the marrow-enriched DBM (Fig. 8E, G), and the collagen fibers of lamellar bones were massive and disorganized (Fig. 8G). In contrast, abundant osteons and ordered collagen fibers were evident in the SAP/DBM, indicating that bone remodeling was advancing (Fig. 8F, H).

Discussion

Tissue-engineered bones have been widely documented as one of the most promising strategies for treating large bone defects.[18,19] However, the classical tissue engineering strategy is associated with some drawbacks, such as prolonged duration, high costs, critical technique requirements, and ethical issues, which limit the generalization and applications in clinical practice. Developing a compound microenvironment, in which MSCs, cytokines related with cell growth, ECM supporting cell adhesion and movement, and other dynamic factors such as strength and stability can be integrated in a rapid and cost-effective manner, is extremely urgent. In this article, we established a special composite by modifying DBM with a SAP, and used it for bone marrow enrichment via a simple SCR strategy. The resulting

composite was implanted to repair critical-sized femoral defects in goats.

Bone marrow delivery via local approaches can promote bone repair, and it has been widely applied in preclinical and clinical trials.[20–23] By enriching autologous bone marrow, the SCR strategy can produce composites comprised of MSCs and cytokines.[12] This strategy has certain advantages when treating bone defects in clinical practice. It can be implemented simply in the operating room. Thus, it is more cost effective than classical tissue engineering approaches as cell expansion *in vitro* is avoided. Moreover, loss of bone marrow, a common problem in the percutaneous bone marrow grafting, can be reduced to a great extent.

Derived from natural bones, DBM grafts can offer the necessary strength and stability for bone defect repair. Although the osteoconductivity of DBM has been broadly confirmed, they are usually implanted with autologous bones because of the lack of bioactivity.[10] In this study, an SAP was developed as an artificial alternative to ECM.[24] SAPs can promote the retention of cells and growth factors by the nano-fiber mesh and electrostatic forces of the amino acids.[12] Moreover, SAPs can provide support for cell growth, proliferation, and differentiation. SAP RADA16-I has been proven with satisfactory safety *in vitro* and without noticeable immunogenicity and proinflammatory responses *in vivo*.[25,26] The initial transformation and degradation products of RADA16-I are natural amino acids, which are innocuous and can be metabolized through biochemical pathways *in vivo*.[27]

A feasible tissue engineering scaffold should not only facilitate cell attachment and proliferation, but also should allow cell infiltration and ultimately promote tissue regeneration. The present nano-fiber scaffold provided a 3D and adequately porous spatial structure that was suitable for the infiltration and ingrowth of gMSCs (Fig. 4). As for cell adhesion, Prieto *et al.* have shown that RAD sequence has no significant difference on the RGD sequence of integrin.[28]

The majority of differentiated gMSCs *in vitro* was from the seeded gMSCs, and minority of differentiated gMSCs was from the enriched bone marrow.[12] The cell type will be clarified in an upcoming study on the mechanism underlying the osteogenesis of the bone marrow-enriched scaffolds. The proliferation assays of gMSCs showed that SAP/DBM scaffolds were more beneficial for cell proliferation than DBM scaffolds (Fig. 3). The proliferation peak of gMSCs on both scaffolds occurred from 3 to 7 days, and the proliferation rate on the SAP/DBM scaffolds was higher than that on the DBM scaffolds. From 7 to 14 days, the proliferation rate slowed down, and the trend for SAP/DBM scaffolds obviously increased. However, the proliferation rate on the SAP/DBM scaffolds was lower than that on the DBM scaffolds after 3 days. Therefore, we suppose the SAP could regulate the proliferation status of cells on different stages, and improve the capability of cell growth. The suppositions are consistent with osteogenetic differentiation of gMSCs, and will be further elaborated.

RADA16 can induce cell differentiation itself.[29,30] In this study, we evaluated the osteogenetic induction of gMSCs in the postenriched SAP/DBM composite. The number and skeleton of gMSCs in the postenriched SAP/DBM scaffolds were more superior to those in the DBM (Fig. 4). The adhesive and proliferative capacities of gMSCs in the postenriched SAP/DBM scaffolds were greater than those in the DBM (Fig. 3). To further assess the osteogenic differentiation of gMSCs further, we detected the gene expressions of *ALP*, *OCN*, *OPN*, and *Runx2* (Fig. 5). *ALP* is an early marker of mature osteoblasts. *OPN* plays crucial roles for controlling bone mineralization. *OCN* is a special marker of bone formation and osteoblastic activity. *Runx2* is involved in the signal transduction of ECM and its activation can increase the transcriptional activity of the osteocalcin gene. At 7 days, *ALP* mRNA expression levels in the SAP/DBM composite was significantly higher than that in the DBM, and *ALP* levels were downregulated at 14 days, which was consistent with the secretory stage of *ALP*. However, *OCN* and *Runx2* mRNA expression levels were significantly lower at 7 days. No significant difference in *OPN* mRNA expression was detected between the SAP/DBM and DBM, and *OCN*, *OPN*, and *Runx2* expression levels were upregulated at 14 days; the expression levels of all of these genes were significantly higher in the SAP/DBM, compared with the DBM. The increased trend of gMSCs in the SAP/DBM were consistent with the proliferation of gMSCs; this result could be attributed to the nano-fiber structure of the SAP, which acted as a controlled release system[31] and made the enriched growth factors and cytokines secreted by gMSCs release in a controlled manner.

Currently, no satisfactory results have been reported regarding the clinical application of large bone grafts modified with SAPs. One reason is that the reconstruction of large bone defects remains a challenge.[32] The goat critical-sized femoral defect model has been extensively used for evaluating the reparative efficacy of bone grafts.[13,33,34] In this study, the marrow-enriched SAP/DBM composites showed superior osteogenesis and an advanced healing effect. As revealed by BSI, higher bone metabolism activity was detected in the REC of the SAP/DBM than the DBM at 2 and 4 weeks postoperation (Fig. 6). At 8 weeks, micro-CT suggested bone union and nonunion for the SAP/DBM and DBM, respectively (Fig. 7). These results were further supported by the results of histology that showed circuitous trabecular and cartilage-like fibers for the SAP/DBM and DBM, respectively (Fig. 8). However, there was no significant difference in the BMD between the SAP/DBM and DBM at 8 weeks. This result might be attributed to the slow release of growth factors for mineralization in the SAP/DBM. At 16 weeks, bone remodeling and trabecula structure in the SAP/DBM were superior to that in the DBM from both micro-CT and histology results. We here hypothesize that the efficacy mechanism for the SAP/DBM composite is: (i) the osteogenetic composition of bone marrow, mostly containing stem cell and growth factors, was transplanted *in vivo* to start the osetogenetic function of the host. The supposition resulted from superior bone formation and because the number of stem cells transplanted *in vivo* was minor. (ii) The SAP/DBM composite could recruit substantially more stem cells and growth factors of the host by the nano-fiber structure characteristics and by mimicking ECM. (iii) The release system of the SAP/DBM could control the osteogenesis at different stage. These viewpoints were consistent with some scholars, for example, Zimmermann *et al.*[35] reported that short-term stem cell survivals after *in vivo* implantation. Tsso *et al.* proposed that transplanted MSCs recruited a host's osteoprogenitor cells for

bone repair.[36] We suppose that MSCs and growth factors with enriched-marrow start the osteogenic function, and the host's MSCs and growth factors play a more important role for bone formation. However, related mechanism need to be elucidated by the following studies. It was notable that the union of unilateral cortical bone in the DBM was incomplete (Fig. 7F), and that unilateral cortical bone not fused perfectly in the SAP/DBM (Fig. 7H); we suppose that the healing time of 16 weeks is relatively short, compared with 6–12 months.[37,38] Regardless, these results indicated that the approach of immediate implantation after construction induced satisfactory outcomes. Moreover, this approach possessed advantages over traditional tissue engineering constructs, such as convenience, low risk, time savings, and ethical compliance.

Conclusion

SAPs hold great potential in clinical application because they are applicable to various types of cells and growth factors. SAPs has a similar microstructure to ECM, and the application involves low risk. These characteristics allow SAPs to act as modification materials for various lacunar or porous bone grafts to maintain cell attachment and proliferation. In this study, we evaluated the osteogenic differentiation capacity of gMSCs in a marrow-enriched SAP/DBM composite *in vitro* and the efficacy of the marrow-enriched SAP/DBM composite for repairing a critical-size femoral defect in goats. Our findings suggest that the post-enriched composite significantly enhanced the cellular activities of gMSCs compared to that observed for the DBM. Complete reconstruction of the large bone defect was achieved after implantation of the bone marrow-enriched SAP/DBM composite. These results indicate that immediate implantation after bone marrow enrichment could be a new strategy for treating large bone defects in the context of tissue engineering.

Acknowledgments

We thank Quanfang Wei, Jianhong Mi and Jun Zhao for excellent technical support. This study was funded by the National High Technology Research and Development (863) Program of China (2012AA020504), the Military Foundation (BWS11C040), and the Foundation of Southwest Hospital (SWH2013JS07).

Disclosure Statement

No competing financial interests exist.

References

1. Oerlemans, A.J., van Hoek, M.E., van Leeuwen, E., van der Burg, S., and Dekkers, W.J. Towards a richer debate on tissue engineering: a consideration on the basis of NEST-ethics. Sci Eng Ethics **19,** 963, 2013.
2. Dong, S., Guo, H., Zhang, Y., Li, Z., Kang, F., Yang, B., Kang, X., Wen, C., Yan, Y., Jiang, B., and Fan, Y. rFN/Cad-11-modified collagen type II biomimetic interface promotes the adhesion and chondrogenic differentiation of mesenchymal stem cells. Tissue Eng Part A **19,** 2464, 2013.
3. Amable, P.R., Teixeira, M.V., Carias, R.B., Granjeiro, J.M., and Borojevic, R. Protein synthesis and secretion in human mesenchymal cells derived from bone marrow, adipose tissue and Wharton's jelly. Stem Cell Res Ther **5,** 53, 2014.
4. Betsch, M., Schneppendahl, J., Thuns, S., Herten, M., Sager, M., Jungbluth, P., Hakimi, M., and Wild, M. Bone marrow aspiration concentrate and platelet rich plasma for osteochondral repair in a porcine osteochondral defect model. PLoS One **8,** e71602, 2013.
5. Hernigou, P., Poignard, A., Beaujean, F., and Rouard, H. Percutaneous autologous bone-marrow grafting for nonunions. Influence of the number and concentration of progenitor cells. J Bone Joint Surg Am **87,** 1430, 2005.
6. Ateschrang, A., Ochs, B.G., Ludemann, M., Weise, K., and Albrecht, D. Fibula and tibia fusion with cancellous allograft vitalised with autologous bone marrow: first results for infected tibial non-union. Arch Orthop Trauma Surg **129,** 97, 2009.
7. Bokhari, M.A., Akay, G., Zhang, S., and Birch, M.A. The enhancement of osteoblast growth and differentiation *in vitro* on a peptide hydrogel-polyHIPE polymer hybrid material. Biomaterials **26,** 5198, 2005.
8. Erickson, I.E., Huang, A.H., Chung, C., Li, R.T., Burdick, J.A., and Mauck, R.L. Differential maturation and structure-function relationships in mesenchymal stem cell- and chondrocyte-seeded hydrogels. Tissue Eng Part A **15,** 1041, 2009.
9. Chen, J., Shi, Z.D., Ji, X., Morales, J., Zhang, J., Kaur, N., and Wang, S. Enhanced osteogenesis of human mesenchymal stem cells by periodic heat shock in self-assembling peptide hydrogel. Tissue Eng Part A **19,** 716, 2013.
10. Fischer, C.R., Cassilly, R., Cantor, W., Edusei, E., Hammouri, Q., and Errico, T. A systematic review of comparative studies on bone graft alternatives for common spine fusion procedures. Eur Spine J **22,** 1423, 2013.
11. Macisaac, Z.M., Rottgers, S.A., Davit, A.R., Ford, M., Losee, J.E., and Kumar, A.R. Alveolar reconstruction in cleft patients: decreased morbidity and improved outcomes with supplemental demineralized bone matrix and cancellous allograft. Plast Reconstr Surg **130,** 625, 2012.
12. Hou, T., Li, Z., Luo, F., Xie, Z., Wu, X., Xing, J., Dong, S., and Xu, J. A composite demineralized bone matrix—self assembling peptide scaffold for enhancing cell and growth factor activity in bone marrow. Biomaterials **35,** 5689, 2014.
13. Hou, T., Li, Q., Luo, F., Xu, J., Xie, Z., Wu, X., and Zhu, C. Controlled dynamization to enhance reconstruction capacity of tissue-engineered bone in healing critically sized bone defects: an *in vivo* study in goats. Tissue Eng Part A **16,** 201, 2010.
14. Chang, Z., Hou, T., Wu, X., Luo, F., Xing, J., Li, Z., Chen, Q., Yu, B., Xu, J., and Xie, Z. An anti-infection tissue-engineered construct delivering vancomycin: its evaluation in a goat model of femur defect. Int J Med Sci **10,** 1761, 2013.
15. Lee, K., and Goodman, S.B. Cell therapy for secondary osteonecrosis of the femoral condyles using the Cellect DBM System: a preliminary report. J Arthroplasty **24,** 43, 2009.
16. Viateau, V., Guillemin, G., Calando, Y., Logeart, D., Oudina, K., Sedel, L., Hannouche, D., Bousson, V., and Petite, H. Induction of a barrier membrane to facilitate reconstruction of massive segmental diaphyseal bone defects: an ovine model. Vet Surg **35,** 445, 2006.
17. Lauer, I., Czech, N., Zieron, J., Sieg, P., Richter, E., and Baehre, M. Assessment of the viability of microvascularized

bone grafts after mandibular reconstruction by means of bone SPET and semiquantitative analysis. Eur J Nucl Med **27,** 1552, 2000.
18. Marolt, D., Campos, I.M., Bhumiratana, S., Koren, A., Petridis, P., Zhang, G., Spitalnik, P.F., Grayson, W.L., and Vunjak-Novakovic, G. Engineering bone tissue from human embryonic stem cells. Proc Natl Acad Sci U S A **109,** 8705, 2012.
19. Yamada, Y., Nakamura, S., Ito, K., Umemura, E., Hara, K., Nagasaka, T., Abe, A., Baba, S., Furuichi, Y., Izumi, Y., Klein, O.D., and Wakabayashi, T. Injectable bone tissue engineering using expanded mesenchymal stem cells. Stem Cells **31,** 572, 2013.
20. Connolly, J.F., Guse, R., Tiedeman, J., and Dehne, R. Autologous marrow injection as a substitute for operative grafting of tibial nonunions. Clin Orthop Relat Res **266,** 259, 1991.
21. Le Nail, L.R., Stanovici, J., Fournier, J., Splingard, M., Domenech, J., and Rosset, P. Percutaneous grafting with bone marrow autologous concentrate for open tibia fractures: analysis of forty three cases and literature review. Int Orthop **38,** 1845, 2014.
22. Sugaya, H., Mishima, H., Aoto, K., Li, M., Shimizu, Y., Yoshioka, T., Sakai, S., Akaogi, H., Ochiai, N., and Yamazaki, M. Percutaneous autologous concentrated bone marrow grafting in the treatment for nonunion. Eur J Orthop Surg Traumatol **24,** 671, 2014.
23. Goel, A., Sangwan, S.S., Siwach, R.C., and Ali, A.M. Percutaneous bone marrow grafting for the treatment of tibial non-union. Injury **36,** 203, 2005.
24. Holmes, T.C., de Lacalle, S., Su, X., Liu, G., Rich, A., and Zhang, S. Extensive neurite outgrowth and active synapse formation on self-assembling peptide scaffolds. Proc Natl Acad Sci U S A **97,** 6728, 2000.
25. Davis, M.E., Motion, J.P., Narmoneva, D.A., Takahashi, T., Hakuno, D., Kamm, R.D., Zhang, S., and Lee, R.T. Injectable self-assembling peptide nanofibers create intramyocardial microenvironments for endothelial cells. Circulation **111,** 442, 2005.
26. Tang, C., Shao, X., Sun, B., Huang, W., and Zhao, X. The effect of self-assembling peptide RADA16-I on the growth of human leukemia cells *in vitro* and in nude mice. Int J Mol Sci **10,** 2136, 2009.
27. Garbern, J.C., Hoffman, A.S., and Stayton, P.S. Injectable pH- and temperature-responsive poly(N-isopropylacrylamide-co-propylacrylic acid) copolymers for delivery of angiogenic growth factors. Biomacromolecules **11,** 1833, 2010.
28. Prieto, A.L., Edelman, G.M., and Crossin, K.L. Multiple integrins mediate cell attachment to cytotactin/tenascin. Proc Natl Acad Sci U S A **90,** 10154, 1993.
29. Ozeki, M., Kuroda, S., Kon, K., and Kasugai, S. Differentiation of bone marrow stromal cells into osteoblasts in a self-assembling peptide hydrogel: *in vitro* and *in vivo* studies. J Biomater Appl **25,** 663, 2011.
30. Chau, Y., Luo, Y., Cheung, A.C., Nagai, Y., Zhang, S., Kobler, J.B., Zeitels, S.M., and Langer, R. Incorporation of a matrix metalloproteinase-sensitive substrate into self-assembling peptides—a model for biofunctional scaffolds. Biomaterials **29,** 1713, 2008.
31. Gelain, F., Unsworth, L.D., and Zhang, S. Slow and sustained release of active cytokines from self-assembling peptide scaffolds. J Control Release **145,** 231, 2010.
32. Nair, M.B., Varma, H.K., Menon, K.V., Shenoy, S.J., and John, A. Reconstruction of goat femur segmental defects using triphasic ceramic-coated hydroxyapatite in combination with autologous cells and platelet-rich plasma. Acta Biomater **5,** 1742, 2009.
33. Khan, S.N., Cammisa, F.J., Sandhu, H.S., Diwan, A.D., Girardi, F.P., and Lane, J.M. The biology of bone grafting. J Am Acad Orthop Surg **13,** 77, 2005.
34. Reichert, J.C., Wullschleger, M.E., Cipitria, A., Lienau, J., Cheng, T.K., Schutz, M.A., Duda, G.N., Noth, U., Eulert, J., and Hutmacher, D.W. Custom-made composite scaffolds for segmental defect repair in long bones. Int Orthop **35,** 1229, 2011.
35. Zimmermann, C.E., Gierloff, M., Hedderich, J., Acil, Y., Wiltfang, J., and Terheyden, H. Survival of transplanted rat bone marrow-derived osteogenic stem cells *in vivo*. Tissue Eng Part A **17,** 1147, 2011.
36. Tsso, R., Augello, A., Boccardo, S., Salvi, S., Carida, M., Postigliong, F., Fais, F., Truini, M., Cancedda, R., and Pennesi, G. Recruitment of a host's osteoprogenitor cells using exogenous mesenchymal stem cells seeded on porous ceramic. Tissue Eng Part A **15,** 2203, 2009.
37. Fricain, J.C., Schlaubitz, S., Le Visage, C., Arnault, I., Derkaoui, S.M., Siadous, R., Catros, S., Lalande, C., Bareille, R., Renard, M., Fabre, T., Cornet, S., Durand, M., Leonard, A., Sahraoui, N., Letourneur, D., and Amedee, J. A nano-hydroxyapatite—pullulan/dextran polysaccharide composite macroporous material for bone tissue engineering. Biomaterials **34,** 2947, 2013.
38. Nair, M.B., Varma, H., Shenoy, S.J., and John, A. Treatment of goat femur segmental defects with silica-coated hydroxyapatite—one-year follow-up. Tissue Eng Part A **16,** 385, 2010.

Address correspondence to:
Tianyong Hou, PhD
National & Regional United Engineering
Lab of Tissue Engineering
Department of Orthopaedics
Southwest Hospital
The Third Military Medical University
Chongqing 400038
China

E-mail: tianyonghou@126.com

Jianzhong Xu, PhD
National & Regional United Engineering
Lab of Tissue Engineering
Department of Orthopaedics
Southwest Hospital
The Third Military Medical University
Chongqing 400038
China

E-mail: jianzhongxu1963@gmail.com

Received: May 18, 2014
Accepted: December 16, 2014
Online Publication Date: February 10, 2015